# Physical Studies on Deposited Snow. II.*
# Mechanical Properties (1)

by

Zyungo YOSIDA, Hirobumi OURA, Daisuke KUROIWA, Tosio HUZIOKA,
Kenji KOJIMA, Sin-iti AOKI and Seiiti KINOSITA

*Applied Physics Section, Institute of Low Temperature Science.*

(Manuscript Received February, 1956)

## II. Mechanical Properties of Deposited Snow

### §1. Compressive nature of snow.

As is the case with many other substances, snow responds visco-elastically to a force applied to it provided that the force remains so small that it does not break down the snow. M. de Quervain studied the visco-elastic properties of snow and ice by twisting a pillar of snow or ice and found that their mechanical properties could be qualitatively represented by a rheological model composed of a Maxwell unit and a Voigt unit in series connection (1). Extensive investigations on the viscous properties of snow, namely the creep phenomenon of snow, were performed by R. Haefeli as early as 1939 (2), and recently Edwin Bucher, from the rheological point of view, made studies on creep of snow by applying to it torsional, tensile and compressive force (3).

The present authors too studied the visco-elastic properties of snow by compressing a pillar of snow by a pressure not exceeding 30 gr-wt/cm$^2$. The method of compression was adopted since its simplicity allowed many samples of snow to be dealt with in a short time. Then the elastic constant $E$ and the viscous constant $\eta$ measured in the present experiments were compressive Young's modulus and compressive viscous constant respectively. If the Poisson ratio of snow is denoted by $\sigma$, they can be converted to the constants concerning shearing stress by being divided by $2(1+\sigma)$, although the value of $\sigma$ may have to be changed according to whether elastic or viscous phenomenon is concerned. When a pillar of snow is compressed in the axial direction, it must expand laterally provided that $\sigma$ is not zero. Snow layers composing snow cover are always acted upon by the compressive pressure due to their own weights but can not expand laterally and their response to the compressive pressure will differ from that in the case of a snow pillar. One can obtain the constants in the case of snow layer from those in the case of snow pillar by dividing the latter by $1-\frac{2\sigma^2}{1-\sigma}$. But it should be noticed that such a con-

* Contribution No. 307 from the Institute of Low Temperature Science.

version of constants is applicable only in the case when strain produced by the force is limited within a very small magnitude. If the strain becomes large, there happens even such a case that the viscous constants do not coincide with each other in two cases of compression and extension of snow, as shown by Haefeli (2).

The experiments were performed in the cold room attached to the present authors' Institute (4) (5) (6). A circular pillar of snow 5 cm in diameter and 7~15 cm in length was cut out of the snow cover lying on the ground and iron discs 1 mm thick were attached to each of the end planes of the pillar. The discs were applied to the ends of the snow pillar after they had been somewhat warmed by being held between the hands. The thin layer of snow on the end planes was melted by the warmth of the discs and then was frozen again by the prevailing cold to fasten the discs firmly to the ends of the pillar. In Fig. 1, S represents the snow pillar, standing on a wooden table B, with the

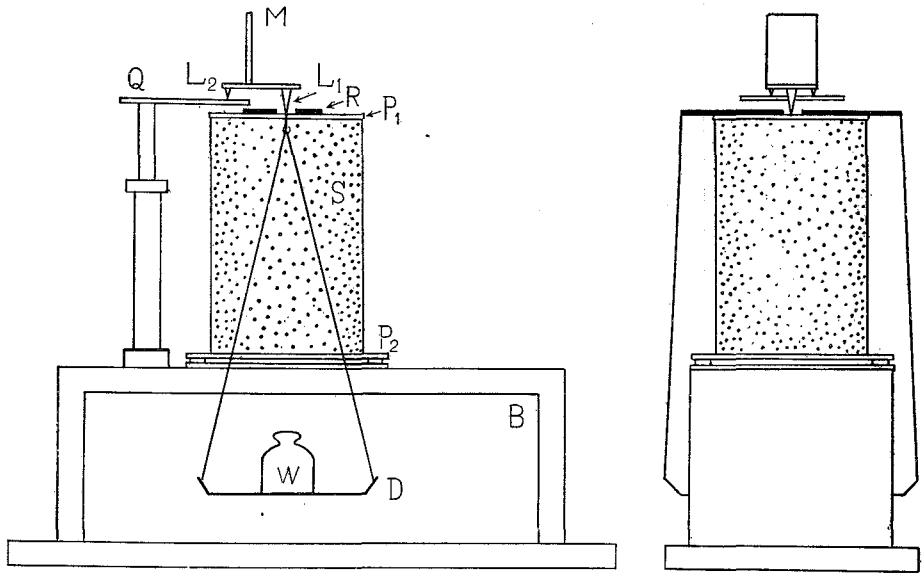


**Fig. 1** Apparatus for measuring the compression of snow pillar.

iron plates $P_1$ and $P_2$ on its upper and lower ends respectively. R is an aluminium ribbon plate which extrudes the margin of the iron plate $P_1$. Strings attached to the two ends of R suspend the aluminium pan D without touching the wooden table B. The brass plate on which the mirror M stands has three pointed legs with its fore leg resting on the iron plate $P_1$ through a hole in the aluminium ribbon plate R while its two rear legs are put in a groove made on the metal plate Q of which the position can be adjusted to any desired height. When a weight W is put on the aluminium pan D the snow pillar is contracted by a small amount $\Delta l$, with the result that the

mirror M is tilted forward by a small angle $\Delta\alpha$ which is proportional to the contraction $\Delta l$. Therefore, by measuring the angle $\Delta\alpha$ by means of the method of scale and telescope, the contraction $\Delta l$ can be accurately determined.

An example of the course of depression observed on the top of a pillar of compact snow is shown in Fig. 2. The top of the pillar of which the initial position is indicated by point P in Fig. 2 was gradually lowered to point O in 4 minutes by the compressive pressure $w'$ caused by the weight of the iron disc $P_1$ and the empty aluminium pan D. $w'$ was 2.01 gr-wt/cm$^2$ in this case. At point O a weight was put on the pan D and the compressive force acting on the snow pillar was increased. Then the top of the pillar was lowered instantly by an amount equal to OA to continue hereafter descending along the line ABC. After point C at which another weight was added to the pan the position of the top of pillar descended as indicated by the line CDEF of which the initial part CD was an instantaneous depression.

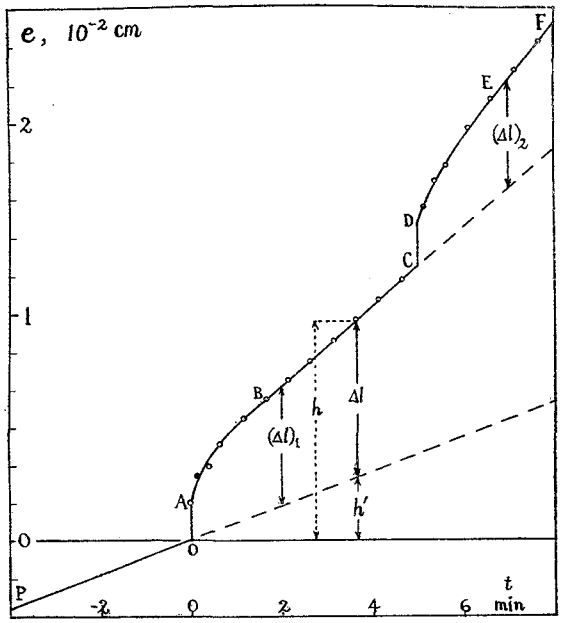


Fig. 2 Depression of the top of snow pillar. At $t=0$ min and at $t=5$ min the compressive pressure $w$ acting on the snow pillar was increased by the same amount respectively.

If the weight was removed immediately after it had been put on the pan D instead of being left to rest on it, the instantaneous depression as indicated by OA or CD in Fig. 2 was almost completely recovered instantly. Therefore such an instantaneous depression must be a purely elastic deformation. The second depression which followed the initial elastic depression and is indicated by the part AB or DE of the depression curve of Fig. 2 is a depression caused by retarded elasticity which can be recovered slowly if the compressive force which has brought it about is removed. In the stage following that of retarded elasticity the depression proceeded at a constant small rate as shown by the straight line segments BC and EF in Fig. 2. The depression due to such a continual contraction of the snow pillar can not be recovered even a long time after the removal of the compressive force. Therefore this continual depression at a constant rate must be the creep phenomenon. But it must be noted that this rate of creep appeared constant only because

the time of application of compressive pressure was short. The rate would have come to decrease gradually if the compressive pressure were left to act on the snow for a much longer time.

In the case of the present experiments the snow pillar was always subjected to a compressive pressure $w'$ representing the dead weight of the iron plate $P_1$ attached to the top of the pillar and of the aluminium pan D shown in Fig. 1. Therefore, when a weight W was put on the pan D and the compressive pressure was increased from $w'$ to $w'+w$, the depression $h$ observed thereafter on the top of the pillar was the result of the action of both $w'$ and $w$. But the part of depression $\Delta l$ due to $w$ alone can be separated from the total depression $h$ by subtracting from it the part $h'$ due to $w'$ which can easily be determined by elongating the straight line segment PO representing the creep depression caused by $w'$ alone into the region after the application of $w$ as shown in Fig. 2.

Fig. 3(a) shows an example of strain-time curve observed at $-8.9°C$ on a pillar of compact snow of density 0.19 gr/cm$^3$ by applying a compressive pressure $w=1.0\times10^4$ dyne/cm$^2$ for a period of 7 minutes. The strain $e$ in this case is the ratio $\Delta l/l$, where $l$ represents the length of the snow pillar. The strain due to the dead weight $w'$ is eliminated in this curve in the manner explained in the previous paragraph. At the moment of application of the com-

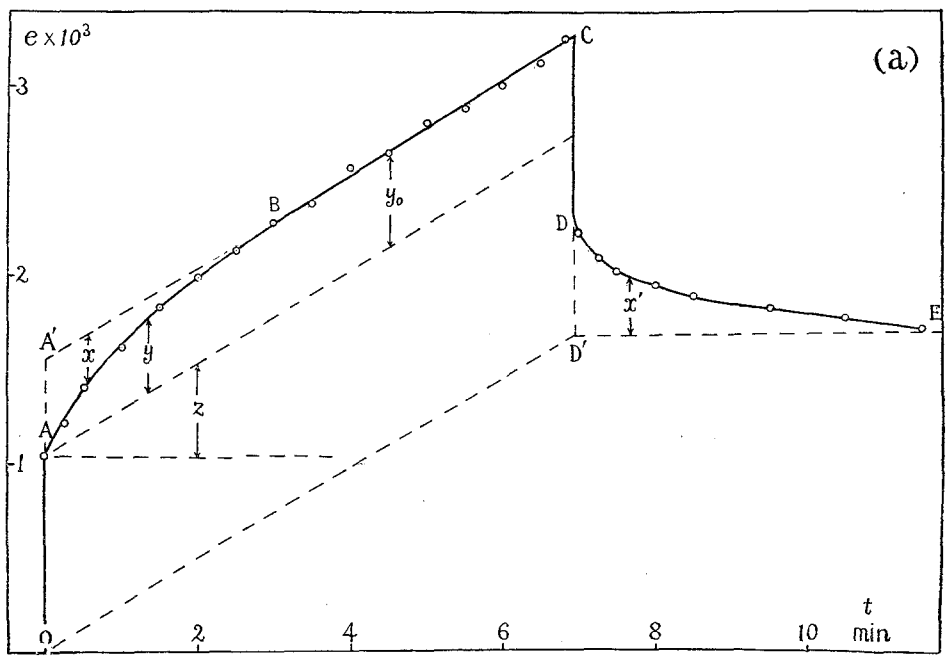


**Fig. 3** (a) Compressive strain $e$ produced on the snow pillar. Compressive pressure was applied at $t=0$ min and was removed at $t=7$ min.

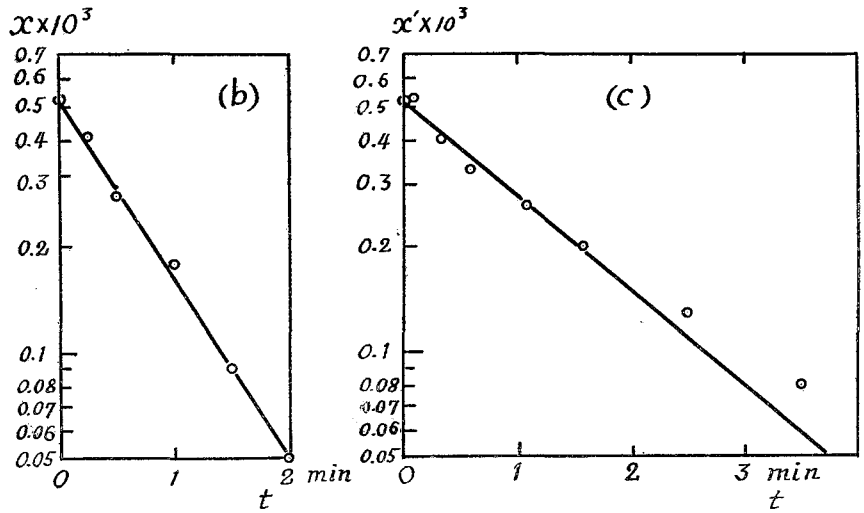


Fig. 3 (b) (c) The logarithm of $x$ and $x'$ shown in Fig. 3 (a) decreases linearly with the increase of time $t$.

pressive pressure $w$ an instantaneous elastic strain OA appeared. Then the period of retarded elasticity lasted for about 3 minutes in which the strain increased at a decreasing rate up to point B to be followed by the period of creep represented by the straight line BC. At point C the compressive pressure $w$ was suddenly removed. The strain was instantly decreased to point D by an amount almost equal to the initial elastic increase OA. The recovery of strain was not completed to that extent but the strain continued to decrease along the line from D to E to overcome that part of strain caused by the retarded elasticity in the period from A to B. After point E no or little change was observed in the strain. However the total strain which had been produced up to the moment of removal of the compressive pressure $w$ was not entirely recovered since the creep phenomenon had acted to set up a permanent strain corresponding to point E in the time during which the compressive pressure had been being applied.

The final value of the strain due to the retarded elasticity alone is equal to the distance $y_0$ between the straight line BC and a straight line drawn parallel to it through point A. The amount DD′ of the slow recovery of strain in the period following point D is almost the same as that of $y_0$, which shows that the strain caused by retarded elasticity is actually recovered in this period. The strain $y$ due to retarded elasticity slowly increased to reach its final value $y_0$ and $x=y_0-y$ was found to be diminished with time exponentially as is shown by the annexed figure (b) of Fig. 3 in which one can see that $log_{10}x$ decreases in a fairly good linear relation to the time $t$. Also in the case of recovery of the strain due to retarded elasticity, the strain $x'$ corresponding

to the strain $x$ in the case of production of retarded elasticity strain decreases with time exponentially as shown in another annexed figure (c) of Fig. 3. De Quervain obtained by torsional experiments almost the same results as here described but he found that the course of change in $x$ and $x'$ somewhat deviated from exponential curves (1). This deviation seems to have arisen from the fact that the time of application of force was longer in his case than in the present case.

Such being the case, one can see that the compressive behavior of snow can be represented by that of the simple models widely used in rheology. The schematical figure on the left side of Fig. 4 shows a combination of two of the fundamental rheological unit models: the Maxwell unit model and the

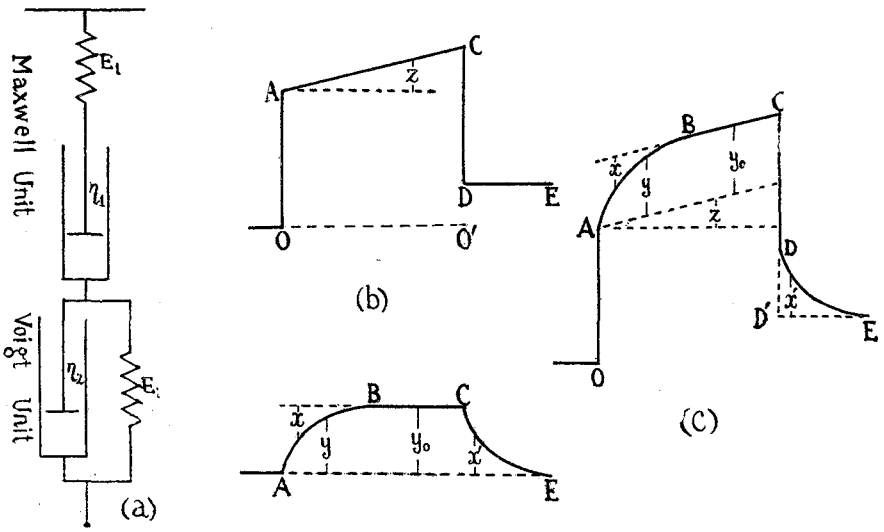


Fig. 4 Left: Rheological model representing the compressive nature of snow. Centre: Upper and lower figures show the strain caused on Maxwell and Voigt unit models by a compressive pressure which continues to act for a certain time interval. Right: Sum of the two strains shown by the central figures. This is nothing but the strain shown by the model on the left side.

Voigt unit model. The Maxwell unit model is composed of a spring with elastic constant $E_1$ and a dash-pot with viscous constant $\eta_1$ in series connection; the Voigt unit model is composed of a spring with elastic constant $E_2$ and a dash-pot with viscous constant $\eta_2$ in parallel connection. When a compressive force is applied for a certain period of time the strain $e_1$ on a Maxwell unit model will be as shown in the central upper figure of Fig. 4. In this case the strain $e_1$ is composed of pure elastic strain $e_1'=OA$ and creep strain $e_1''=O'D$, of which the former alone can be recovered by removal of the compressive force as shown by the vertical segment CD. The Voigt unit

model represents the mechanism of the appearance of retarded elasticity. The pure elastic response of the spring $E_2$ is retarded by the viscous action of the dash-pot $\eta_2$ and the course of change in the strain $e_2$ in this unit will be shown by the curve drawn in the central lower part of Fig. 4. The total strain $e=e_1+e_2$ appearing on the combination of the Maxwell unit model and the Voigt unit model thus comes to be represented by figure (c) on the right side of Fig. 4 which resembles very much the strain-time curve of Fig. 2 observed on the actual snow. If the compressive force applied is $w$, the instantaneous elastic strain OA and the parts of strain represented respectively by $x$, $y$, $z$ and $x'$ in (c) of Fig. 4 are represented by the following mathematical formulae:

$$\mathrm{OA}=w/E_1 \tag{1}$$

$$x=(w/E_2)\,exp\,(-t/\tau_2) \tag{2}$$

$$y=y_0-x=(w/E_2)\{1-exp(-t/\tau_2)\} \tag{3}$$

$$z=(w/E_1)(t/\tau_1) \tag{4}$$

$$x'=(w/E_2)\,exp\,(-t/\tau_2), \tag{5}$$

where $\tau_1=\eta_1/E_1$ and $\tau_2=\eta_2/E_2$ are time constants called relaxation time and retardation time respectively.

The close resemblance between the strain-time curve shown in Fig. 3 which was obtained with actual snow and that shown by the rheological model suggests that the compressive nature of snow can be characterised by a set of four constants $E_1$, $E_2$, $\eta_1$, $\eta_2$ or of $E_1$, $E_2$, $\tau_1$, $\tau_2$. Indeed the following values can be obtained for these characteristic constants by the use of that part of the strain-time curve OABC of Fig. 3(a) which belongs to the period during which the compressive pressure $w$ was acting and by the aid of the formulae from (1) to (4):

$$E_1=0.90\times10^7\ \mathrm{dyne/cm^2},\quad \tau_1=4.25\ \mathrm{min.}$$
$$E_2=1.92\times10^7\ \mathrm{dyne/cm^2},\quad \tau_2=0.85\ \mathrm{min.}$$

If the compressive nature of the snow can be completely represented by the rheological model, the strain $x'$ which decreases gradually after the compressive pressure is removed should be represented by formula (5) with the same values of $E_2$ and $\tau_2$ as those given above. But the value of $\tau_2$ must be changed to $\tau_2'=1.19$ min in order to make the observed value of $x'$ coincide with the computed value of $x'$, although the value of the elastic constant $E_2$ needed not be changed from the above value. The pure elastic recovery represented by the vertical segment CD was found equal to OA, which shows that the other elastic constants $E_1$ too had not changed just as $E_2$ had not.

However the above described example is one of the most simple cases of

strain-time curve observed on the actual snow. In many cases not only the time constants $\tau_1$ and $\tau_2$ but also the elastic constants $E_1$ and $E_2$ were found to change when the snow had been under the action of a compressive pressure. This fact show that the snow is subject to an irreversible change in its mechanical property while it is being influenced by a pressure, which one can expect arises from its fragile structure. Although it is certainly a weak point that the characteristic constants are changeable, they are still indispensable constants to characterise the compressive nature of snow.

Ice itself, the material constituting snow, also shows a visco-elastic property much like that of snow. De Quervain twisted a circular pillar of ice by a force of constant moment and obtained a strain-time curve similar to that of Fig. 3 (1). But he found, unlike in the case of snow, that the instantaneous recovery of strain at the moment of removal of the force was much smaller than the instantaneous strain produced at the application of the force. T. Tabata, one of the researchers of the authors' Institute, loaded a beam of sea-ice with a weight at its centre (7). The dip of the centre of sea-ice beam changed with time just like the curve of Fig. 3 without showing appreciable difference between the instantaneous changes at the moments of application and removal of the weight.

For practical purposes the fact that there are four constants to characterise the compressive nature of snow may pose a cumbersome circumstance. The present authors believe that in many cases the snow can approximately be represented by a simple Maxwell model in which case the elastic constant of the model should be chosen as the ratio $OA'/w$ instead of $OA/w$, where $OA'$ and $OA$ are strains shown in Fig. 3, while the viscous constant should be chosen as the same as before. If the two constants in this approximation are denoted by $E_M$ and $\eta_M$, the relaxation time $\tau_M$ is given by $\eta_M / E_M$. Rheology teaches that any substance of which the mechanical property can be represented by a Maxwell model makes response to a mechanical action like a solid substance in the case when the action lasts only for a time shorter than $\tau_M$ while it responds like a liquid substance to a mechanical action which continues for a time much longer than $\tau_M$. Such a substance may be said to have a memory which lasts only for the relaxation time $\tau_M$. When a constant force acts on it for a time longer than $\tau_M$ causing its deformation, it forgets its real undeformed initial state and acts as if the deformed state in which it was $\tau_M$ before were the true original state, trying to return to that state by its elastic strength.

It is noted that the results obtained concerning the compressive nature of snow described above in this section will be formally applied also to the nature which snow shows when acted on by tensile or shearing force. Indeed de Quervain has shown that this is the case with shearing force (1). In the following section experimental values of characteristic constants obtained on

the compressive nature of many samples of snow will be presented.

## §2 Characteristic constants determining the compressive nature of snow.

(*a*) *Non-dependence of the constants $E_1$ and $\eta_1$ on the strength of compressive pressure.* As explained in the previous section the compressive nature of snow can be characterised by a set of four constants $E_1$, $E_2$, $\eta_1$, $\eta_2$ or $E_1$, $E_2$, $\tau_1$, $\tau_2$. Among these four $E_1$ and $\eta_1$ are the constants which can be most easily determined, the former being the ratio of the compressive pressure to the instantaneous strain produced at the moment of application of that pressure while the latter is the ratio of the compressive pressure acting on the snow to the time rate of change in the strain which the snow shows some time after the application of that pressure.

In order to learn whether the constant $E_1$ is independent or not of the strength of the compressive pressure $w$, that is, whether or not the instantaneous strain $e_1'$ produced by $w$ increases in proportion to the increase in $w$, compressive pressure of different strengths was applied on each of various snow samples cut out of one and the same layer of the snow cover. On such samples of the same nature the experiments were performed in such a way that one of the samples was stood on the wooden table shown in Fig. 1 of the previous section and a weight was put on the pan D, and then that sample was replaced by another one and a different weight was applied and so on. In these cases a compressive pressure $w'$ due to the dead weight explained in the previous section had been acting before the weight was put on the pan D. Therefore the compressive pressure due to the weight cannot be said to have

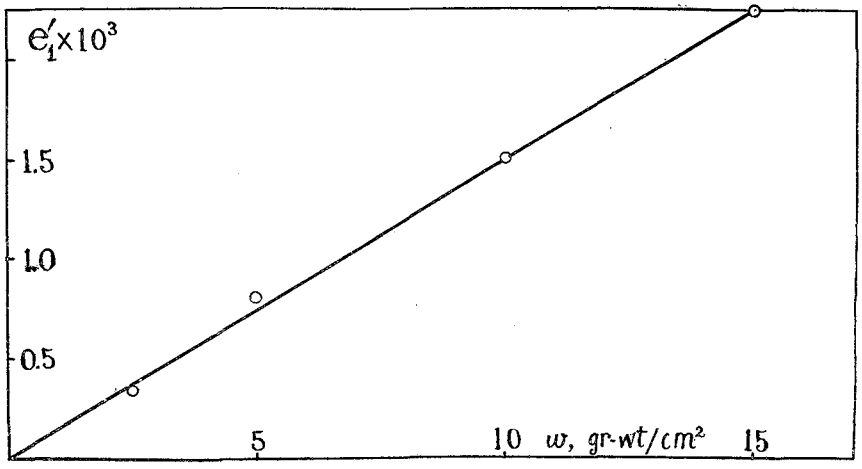


Fig. 5 Instantaneous elastic strain $e_1'$ produced at the moment of application of compressive pressure $w$ increases in proportion to the increase in $w$, so long as $w$ is applied to snow in the virgin state.

been applied on snow which is in the virgin state, that is, in a state completely free from any stress. But, even if it were so, the snow sample may be thought to have been at least nearly in the virgin state, for the pressure $w'$ was actually much smaller than the pressure $w$. Fig. 5 shows the results of these experiments. The instantaneous strain $e_1'$ produced by $w$ is in good proportion to $w$, which fact shows that the elastic constant $E_1$ is not dependent upon the strength of $w$.

When the compressive pressure $w$ was added to the snow which had already been being stressed, the instantaneous strain $e_1'$ did not show such a simple relation as above. Indeed the instantaneous strains OA and CD shown in Fig. 2 of the previous section each of which was produced by a compressive pressure of the same intensity were not of the same amount, CD being smaller than OA. Discussions on this subject will be presented below in article (*d*) of this section.

The viscous constant $\eta_1$ can be determined by dividing the total pressure $w'+w$ actually acting on the snow by the time rate of change $\dot{e}$ in the strain in these regions where the strain-time curve comes to be straight as shown by the regions from B to C or from E to F in Fig. 2. Fig. 6 shows the relation between $\dot{e}$ and $w'+w$ and three of the curves shown therein are straight lines passing through the origin, which shows that $\eta_1$ is not dependent upon the intensity of $w'+w$. The lowest curves (D) presents an exceptional case in that $\dot{e}$ increases with decreasing rate as $w'+w$ is increased. In the cases of metals $\dot{e}$ increases with the increase of force more rapidly than in proportion to it and J. W. Glen showed that this is the case also with ice (8). Therefore the case of curve (D) inverse to the general case must have arisen from the

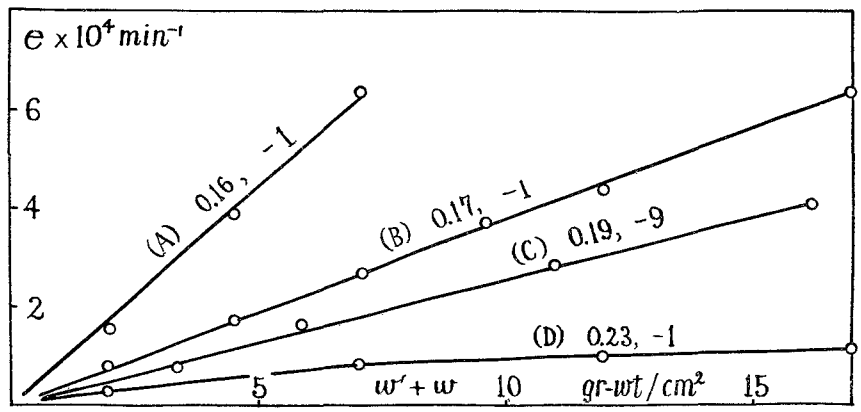


Fig. 6 Time rate of change $e$ of strain observed some time after the application of compressive pressure $w$ increases as a rule in proportion to the pressure $w'+w$ actually acting on the snow, $w'$ being the pressure due to the dead weight. Two figures attached to each of the curves, for example 0.16 and $-1$ on curve (A), are density and temperature respectively.

peculiar texture of snow consisting of many minute ice granules and rods connected with each other in a very complicated way but not from the properties of ice itself. The cases of the other three curves should be considered rather to be special ones peculiar to the condition that the compressive pressure was kept to a small value in the present experiments. Indeed the compressive pressure was always kept not to exceed 30 gr-wt/cm$^2$ in the present experiments as a precaution against breaking down the snow sample.

(*b*) *The characteristic constants and the temperature.* The compressive nature of snow is remarkably influenced by the temperature. Fig. 7 shows strain-time curves observed on snow samples of the same nature at three different temperatures. The compressive pressure applied on them at $t=0$ was of the same magnitude, $1.00\times10^4$ dyne/cm$^2$, in all three cases. The strain was diminished generally as the temperature lowered, which shows that the characteristic constants were enlarged as the temperature was decreased. The course of change in the four characteristic constants $E_1$, $E_2$, $\eta_1$, $\eta_2$ with temperature determined on snow samples of different densities is shown in Fig. 8 with the different symbols for the different densities. Although the points representing the experimental values of the constants are scattered, the tendency for all the constants to increase with lowering temperature is clearly shown; it would be approximately represented by the broken lines drawn in the figures.

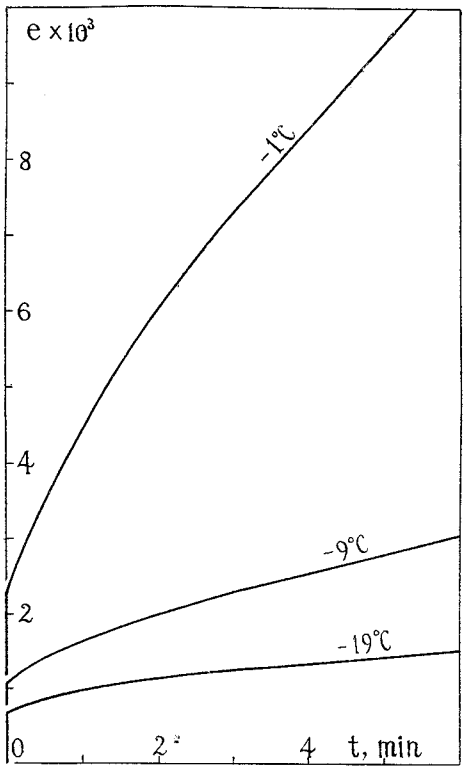


**Fig. 7** Strain-time curve of snow is greatly influenced by temperature. Density of snow: 0.16.

Among the four characteristic constants, $\eta_1$ is the most important one in the sense that it determines the creeping velocity of snow when it is acted on by a constant pressure for a long time as in the case of snow layers lying in the lower part of natural snow cover. It is known that the viscous constant $\eta$ of a solid and of a liquid is in general roughly expressed as to its dependence on the temperature by a mathematical formula of the form:

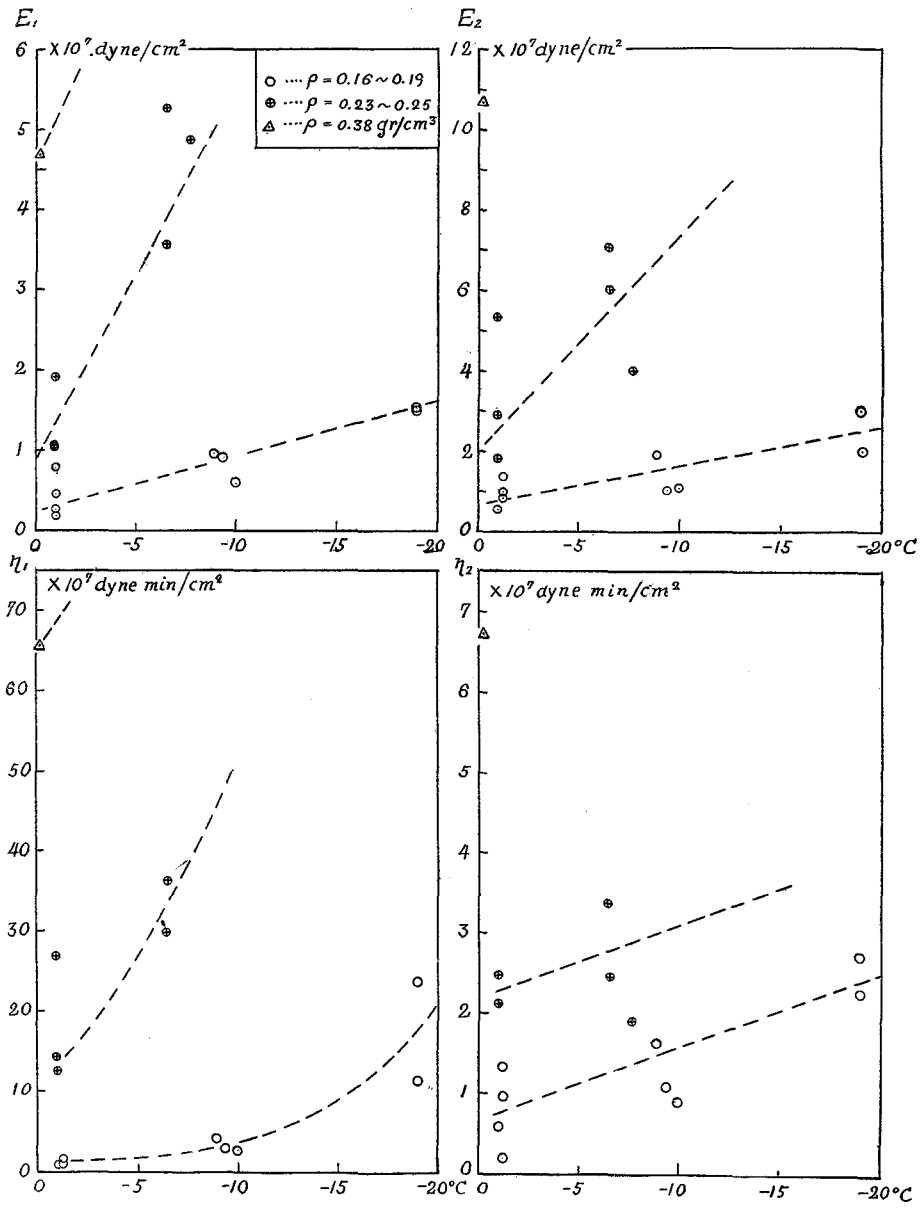


Fig. 8 Four characteristic constants and temperature.

$$\eta = A\, exp\,(Q/RT), \qquad (1)$$

where $A$ and $Q$ are constants characteristic to the substance while $R$ and $T$ denote the universal gas constant and the absolute temperature respectively. The linear relations between $log_{10}\eta_1$ and $1/T$ shown in Fig. 9 then indicate that the viscous constant $\eta_1$ of snow also satisfies the above formula as the

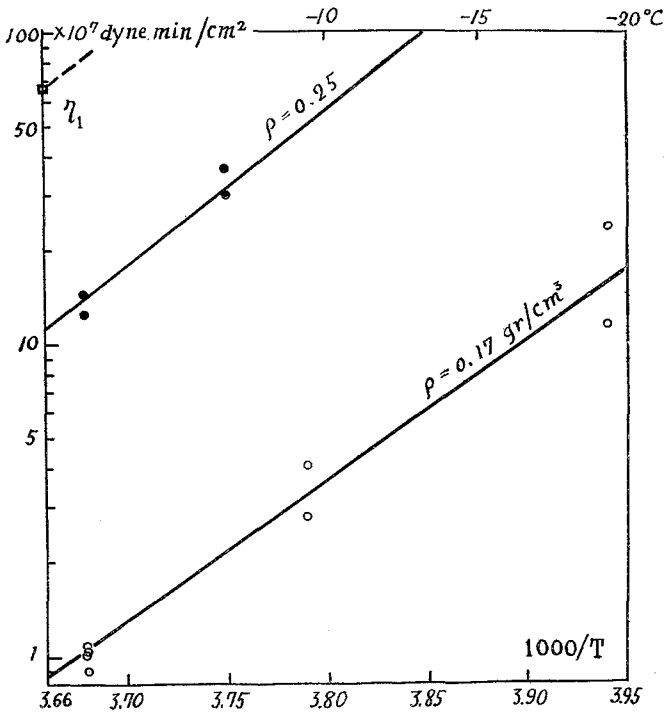


Fig. 9 $log_{10}\eta_1$ versus reciprocal of absolute temperature.

other substances do. The explicit forms of the relations are:

$$\eta_1 = 1.58\times10^{-10}\, exp\,(10.5\times10^3/T)\ \text{dyne·min/cm}^2 \quad \text{for density 0.17,}$$

$$\eta_1 = 1.10\times10^{-11}\, exp\,(11.9\times10^3/T)\ \text{dyne·min/cm}^2 \quad \text{for density 0.25,}$$

which yield respectively

$$Q = 20.8 \quad \text{and} \quad 23.8\ \text{kcal/mole.}$$

Haefeli gives in his paper (2) the numerical results of his observations on strain produced on snow pillars of the same density 0.32 but of different temperatures by the same compressive pressure 64 gr-wt/cm². The present authors computed the value of $Q$ from his data and it turned out to be:

$$Q = 13\ \text{kcal/mole.}$$

Bucher gives in his paper (3) a figure in which are presented nine curves showing the relation between $log_{10}\eta_i$ and temperature, each of them concerning different sorts of snow. The values of $Q$ computed by the present authors on each of the curves by regarding $log_{10}\eta_i$ as decreasing in linear relation to the reciprocal of absolute temperature were found to lie in the range from 10 to 20 kcal/mole.

Snow is composed of a large number of ice elements such as ice granules and ice bonds connecting them with each other. When a sample of snow is undergoing viscous flow under the action of a compressive pressure $w$, the ice elements are imparted with stress which varies from one element to the other with the result that each of the elements flows at a different rate. But, on one and the same element, as the first approximation, the stress will be proportional to the intensity of the compressive pressure $w$ and consequently the flow rate of this element will be in proportion to the ratio $w/\eta_i$, where $\eta_i$ denotes the viscous constant of ice. Since this must be the case in respect to every ice element of the snow, it should flow as a whole at a rate proportional to $w/\eta_i$, which indicates that the viscous constant $\eta_i$ of snow is proportional to that of ice $\eta_i$. Therefore, if the viscous constant $\eta_i$ of ice depends on the temperature in the form of mathematical formula (1), the value of $Q$ observed on ice must coincide with that observed on snow. J. W. Glen (8) made experimental studies on the creep of ice and found that formula (1) held for ice with

$$Q = 31.8 \text{ kcal/mole.}$$

The above value of $Q$ obtained on snow by the present authors is about two-thirds of the value obtained by Glen. This difference may be attributed to the facts that Glen's value was computed on the base of viscous constants observed on ice many hours after the application of the compressive force while the present authors used for their computation the values of viscous constants which snow showed in the time of application of compressive force not longer than a few tens of minutes.

(*c*) *The characteristic constants and the density of snow.* Although a definite relation cannot be expected to exist between the characteristic constants and the density of snow, some loose relationship, if not a definite one, may be found between them. In Fig. 10 the elastic constants $E_1$ is plotted against the density $\rho$ of snow for temperature ranges from $-1°C$ to $-3°C$ and from $-5°C$ to $-15°C$. The triangular mark in Fig. 10(b) indicates the experimental value obtained by de Quervain (1). $E_1$ increases slowly with the increase in $\rho$ while the latter remains smaller than 0.3 but begins to increase rapidly when the density comes to exceed 0.3. The broken lines in Fig. 10, which are drawn in order to show even though roughly the increasing tendency of $E_1$ with $\rho$ for

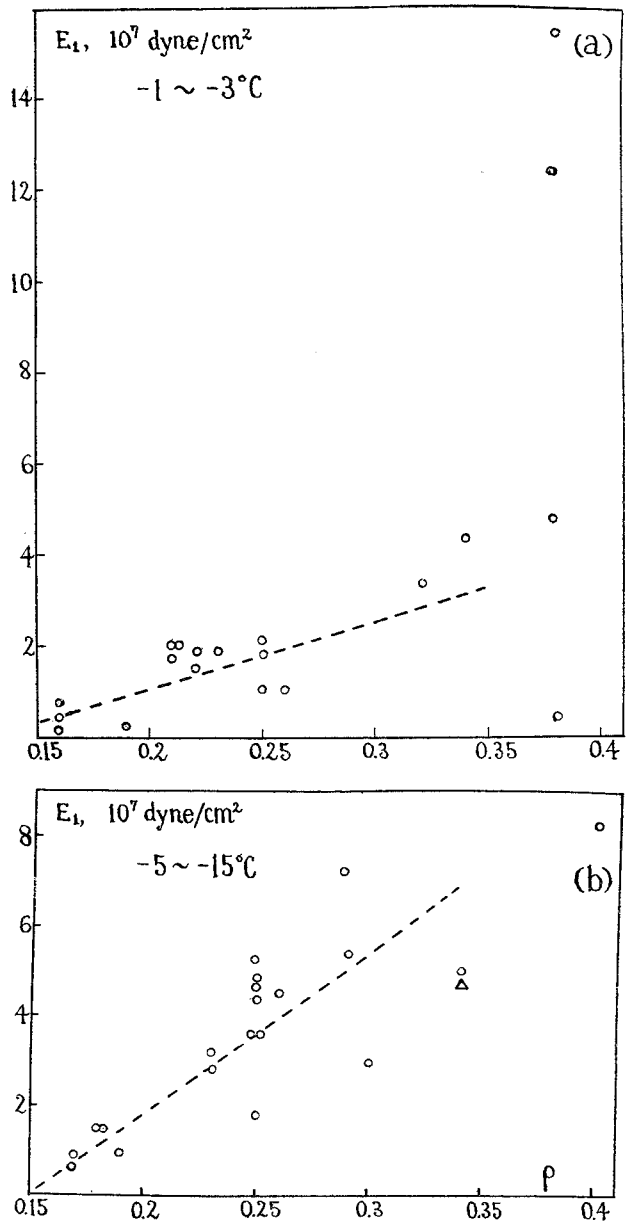


**Fig. 10** $E_1$ versus density $\rho$ of snow. (a) Temperature: $-1\sim-3$°C. (b) Temperature: $-5\sim-15$°C; triangular mark is according to de Quervain.

values smaller than 0.3, can be mathematically expressed by:

$$E_1(10^7\ \text{dyne/cm}^2) = -1.5+(40/3)\rho \quad \text{for} \quad -1\sim-3°\text{C}$$
$$E_1(10^7\ \text{dyne/cm}^2) = -5.4+36\rho \quad \text{for} \quad -5\sim-15°\text{C}.$$

The viscous constant $\eta_1$ increases with the increasing density $\rho$ of snow. The reciprocals of $\eta_1$ are shown in Fig. 11 in relation to the density for two different ranges of temperature from $-1°C$ to $-3°C$ and from $-5°C$ to $-15°C$. The triangular mark in Fig. 11 (b) represents the value obtained by de Quervain (1). $1/\eta_1$ seems to decrease linearly with increasing $\rho$. The straight lines showing this tendency can be expressed by:

$$1/\eta_1(10^7 \text{ dyne}\cdot\text{min/cm}^2) = 2-6.5\rho \quad \text{for } -1\sim-3°C$$

$$1/\eta_1(10^7 \text{ dyne}\cdot\text{min/cm}^2) = 0.85-3\rho \quad \text{for } -5\sim-15°C.$$

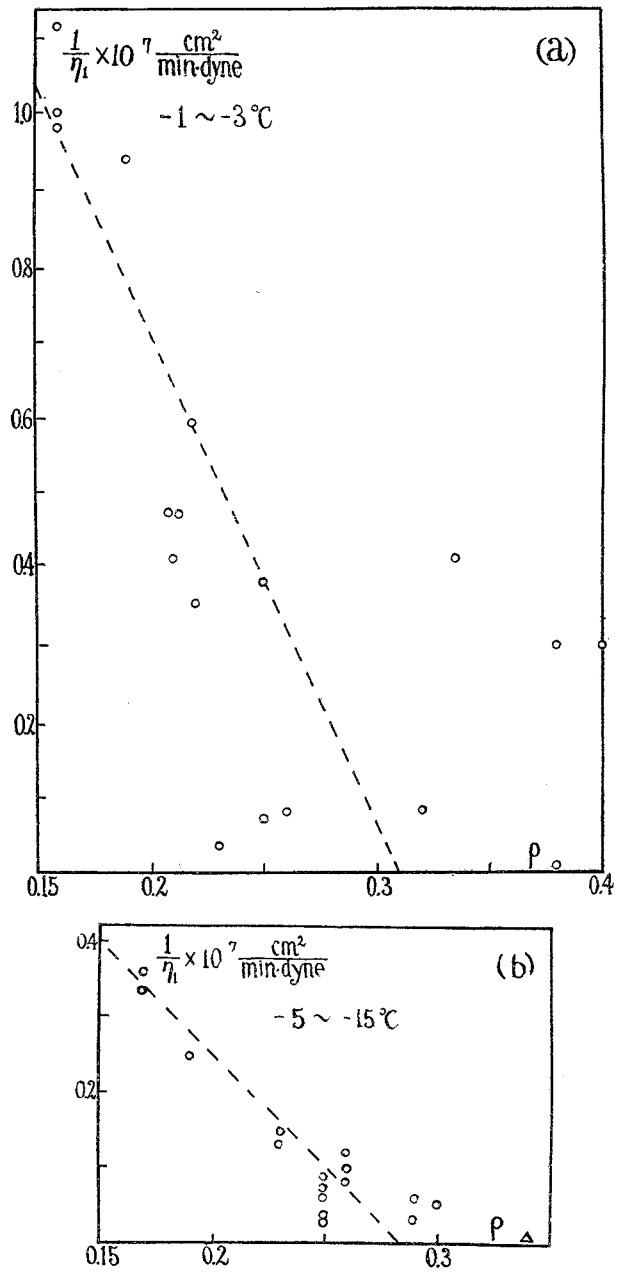


Fig. 11 Reciprocal of $\eta_1$ versus $\rho$. (a) Temperature: $-1\sim-3°C$. (b) Temperature: $-5\sim-15°C$; triangular mark is due to de Quervain.

The second elastic constant $E_2$ is usually larger than $E_1$; $E_2$ is from two to four times as large as $E_1$ when the snow density is in the range 0.1~0.2 gr/cm$^3$ and the temperature is higher than $-1.5°C$, but with increasing density and with decreasing temperature the ratio $E_2/E_1$ tends to diminish to become less than 2 when the density exceeds 0.2 gr/cm$^3$ and the temperature becomes lower than about $-10°C$. The possibility is not excluded that $E_2$ is less than $E_1$ although such a case rarely occurs.

The second viscous constant $\eta_2$ is less than $\eta_1$ although the inverse cases are not considered impossible as rare cases. $\eta_2$ amounts to from seven- to nine-tenths of $\eta_1$ for the snow density $0.1\sim0.2$ gr/cm$^3$ and for the temperature higher than $-1.5$°C but it is reduced to about one-tenth of $\eta_1$ when the density and the temperature become larger than 0.2 gr/cm$^3$ and lower than about $-10$°C respectively.

The relaxation time $\tau_1$ which is equal to the ratio $\eta_1 E_1$ usually lies in the range from 4 min to 15 min. The maximum and minimum values of $\tau_1$ observed were 25.6 min and 1.31 min respectively. No definite relation was found between $\tau_1$ and the density or the temperature. The retardation time $\tau_2$ of snow which is equal to the ratio $\eta_2/E_2$ ranges from about half a minute to about one minute. Here also no definite relation was found between $\tau_2$ and the density of snow or the temperature.

As stated in the previous section § 1, it is a practical convenience to consider the snow as represented by a Maxwell unit model with two characteristic constants $E_M$ and $\eta_M$. $\eta_M$ is equal to $\eta_1$ and $E_M$ is related with $E_1$ and $E_2$ by the formula:

$$\frac{1}{E_M}=\frac{1}{E_1}+\frac{1}{E_2}.$$

The relaxation time $\tau_M$ in this case turns out to be $\tau_M=\eta_M/E_M$ and there holds the equation:

$$\tau_M=\eta_M/E_M=(\eta_1/E_1)+(\eta_1/E_2)=\tau_1+(\eta_1/\eta_2)\tau_2.$$

Since $\eta_1$ is several times larger than $\eta_2$ and $\tau_2$ is only a fraction of $\tau_1$, as stated in the above paragraphs, $(\eta_1/\eta_2)\tau_2$ will be nearly of the same magnitude as $\tau_1$. Therefore the relaxation time $\tau_M$ may be considered twice as large as $\tau_1$ which ranges usually from 4 min to 15 min.

(*d*) *The characteristic constants influenced by the compressive pressure which has previously been applied to the snow.* It was noted in article (*a*) of this section that the elastic constant $E_1$ observed on snow in the virgin state does not coincide with that observed when the snow is already stressed. Generally speaking the rheological property of snow is remarkably influenced by the compressive force which has been applied and by the way in which it has been applied as shown by the following example. The compressive pressure $w$ acting on a pillar of snow was varied step by step at the time points A, B, C, ····· in such a way as indicated by the angular figure shown in Fig. 12(a). The curve in Fig. 12(b) shows schematically the course of change in the strain $e$ caused by $w$, the snow being now regarded as represented by a single Maxwell model for the sake of simplicity. Let the abrupt change in $e$ indicated by the length of vertical segments in Fig. 12(b) be denoted by $\Delta e$. Then the varia-

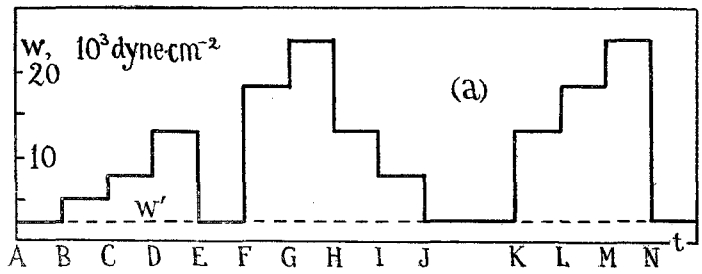


Fig. 12 (a) Compressive pressure $w$ acting on the pillar of snow is changed step by step as shown in this figure. $w'$ is compressive pressure exerted by dead weight which cannot be eliminated in the case of the present experiments.

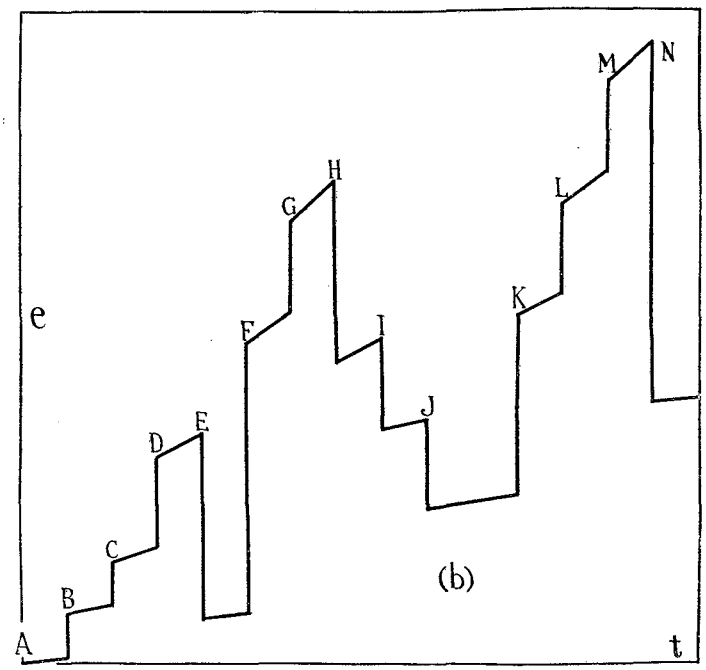


Fig. 12 (b) Schematic representation of strain $e$ produced in the pillar of snow by the compressive pressure shown in figure 12 (a).

tion $\Delta w$ in $w$ which is the same as the length of vertical segments in Fig. 12(a) yields, when divided by $\Delta e$, the elastic constant $E_M$ of the snow. This is not confined only to the cases of positive values of $\Delta w$ and of $\Delta e$ at such time points as B, C, D, but it applies also to the cases of negative $\Delta w$ and $\Delta e$ as at the time points E, H, I. The small circles in Fig. 12(c) represent the values of $\Delta w$ and $\Delta e$ observed at the time points indicated by the annexed capital letters. If straight lines are drawn from the origin towards the circles

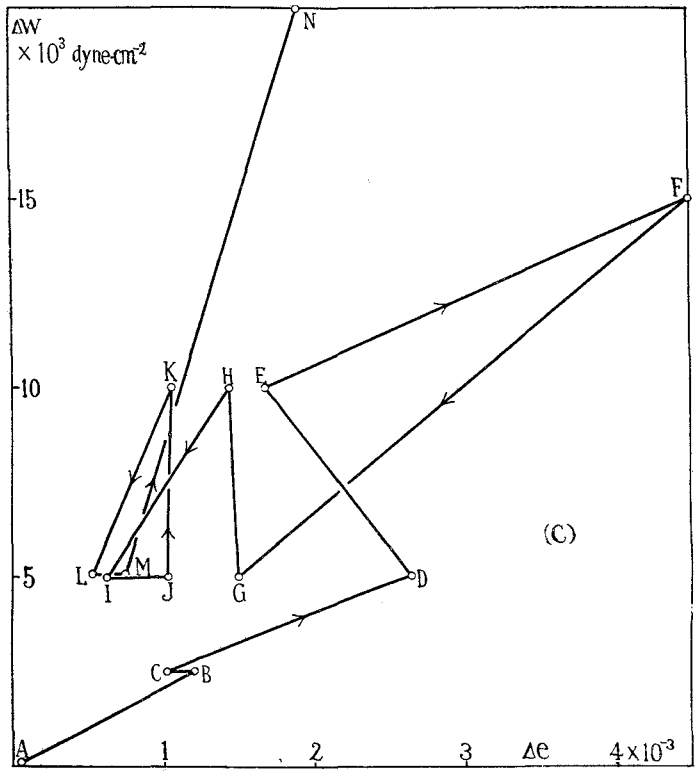


**Fig. 12** (c) $\Delta w$: magnitude of stepwise change in $w$ at time points indicated by the capital letters in figure 12 (a). $\Delta e$: instantaneous change in strain produced by $\Delta w$.

the tangent of their slope angle $\alpha$ is equal to the elastic constant $E_M$ and therefore, if $E_M$ were the real characteristic constant not dependent on the compressive pressure exerted on the snow in the past, all the circles would have to lie on a straight line passing through the origin. But the actual case is wholly contrary to this as shown in the figure. The slope angle $\alpha$, therefore the elastic constant $E_M$, tends to increrse as the time of application of compressive pressure is elongated although decrease in $\alpha$ instead of increase is found exceptionally in the cases of transfers such as from E to F, from I to J and from L to M.

The viscous constant $\eta_M$ too is not unrelated with the previous stress. In Fig. 12(d) the time rate of change $\dot{e}$ of the strain is plotted against the compressive pressure $w$ shown in Fig. 12(a) for each time interval during which $w$ is kept constant. The capital letter attached to the circle in the figure shows the time interval following the time point indicated by that letter, for example, the circle marked G belongs to the time interval from time point G

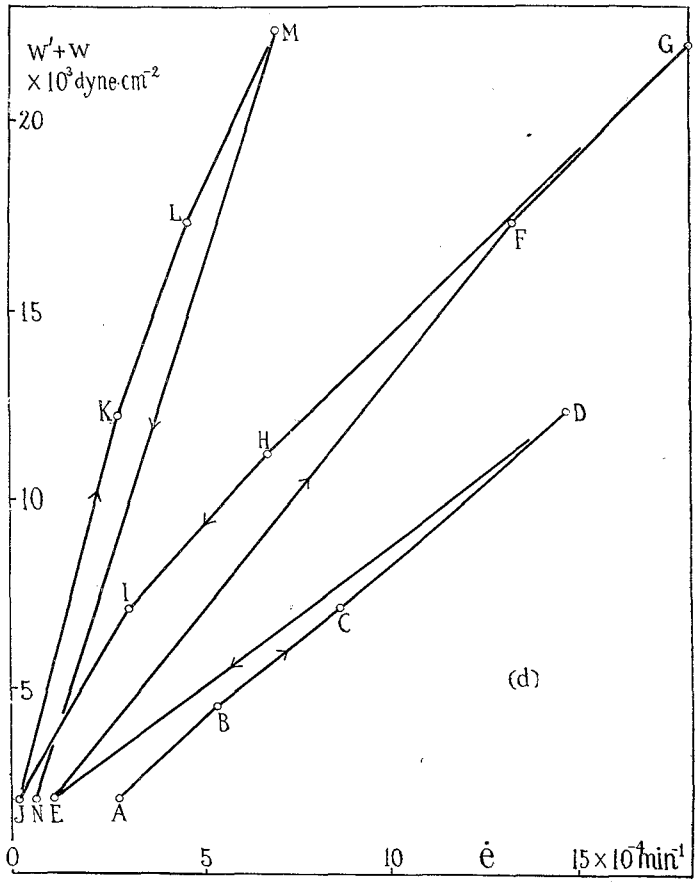


Fig. 12 (d) $\dot{e}$: time rate of change in strain $e$ in the time interval during which the compressive pressure $w'+w$ is kept constant. Capital letter attached to the small circle in this figure shows the beginning time point of the time interval.

to time point H. The tangent of the slope angle of the straight lines drawn from the origin towards the circle gives the viscous constant $\eta_M$. $\eta_M$ is the same as $E_M$ in that $\eta_M$ shows the tendency to increase with the increase of the time of application of the previous stress, but its influence appears here to be simpler than in the case of $E_M$. The circles in Fig. 12(d) can be divided into three groups in each of which the circles are distributed nearly along a straight line passing through the origin. Setting aside the continually acting compressive pressure $w'$ due to the dead weight, the compressive pressure $w$ was applied, as shown in Fig. 12(a), in three intermittent intervals B~E, F~J, K~N and to each of these intervals corresponds each of the groups of circles shown in Fig. 12(d). Therefore it can be said that $\eta_M$ is maintained at almost constant

value so long as the application of compressive pressure is not interrupted and that the interruption effects a discontinuous increase in the value of $\eta_M$. The curves shown in Fig. 6 were obtained by increasing step by step the compressive pressure on snow in the virgin state and therefore correspond to the ascending part ABCD of the first branch of the curve shown in Fig. 12(d). De Quervain, in his torsion experiments on snow, changed step by step the torsional moment acting on the snow cylinder between the extreme values $-P_0$ and $+P_0$ and found that the relation between the torsional moment and the time rate of change in strain could be represented by a narrow hysteresis loop (1). Each of the branches of the curve shown in Fig. 12(d) is similar in form to one half of de Quervain's hysteresis loop.

In order that the discontinuous increase in $\eta_M$ is to be effected, it is necessary that the time of interruption of the compressive pressure amounts at least to several minutes. When the time of interruption was reduced to several seconds no effect was observed and the change in $\dot{e}$ was the same as that which would have been observed if $w$ were changed without interruption. The retardation time $\tau_2$ is of the order of magnitude of one minute as stated in the previous article (*c*), which shows that several minutes are needed for the strain due to retarded elasticity to be completely recovered. It is therefore supposed that the discontinuous increase in $\eta_M$ would have some bearing on the process of the retarded elasticity.

(*e*) *Some notes on the present experiments.*

(*i*) If the iron plates $P_1$ and $P_2$ shown in Fig. 1 were merely attached to the end planes of the snow pillar, the plates did not touch the end planes with their whole surface with the result that the snow pillar was stressed unevenly in the neighbourhood of its ends. Such an uneven distribution of stress clearly causes an error in the measurement of strain. It was for the purpose of avoiding such an end effect that the iron plates were frozen to the ends of the snow pillar as explained in the previous section. In order to learn whether the end effect could be eliminated or not in such a way, $E_M$ and $\eta_M$ were measured on two pillars of snow of the same nature but of different lengths. If the end effect was wholly eliminated the results should be the same in both of the two cases. The results of experiments made on snow pillars 7.5 cm and 15 cm long are shown in Table 1. Agreement of the results is good in

TABLE 1

| Length of the pillar (cm) | $E_M$ ($10^7$ dyne/cm$^2$) | | | $\eta_M$ ($10^7$ dyne·min/cm$^2$) | | |
|---|---|---|---|---|---|---|
| 7.5 | 1.5 | 1.5 | 3.2 | 2.4 | 2.8 | 14 |
| 15.0 | 1.4 | 1.1 | 3.2 | 2.1 | 1.7 | 17 |
| Density of snow (gr/cm$^3$) | 0.21 | 0.22 | 0.25 | 0.21 | 0.22 | 0.25 |

the case of large snow density 0.25 while there are some differences in the cases of smaller snow density. These differences may be partly due to incomplete elimination of the end effect, but they may be mostly attributed to an uncontrollable change caused in the fragile structure of snow of smaller density by such treatments as cutting or as freezing the iron plate to the snow pillar before the experiments were begun.

(*ii*) The snow pillars used in most cases of experiments were those which were cut out in the horizontal direction from the snow layers composing snow cover. Since the snow layers are being loaded in the vertical direction under the natural conditions their properties may not be the same in both the horizontal and the vertical directions. Two pillars cut out from the same snow layer of large thickness, one vertically and the other horizontally, gave the results shown in Table 2. Although the values of $E_M$ and $\eta_M$ obtained on the vertically cut pillar and the horizontally cut one are not the same, small difference between them indicates that snow layers are at least nearly isotropic in their rheological properties.

TABLE 2

| | $E_M$ (dyne/cm$^2$) | | $\eta_M$ (dyne·min/cm$^2$) | |
|---|---|---|---|---|
| Density of snow | 0.21 | 0.23 | 0.21 | 0.23 |
| Vertical | 1.6 | 2.2 | 2.1 | 7.0 |
| Horizontal | 1.5 | 2.3 | 2.4 | 7.6 |

## §3 Viscous compression of snow layers composing snow cover.

The viscous compression of snow by the creep phenomenon described in the preceding two sections was the compression taking place within an observation time not longer than 10 minutes or thereabouts. When the compressive pressure was left to act on the snow pillar for hours instead of having been removed soon after its application, it was observed that the rate of shortening of the pillar came gradually to diminish. This is in accord with Glen's observation on ice extending over several tens of hours showing gradual decrease of time rate of change in the strain of ice (8). Since, however, it was difficult to make a long run observation lasting for hours or days employing the methods described above, the rate of compression of snow layers composing snow cover was studied by the present authors for a long time as they were loaded by their own weights (9). If the thickness of the $i$-th layer is denoted by $h_i$ and the density of snow composing that layer is denoted by $\rho_i$, the rate of change in strain $\dot{e}_i$ of the $i$-th layer can be expressed by

$$(-dh_i/dt)/h_i \quad \text{or} \quad (d\rho_i/dt)/\rho_i,$$

provided that the mass of snow composing the $i$-th layer is kept unchanged.

The compressive pressure acting on that layer is given by

$$w_i = \tfrac{1}{2}\rho_i h_i + \sum \rho_j h_j,$$

where $\rho_j$'s, $h_j$'s are the density and thickness of the layers lying above the $i$-th layer respectively. Hence the viscous constant

$$\eta_i = w_i / \dot{e}_i$$

of snow composing the $i$-th layer can be determined if $\rho$ and $h$ are observed for a long time on every layer of the snow cover. In this case, however, the snow layer is not only acted on by the compressive pressure but it undergoes a metamorphosis which would proceed even if there were no compressive pressure. Therefore the viscous constant here cannot be regarded in the strict sense as of the same nature as the viscous constant $\eta_1 (= \eta_M)$ of the previous section.

In the snow cover on the flat ground near the building of the Institute a hole was made and the stratified structure of the snow cover was disclosed on its wall as shown in Fig. 13. The snow layer between two adjacent dark lines looking uniform in its appearance belonged to one snow fall which had taken place in the past. The date of that snow fall read on the register of snow falls in the past gave the time $t$ which had passed since the formation of the snow layer. The wall of hole was advanced inwards into the snow cover every five or six days by cutting off more than 50 cm thickness of snow forming the wall and the density $\rho$ of snow and the thickness $h$ were observed accurately on each of the snow layers. Commonly the boundary of two snow layers deposited on two different snow falls with an interval of a few days between them is not very distinct, accordingly coloured water is often sprayed on the wall of snow to make the boundary manifest itself clearly. But in the present case no such procedure was needed

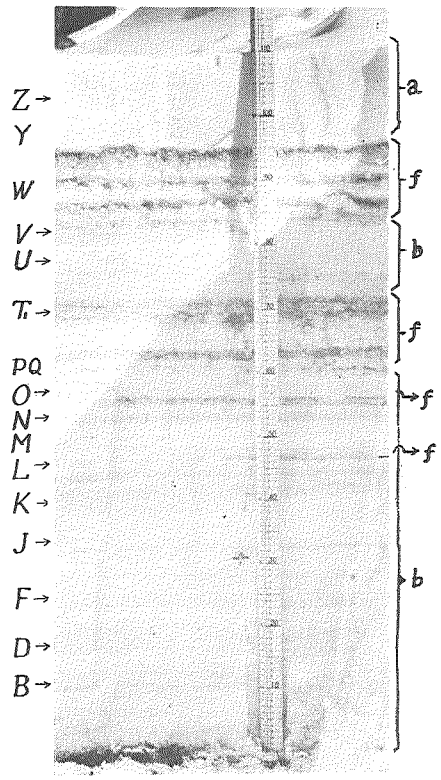


Fig. 13 The wall of hole made in the snow cover (March 4th, 1955).

because soot particles coming from the university smoke-stacks deposited on the snow surface during the interval between snow falls to make the boundaries of snow layers appear distinctly dark. The density $\rho$ of snow was determined by weighing a sample of snow 30.0 mm thick, 58.0 mm wide and 70.0 mm long taken out from snow layer by thrusting the sampler into the wall of the hole.

The temperature of snow observed at various heights above ground by inserting a thin alcohol thermometer into the wall of the hole was found rarely to be lower than $-6°C$, being almost in all cases higher than $-3°C$ in the lower half of the snow cover. The temperature influences the viscous constant as shown in the previous section. But in the following study the influence of change in temperature on viscous constant of snow will be left out of consideration, since the change of temperature was confined within a narrow range below 0°C as noted above.

The positions of the boundaries of snow layers are shown in Fig. 14 against the dates from 25th Dec. 1954 to 31st March 1955. The layers are

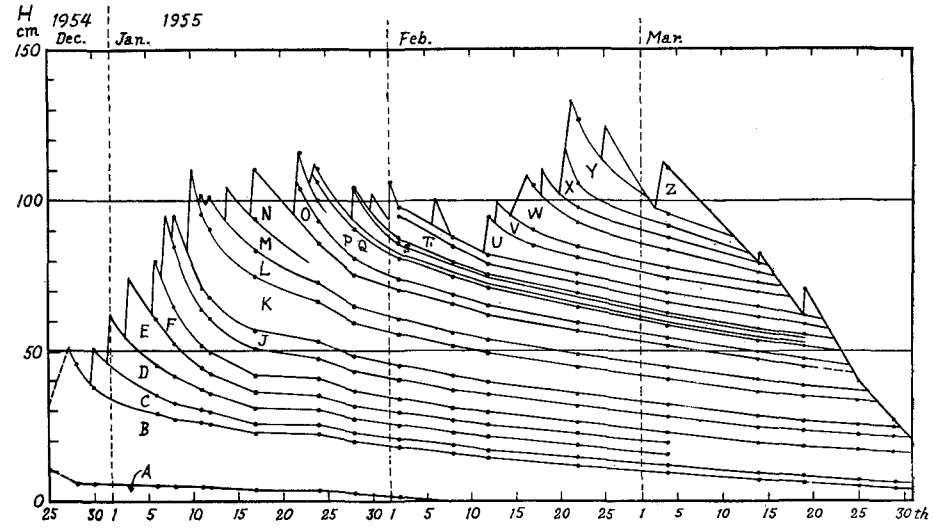


**Fig. 14** Snow layers composing snow cover.

labeled A, B, C,····· beginning at the lowest layer. Fig. 15 is the mass diagram of the snow layers; the mass $m$ of snow per horizontal square centimeter belonging to a snow layer is represented by the width of zone marked with the letter of that layer. Of course $m$ is equal to the prod ct of the height of layer and the density of snow. From this diagram the compressive pressure $w$ acting on any layer at any time can be read at once.

The zones lying below zone PQ seem to keep their width, that is their mass $m_i$, constant up to a short time before their disappearance, except layers A and B of which the lower parts are cut off by the line representing the

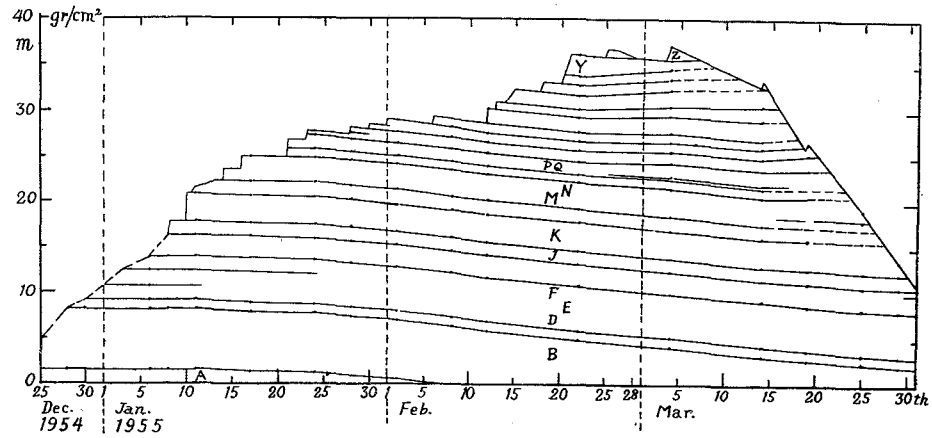


Fig. 15 Diagram of mass of snow cover. The mass $m$ of snow composing a snow layer shown in Fig. 14 is equal to the width of the zone of this figure identified by the same letter as the snow layer.

ground surface, being melted and absorbed by soil. Of course the actual values of the product $m_i=\rho_i h_i$ computed from $\rho_i$ and $h_i$ observed on different days did not completely coincide with each other, which was expected when the errors of measurement were taken into consideration. But the fact that the width of each of the zones looks unchanged so far as they appear in the figure may be taken for an evidence that the mass $m_i$ actually remained constant in each of the layers.

As shown in §2 of Number I of this series of papers previously published, the density of the snow composing the snow cover changes owing to tranfer of water vapour through the snow caused by temperature gradient existing in it. Obviously such a change in density brings about a change in the mass $m_i$ of the snow layer. But the change in density due to this cause cannot be expected to exceed 0.001 gr/cm³ during a month as will be seen from the data given in §2 of Number I. This amount of change in density is negligibly small in comparison with the actually observed change in density of the snow layers. Therefore there can be considered no reason for any great change in the value of $m_i$ except the thawing of snow. Zone Y became narrower with the lapse of time as shown in Fig. 15, which must have been due to thawing of layer Y. Although each of the zones lying below zone Y began to thicken more or less some days before it disappeared by absorption of thaw water coming from above, the zones lying below zone PQ seem to have been subjected to no such influence at least up to the middle of March.

The rate of change in strain $\dot{e}_i$ of a snow layer is primarily given by

$$\dot{e}_i=-(dh_i/dt)/h_i,$$

and it can be replaced, as noted above, by

$$\dot{e}_i = (d\rho_i\ dt)/\rho_i,$$

provided that $m_i = \rho_i h_i$ is kept constant. But, as a matter of fact, $h_i$ cannot be measured with sufficient accuracy for $\dot{e}_i$ to be computed from it, because the boundaries of snow layers are generally not so sharply defined as to permit such accurate observation. On the other hand, the density $\rho_i$ can be determined with considerable accuracy. Hence the determination of the viscous constant was confined to layers B, F, J, K, MN (two layers M and N distinguished at first gradually fused into one layer) and O for the period during which their mass $m_i$ remained constant, that is, up to the middle of March.

In Fig. 16 the density $\rho_i$ of snow composing the above six layers is plotted against the lapse of time $t$ counted from the day after the one when the layer

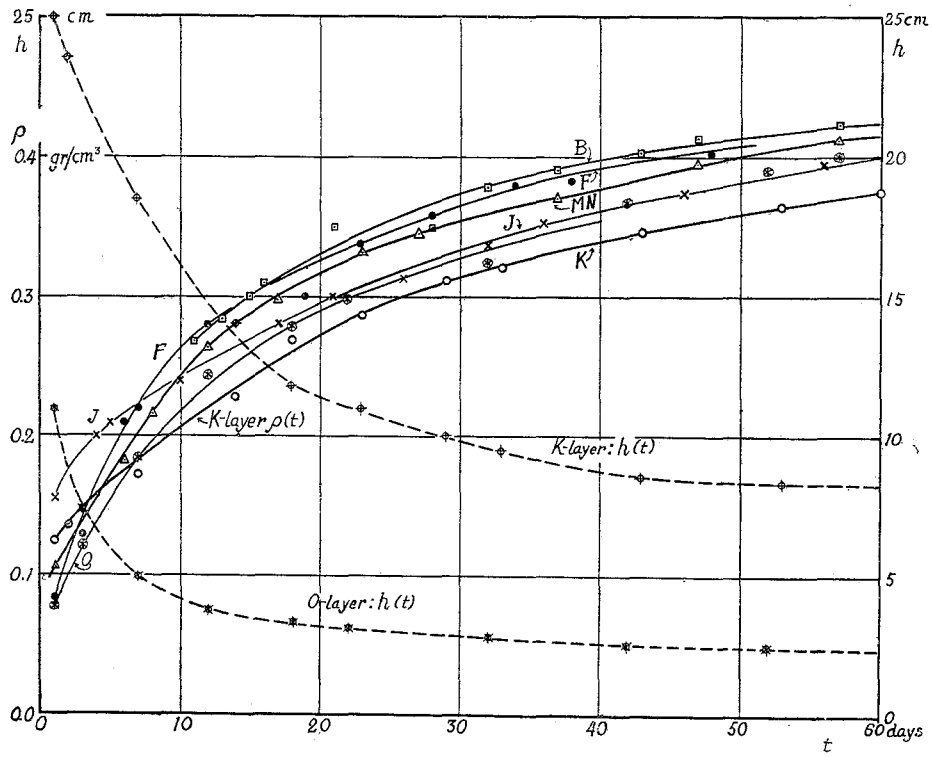


Fig. 16 The density $\rho$ of snow layer is plotted against $t$, the number of days elapsed since that layer was deposited. The height $h$ of snow layer is also plotted for two snow layers K and O.

was deposited. Thickness $h_i$ of snow layer too is plotted for two layers K and O. From the smooth curves drawn in such a way that they pass the observation points as near as possible the change $\Delta\rho_i$ in the density taking place during one day was determined. Then the time rate of change in the strain $\dot{e}_i$ could be given by

$$\dot{e}_i = (\Delta\rho_i/\Delta t)/\rho_i ,$$

where $\Delta t$ means time interval equal to one day. It should be noticed that the value of $\rho_i$ in the denominator of the above formula is not the initial one at $t=0$ but the current value which the density showed on the day of determination of $\Delta\rho_i$. Therefore the above formula can be replaced by

$$\dot{e}_i = \Delta(\log_e \rho_i)/\Delta t.$$

In the case of experiments described in the preceding two sections of this paper it was of no importance whether the initial or current value was used for determining the value of strain $e$, since the difference between the two was very small owing to the short period of observation. But, in the long time of observation of the present case, the current value departed much from the initial one and here the strain $e_i$ was computed after Hencky's definition which uses the current value instead of the initial one (10).

Fig. 17 shows how the viscous constant $\eta$ of snow increases as time goes on. $\eta$ is shown in logarithmic scale by the unit of gr-wt·day/cm$^2$. Fig. 11(a) of the previous section shows the relation between snow density and the reciprocal value $1/\eta$ of viscous constant determined experimentally at temperatures higher than $-3$°C. From that figure it is indicated that the value of $1/\eta$ is $1\times10^{-7}$ cm$^2$/min·dyne or more for the snow having density 0.15 or less, which densities the snow layers concerned here must have had at $t=0$, that

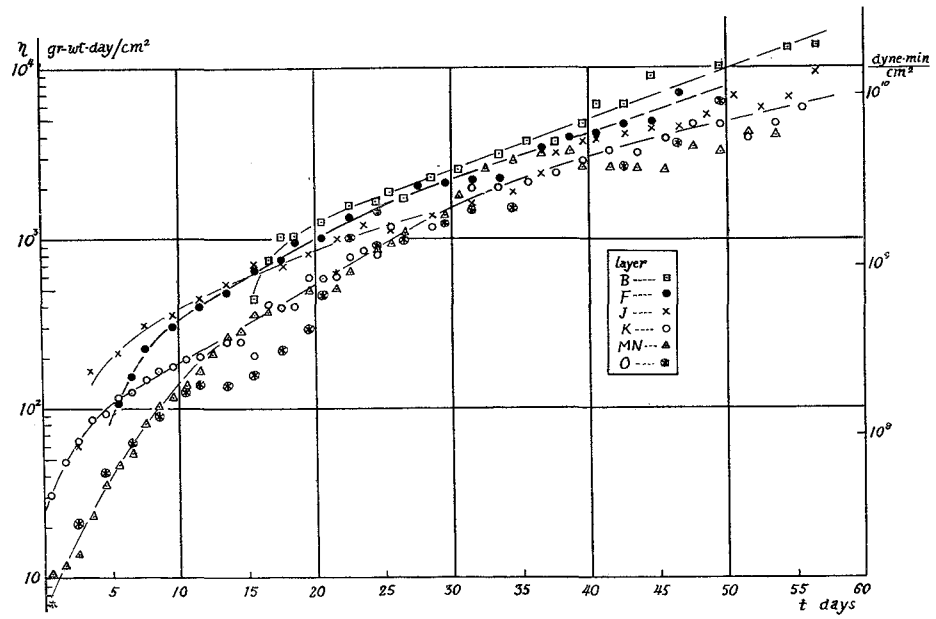


**Fig. 17** Compressive viscous constant $\eta$ versus number of days $t$.

is, on the next day after their formation. $1/\eta = 1 \times 10^{-7}$ cm$^2$/min·dyne gives $\eta = 7$ gr-wt·day/cm$^2$, while Fig. 17 shows that $\eta$ observed on the snow layers lies in the range from 7 to 13 gr-wt·day/cm$^2$ at $t=0$, which is an indication of a good accord between the result of previous experiments and that of observations made on the actual natural snow layers.

As was noted in §1, the conditions under which snow was positioned was not the same in both the cases of experiments on snow pillar and of observations on snow layer. In the former case the snow was free to expand laterally perpendicular to the direction of the compressive pressure, while in the latter case such a lateral expansion was completely prevented. Haefeli made an experiment in which he compressed two pillars of snow with the same pressure, lateral expansion being allowed in one case and prevented in the other (2). He found that the pillar with free side surface was contracted about 10% more than that with prevented surface. Although this is only a single example it may be considered to prove that the difference produced in the value of viscous constant due to whether lateral expansion of snow is allowed or not will be not very great.

Since the snow crystals deposited to form the snow layers were not the same for each of the six it is not strange that the curves shown in Fig. 17 do not coincide with each other. Indeed the snow crystals which fell to form snow layers K and N were very different from each other as shown by the two series of microphotographs in Fig. 18, Pl. I at the end of this book showing metamorphosis of snow crystals in the respective snow layers. The figure annexed to each of the photographs indicates the number of days after the snow layer was deposited. The uppermost two photographs of the snow crystals which were taken one or two days after they had fallen to the ground show still clearly their initial forms. In the case of snow layer K the crystals were composed of thick broad leaves, while in the case of snow layer N they were ordinary dendritic crystals on which many cloud droplets had been attached. Up to about twenty days after the formation of snow layers the mode of metamorphosis was somewhat different in the two cases as shown by the photographs, but thereafter the two snow layers seem to have followed the same course of metamorphosis. The snow crystals of snow layer K were the strongest in structure among all snow crystals which were deposited to form the snow layers observed in the present research. As will be shown below in Fig. 19, the viscous constant $\eta$ of snow layer K was the largest at first while it descended to the smallest after a long time, which must have been the result of the very strong structure of the crystals which formed this snow layer. The more a snow layer contracts, the larger its viscous constant becomes. The strong structure of the snow crystals composing layer K seems to have kept it from contracting at the same rate as the other snow layers with the result that it was delayed in enlarging its viscous constant.

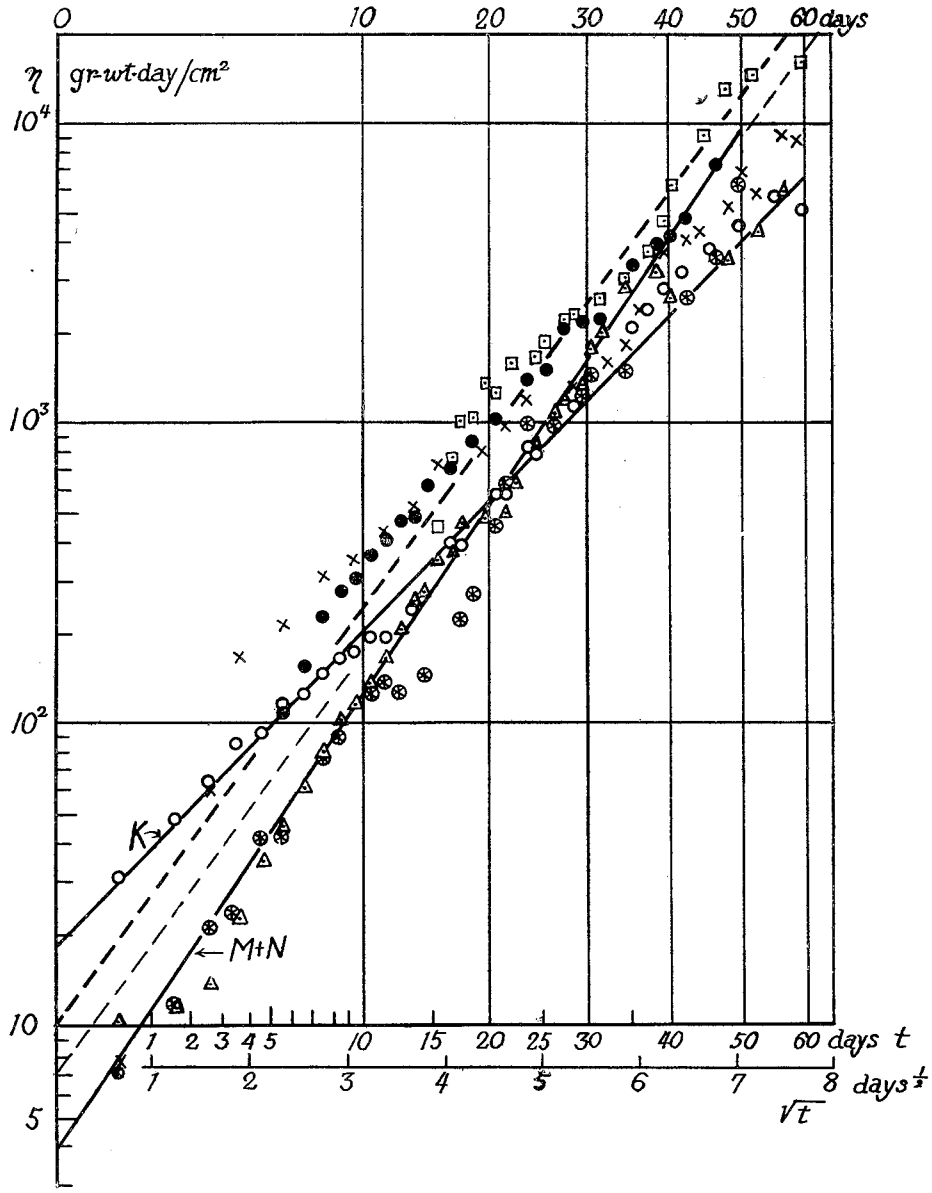


**Fig. 19** $log_{10}\ \eta$ versus $\sqrt{t}$.

But the departures between the curves of Fig. 17 are not very large and one can say generally that the viscous constant of snow layer increases in such a way that it is of the order of magnitude $10^1$ gr-wt·day/cm² in the first week after the formation of the snow layer, $10^2$ gr-wt·day/cm² in the second week, $10^3$ gr-wt·day/cm² in the following four weeks and $10^4$ gr-wt·day/cm² thereafter.

When $log_{10}\eta$ is plotted against the square root of $t$ the points representing the values observed on one snow layer are arranged along a straight line as shown in Fig. 19. Hence the relation between $\eta$ and $t$ can be expressed by

$$\eta=\eta_0 \, exp\,(a\sqrt{t}),$$

and the numerical calculation of $\eta_0$ and $a$ from the position and the slope of the straight lines shows that $\eta_0$ and $a$ are in the ranges 3.9~18.0 gr-wt·day/cm$^2$ and 0.75~1.10 day$^{-\frac{1}{2}}$ respectively. Therefore, as an average value, $\eta$ can be given by

$$\eta=10 \, exp\,\sqrt{t} \text{ gr-wt·day/cm}^2,$$

where $t$ should be counted by days.

Not only the viscous constant $\eta$ but also the density $\rho$ of snow increases with the time $t$ and there can be found a linear relation between $log_{10}\eta$ and $\rho$ as shown by the straight lines of Fig. 20, each of them corresponding to one of the six snow layers on which the observations were made. Then $\eta$ is given by the following mathematical function of $\rho$:

$$\eta=\eta_0' \, exp\,(b\rho)\,.$$

From the fact that all the straight lines in Fig. 20 are parallel to each other the constant $b$ in the above formula turns out to be of the same magnitude for all of the snow layers. The numerical value of $b$ is found to be 21.0 cm$^3$/gr. $\eta_0'$ is 2.2 gr-wt·day/cm$^2$ for snow layer K and 0.81 gr-wt·day/cm$^2$ for snow layer MN; for the other snow layers it takes values between these two. Then the average formula expressing the dependency of $\eta$ on $\rho$ is given by

$$\eta=1.5 \, exp\,(21\rho) \text{ gr-wt·day/cm}^2\,. \qquad (1)$$

In article (*c*) of the previous section another average relation holding at temperature higher than $-3$°C:

$$1/\eta=(2-6.5\rho)\times10^{-7} \text{ cm}^2/\text{dyne·min}$$

was given which is equivalent to

$$\eta=10/(2.88-9.4\rho) \text{ gr-wt·day/cm}^2\,. \qquad (2)$$

$\eta$ in formula (2) is viscous constant in the initial stage of creep while in formula (1) $\eta$ means viscous constant in the next stage of creep extending over many weeks. But there is another difference between those two average formulae, namely, that formula (1) is the average of relations between $\eta$ and $\rho$ each of which is determined on one and the same snow layer while formula (2) is based on data obtained on many snow samples which are taken at random from different snow layers composing snow cover.

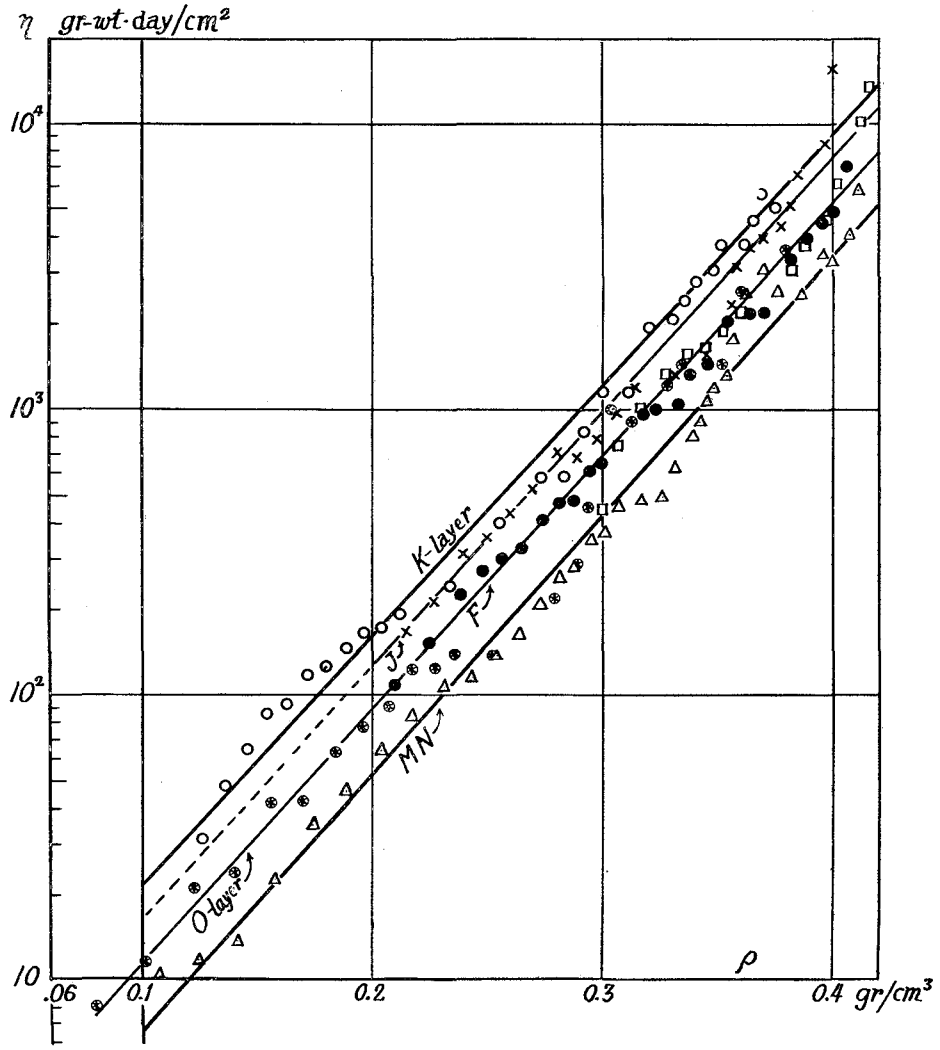


Fig. 20 $log_{10}\eta$ versus density $\rho$ of snow.

Change in thickness $h$ of a snow layer with time $t$ has heretofore been formulated by several researchers, for example, R. Saito gave the following formula for snow deposited in Sapporo (11):

$$h/h_0=0.09/\{0.34-0.25\,exp\,(-0.067t)\}, \qquad (3)$$

and K. Ishiwara, from the observational data on snow deposited on the north side of the main mountain-range of Honshu, derived the formula (12):

$$h/h_0=1-\{t/(2.23+1.13t)\}. \qquad (4)$$

In both the formulae $h_0$ is the value of $h$ at $t=0$ and $t$ should be counted

by days. They are average formulae derived from observations on many snow layers. It is noted that the above two formulae are purely empirical ones. Saito and Ishiwara seem to be of the opinion that the thickness of snow layer is decreased by the action of its metamorphosis, which is the reason why no term respecting compressive pressure is present in their formulae. But it is incomprehensible to the present authors that the metamorphosis of snow itself can exert a force to contract snow provided that no liquid water takes part in the metamorphosis. So far as the metamorphosis takes place by the sublimation process alone, without being acted on by any mechanical force, the space occupied by a mass of snow will undergo no change as a whole, even if the ice particles composing it can be rearranged microscopically in their distribution, since from the macroscopic stand point the evaporation and condensation of water vapour are taking place uniformly throughout the snow mass. As shown on p. 53 and on Pl. XIII of the first paper of the present series the temprature gradient existing in the interior of snow can cause the movement of the ice particles composing it, but the movement is nearly the same on each of the particles shifting the space occupied by them as a whole with no change in its volume.

Surface tension of ice may be a cause of the contraction of snow layer. Let an ice cylinder of radius $a$ be considered. The surface tension $\alpha$ of ice strives to contract the cylinder with a force $2\pi a\alpha$ and there appears a compressive pressure $2\pi a\alpha/\pi a^2=2\alpha/a$ in its interior. Hence, if the viscous constant of ice is denoted by $\eta_i$, the cylinder will contract by $2\alpha/a\eta_i$ per unit time and per unit length of it. The ice bonds connecting the ice grains in snow should be undergoing such a contraction that the snow contracts as a whole. But the numerical calculation shows that the contraction of this sort would become appreciable only when the ice bonds were so thin that their diameters are of the order of magnitude 0.01 mm.

If the weight per horizontal unit area of snow layers on top of the snow layer concerned is $w$, there holds the following differential equation between $w$ and the thickness $h$ of that layer:

$$\dot{e}=-\frac{1}{h}\frac{dh}{dt}=\frac{w}{\eta}. \qquad (5)$$

The viscous constant $\eta$ and the number of days $t$ counted from the day after the formation of the snow layer are, as described above, connected by the function:

$$\eta=\eta_0 \exp(a\sqrt{t}). \qquad (6)$$

Hence, if the weight $w$ can be expressed as a function $f(t)$ of $t$, integration of the above differential equation yields the relation:

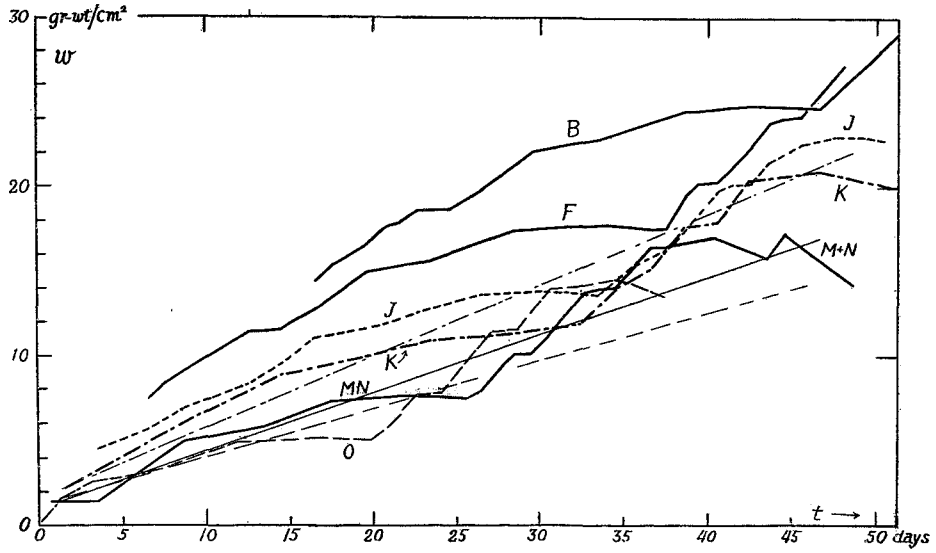


**Fig. 21** Compressive pressure $w$ exerted on a snow layer by the snow layers lying above it.

$$h/h_0 = -\int_0^t f(t)\, exp\,(-a\sqrt{t})/\eta_0 dt\,, \qquad (7)$$

by which $h/h_0$ can be computed. Fig. 21 shows $w$ acting on each of the six snow layers B, F, etc. calculated from the mass-diagram of Fig. 15. The mode of change in $w$ with time $t$ is not very simple, but, in the cases of snow layers K, MN, O, $w$ seems to increase nearly in proportion to $t$ and curves $w$ versus $t$ will be roughly represented by the thin straight lines shown in the figure. Then, if $f(t)$ is put in the form:

$$f(t) = A + Bt\,,$$

the above equation yields

$$\frac{h}{h_0} = \frac{2}{\eta_0 a}[a^2A + 6B - e^{-a\sqrt{t}}\{a^2A(a\sqrt{t}+1) + B(a^3\sqrt{t^3} + 3a^2t + 6a\sqrt{t} + 6)\}]. \qquad (8)$$

The three thick curves in Fig. 22 show $h/h_0$ calculated by the above formula using for the constants $a$, $A$, $B$, $\eta_0$ the figures listed in the following table which were determined by actual measurements on the three snow layers concerned.

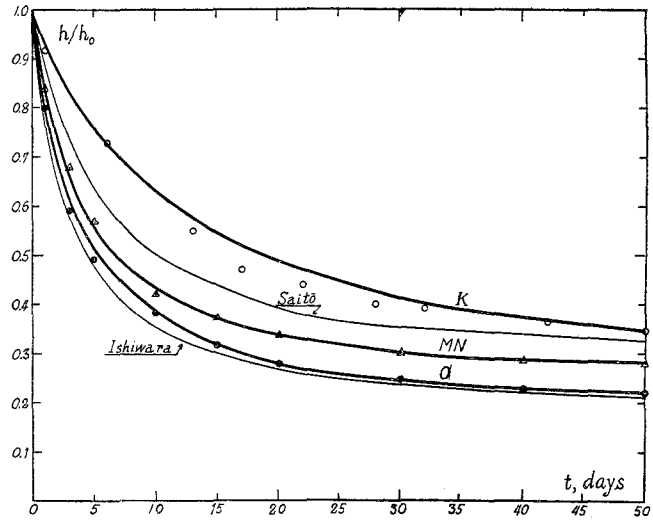


Fig. 22 Computed curves of the height $h$ of snow layer. $h$ is expressed by the ratio to its initial value $h_0$.

| Snow layer | $A$ (gr-wt/cm$^2$) | $B$ (gr-wt/cm$^2$·day) | $\eta_0$ (gr-wt·day/cm$^2$) | $a$ (day$^{-\frac{1}{2}}$) |
|---|---|---|---|---|
| K | 2.0 | 0.42 | 2.02 | 0.75 |
| MN | 1.4 | 0.34 | 0.44 | 1.10 |
| O | 1.5 | 0.28 | 0.43 | 1.02 |

Agreement between the computed curves and the observed values which are indicated by small marks is good, especially in the cases of snow layers MN and O. Curves calculated by formulae (3), (4) of Saito and Ishiwara are also drawn in the figure. If the average is taken on the three thick curves, it will lie near the curve of Saito who derived his formula from observations on snow in Sapporo. Since the snow layers on which the present authors made observations were also those deposited, though in a different winter, in Sapporo, such an agreement between the result of Saito and that of the present authors raises the validity of Saito's formula for representing the average course of change in the thickness of snow layers composing snow cover in Sapporo.

## § 4 The visco-elastic constants in the case of lateral vibration of snow bar.

The snow was subjected to slow change in strain in the experiments which have hitherto been described. In this section there will be reported a study of the visco-elastic properties of snow as shown in response to rapidly changing

strains incident to vibration. One of the present authors and K. Yamaji experimented by making a bar of snow vibrate laterally in the cold room of the Institute (13).

A bar of snow (20~30 cm long, 2~4 cm thick and wide) was suspended horizontally by two loops of string at two nodes of vibration as shown in Fig. 23. Two thin iron plates $I_1$, $I_2$ (0.2 mm thick, 0.8 mm wide, 10 mm long)

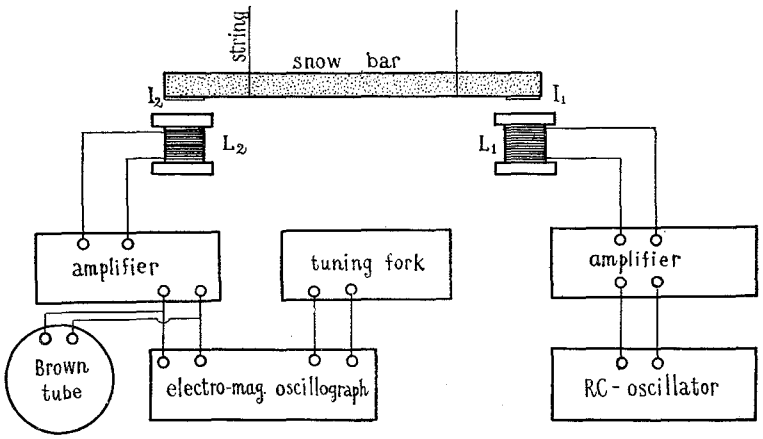


Fig. 23 Equipment for vibrational experiments on snow bar.

were frozen to the snow bar near its ends on the bottom surface. Electromagnets $L_1$, $L_2$ were placed opposite to and 5 mm distant from the iron plates. Electromagnet $L_1$ which was excited by an oscillating electric current coming from the RC-oscillator through the amplifier periodically pulled the iron plate $I_1$ with the result that the snow bar was set in vibration. Iron plate $I_2$ which was now in vibrational motion induced in electromagnet $L_2$ an oscillating electric current which increased or decreased in proportion to the amplitude of vibration of the snow bar. Hence the amplitude of the vibration could be determined by observing through the Brown-tube or registering through the electromagnetic oscillograph the induced current which was magnified by the amplifier. The vibration of the snow bar caused in this way was lateral in its character, that is, the bar was bent upwards and downwards alternately. If the snow bar were supposed to be composed of horizontal thin layers of snow placed one upon another, each of them was subjected to an elongation and a contraction in one period of vibration. Hence the strain to which the snow was subjected in this case is essentially the same sort of strain as treated in the previous sections.

Generally the vibration of the snow bar was very slight. But when the frequency of the RC-ocillator was made to approach a frequency lying in the range from 200 to 300 cycles/sec, the amplitude of vibration began to increase. The amplitude attained a maximum point at a value $f$ of the frequency to

decrease thereafter with the further increase of the frequency. Such a course of change in the amplitude of vibration could be observed by the Brown-tube shown in Fig. 23. The vibration of maximum amplitude at frequency $f$ is obviously the resonance vibration. It was observed with a microscope that the bar of snow was most violently vibrating at its centre, with two nodes of vibration near the ends. Therefore the observed resonance vibration must be that of the fundamental mode.

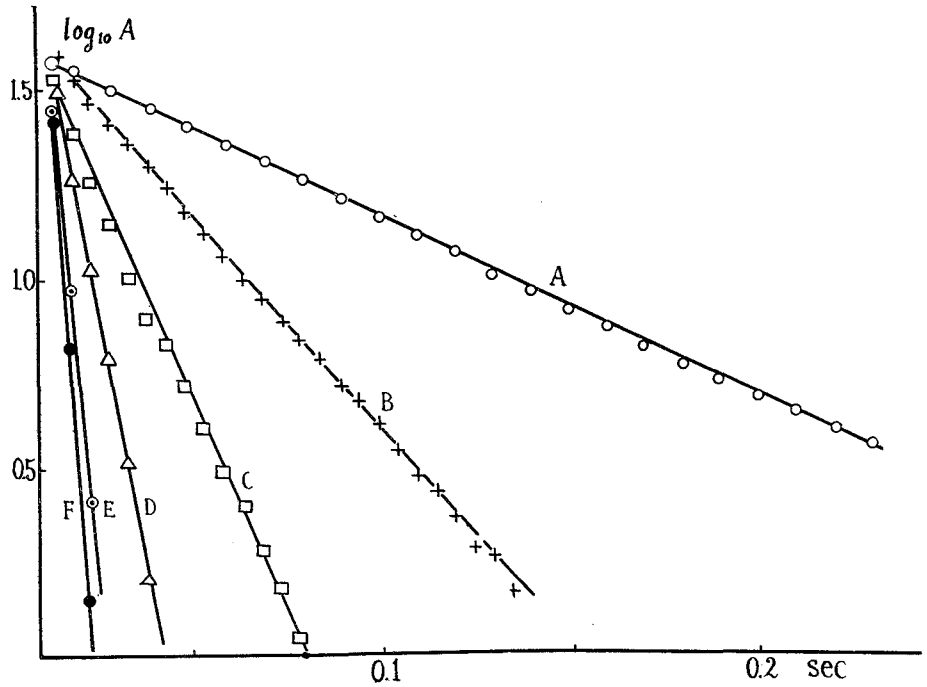


Fig. 25 Logarithm of amplitude $A$ of vibration is diminished linearly with time after the electric current exciting the vibration of snow bar is cut off. Density of snow: 0.33. A: −40°C, B: −30°C, C: −22°C, D: −15°C, E: −10°C, F: −2°C.

When the electric current from the RC-oscillator exciting the resonance vibration in the snow bar was cut off, the vibration began to attenuate as shown in the photographs of Fig. 24, Pl. II at the end of this book. These photographs are reproductions of records registered by the electromagnetic oscillograph. They are taken on one and the same sample of snow of density 0.33 at different temperatures ranging from −3°C to −37°C. The photographs show that the vibration attenuated in a very regular manner at each temperature and indeed it is found that the attenuation is almost perfectly exponential. Fig. 25 shows the relation between the logarithm of the amplitude $A$ of vibration and the time $t$ counted from the cut off of the

exciting electric current. The good linearity between $log_{10} A$ and $t$ shows the exponential attenuation.

Let the work $q$ expressed by

$$q=(Ee+Y\dot{e})\dot{e} \qquad (1)$$

be done in a unit time to a unit volume of a substance when its strain $e$ is being changed at the rate $\dot{e}$. Here $E$ and $Y$ are constants; $E$ is a constant respecting the elasticity of the substance while $Y$ is a constant respecting its internal friction. Then the vibration taking place in such a substance undergoes exponential attenuation after the periodic force which has been applied to the substance to maintain the vibration is cut off. In the case of the lateral vibration of a rectangular bar the amplitude $A$ of vibration attenuates according to the formula

$$A=A_0 e^{-\lambda t} \sin 2\pi f t\,, \qquad (2)$$

where $\lambda$ and $2\pi f$ can be expressed by

$$\lambda=\frac{1}{2K}Y \qquad (3)$$

$$(2\pi f)^2=\frac{1}{K}E-\lambda^2 \qquad (4)$$

$$K=12l^4\rho/m^4b^2\,. \qquad (5)$$

Here $\rho$, $l$, $b$ are the density, the length and the thickness of the vibrating bar respectively while $m$ is a numerical constant characteristic to the mode of vibration. $f$ is the resonance frequency. $m$ is equal to 4.730 in the case

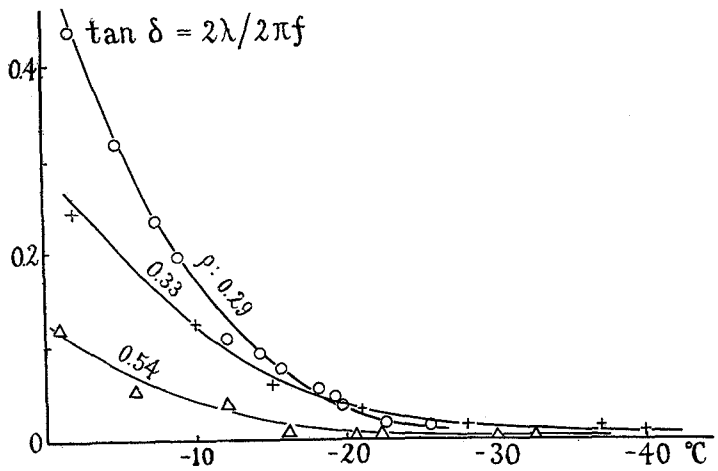


Fig. 26 Vibration loss $tan\,\delta$ and temperature. Figure attached to the curve indicates the density $\rho$ of snow.

of resonance vibration of the fundamental mode.

Since the vibration of the snow bar attenuated exponentially, as described above, the formulae (1) to (5) must hold. The value of $\lambda$ can be determined by the slope of the straight lines shown in Fig. 25 while $f$ is obtained by determining the resonance vibration of the snow bar. Fig. 26 shows the ratio of $2\lambda$ to $2\pi f$ in relation to the temperature for three samples of snow. The ratio $2\lambda/2\pi f$ is nothing other than the vibration loss which is usually expressed by $tan\,\delta$. As seen from Fig. 26, $tan\,\delta$ is at its greatest 0.45, which shows that $(\lambda/2\pi f)^2$ is always less than 0.05. This largest value of $(\lambda/2\pi f)^2$ appears for the snow density 0.29 at the temperature $-3°C$ and $(\lambda/2\pi f)^2$ has values much smaller than the above one for the snow of other densities and for the lower temperatures. Therefore $\lambda$ can be safely neglected against $(2\pi f)^2$ and formula (4) can be simplified to

$$E=\frac{48\pi^2\rho l^4}{m^4b^2}f^2\,. \qquad (6)$$

The constant $E$ respecting the elasticity of the snow can be computed by this formula. The resonance frequency $f$ increased with decrease in temperature as shown in Fig. 27. Therefore $E$ should increase as the temperature is

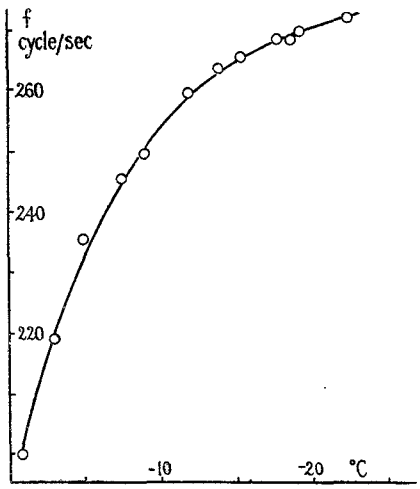


Fig. 27 Resonance frequency $f$ of snow bar and temperature.

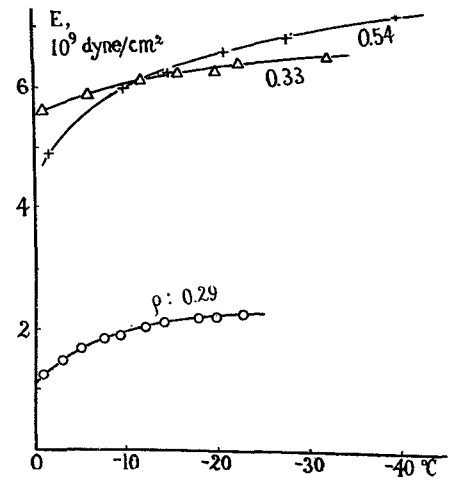


Fig. 28 $E$ versus temperature. $E$: constant respecting the elasticity of vibrating snow bar.

lowered; indeed, the computed values of $E$ plotted in Fig. 28 show the tendency to increase with the decreasing temperature approaching asymptotically to a finite value.

The constant $Y$ respecting the internal friction can be obtained by putting the experimental value of $\lambda$ into formula (3). The more slowly the vibration

attenuates, the smaller $\lambda$, and consequently $Y$ also, becomes. The photographs of Fig. 24, Pl. II show that the attenuation of vibration becomes slower as the temperature is lowered, which results in the decrease of $Y$ with the reduction in temperature. Indeed $Y$ which is computed by formula (3) on the same sorts of snow as those of Figs. 27 and 28 decreases with the decreasing temperature as shown in Fig. 29.

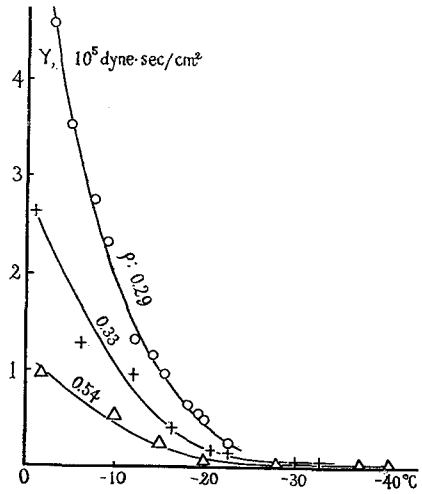


Fig. 29 $Y$ versus temperature. $Y$: constant respecting the internal friction of vibrating snow bar.

Generally it is not an easy task to give an appropriate physical meaning to the constants $E$ and $Y$ which appeared in the above formula (1). If the mechanical property of the snow can be represented by a single Voigt unit model, a spring with elastic constant $E_1$ and a dash pot with viscous constant $\eta_1$ in parallel connection, $E$ and $Y$ are identical with $E_1$ and $\eta_1$ respectively. In this case $E$ and $Y$ are physically interpreted as a pure elastic constant and a pure viscous constant respectively. But if the model is replaced by a single Maxwell unit model in which the spring and the dash pot are connected in series, $E$ and $Y$ turn out respectively to be expressed by

$$E=E_1\frac{\omega^2+\lambda^2}{\omega^2+(\mu-\lambda)^2} \tag{7}$$

$$Y=\frac{E_1^2}{\eta_1}\frac{1}{\omega^2+(\mu-\lambda)^2}\,. \tag{8}$$

In these formulae $\omega$ stands for $2\pi f$ and $\mu$ represents the reciprocal of the relaxation time of the Maxwell unit model, that is $\mu=1/\tau=E_1/\eta_1$. $\lambda$, the attenuation constant of vibration, is given by the equation

$$\frac{2\lambda}{\omega^2-\lambda^2}=\frac{\mu}{\omega^2-\lambda(\mu-\lambda)}\,. \tag{9}$$

In the present experiments on the vibration of snow bar $\lambda^2$ is negligibly small as compared with $\omega^2$ as noted above. Then, if $\mu$ is assumed to be of the same order of magnitude as $\lambda$, the formulae (7), (8), (9) can be reduced to

$$E=E_1 \tag{10}$$

$$Y=E_1^2/(\eta_1\omega^2)=KE_1/\eta_1 \tag{11}$$

$$\lambda=\mu/2=1/2\tau\,. \tag{12}$$

The above assumption made on $\mu$ is found to have been correct since $\mu$ is found here to be of the same order of magnitude as $\lambda$ as shown by formula (12). As was the case with the Voigt model, $E$ is found here also to be the modulus of pure elasticity. The constant $Y$, however, turns out here to be proportional to the reciprocal of the viscous constant $\eta_1$ contrary to the case of Voigt model where $Y$ was the same thing as $\eta_1$.

It should be noticed that formula (1) holds good for the case of Maxwell model only under the condition that the snow bar is subjected to vibrational motion. This is the reason why $\omega$, a constant characterising the vibrational motion, appears in formula (11) besides $E_1$ and $\eta_1$ which are constants of the material. Formula (1) does not always hold in the cases of other general motions.

The Viogt and Maxwell models are only two examples of representation of the mechanical property of the snow and there can possibly be assumed many other models composed of many springs and dash pots to each of which different physical interpretations of $E$ and $Y$ correspond. In the present case of snow it was shown above that $Y$ decreased with the lowering temperature. The viscous constant shows generally a great tendency to increase as the temperature is lowered. Therefore among the conceivable models such sorts of models as the Voigt one in which the viscous constants of the dash pots function so as to make $Y$ increase by enlarging themselves must be excluded in the case of snow, since such models lead to a conclusion contradictory to the experimental fact: the increase of $Y$ with the decreasing temperature. On the other hand such models which are constructed in such a way that the enlargement of viscous constants of the dash pots results in the decrease of $Y$, are allowable. The Maxwell unit model is obviously one of such models and moreover this very model seems to represent the snow in vibrational motion as will be shown below.

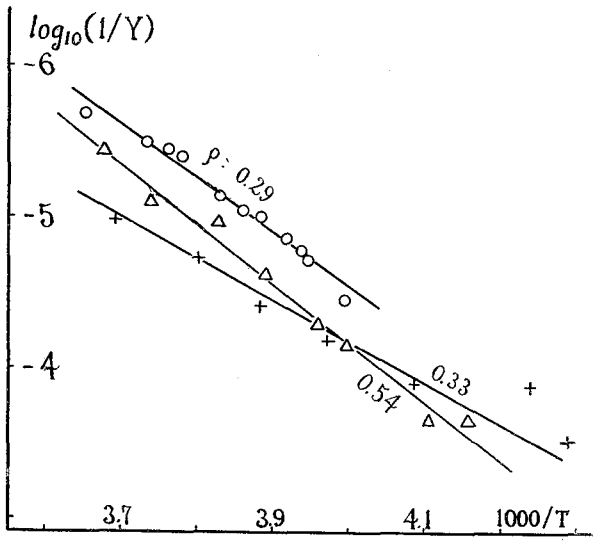


Fig. 30 $log_{10}(1/Y)$ versus $1000/T$. $T$: absolute temperature.

In Fig. 30 the logarithm of the reciprocal of $Y$ is plotted against the reciprocal of the absolute temperature $T$ for three samples of snow; the value of the

logarithm of $1/Y$ is taken along the ordinate axis so as to decrease with the increasing height. The figure shows that $log_e(1/Y)$ and $1/T$ are related linearly to each other, indicating that there exists between them the relation

$$1/Y = A\, exp\,(Q/RT). \tag{13}$$

As was stated in article (*b*) of §2 the viscosity of either a solid or a liquid generally changes with the temperature in proportion to $exp\,(Q/RT)$. Therefore the above relation suggests that $Y$ is such a physical quantity that its mathematical expression contains the viscous constant in the denominator. The value of $Q$ which can be determined from the slope of the straight lines in Fig. 30 turns out to be

$$Q = 18.3,\ 12.7,\ 12.3 \text{ kcal/mole}$$

for the snow samples when the density $\rho = 0.54$, 0.33 and 0.29 respectively. These values are very near those of $Q$ which were found with respect to the first viscous constant $\eta_1$ of snow for the case of statical compression in article (*b*) of §2. Such a coincidence of the values of $Q$ in both cases makes it the more probable that $Y$ is a quantity proportional to the reciprocal of the viscous constant.

Now $Y$ of formula (11) which was obtained by representing the snow by a Maxwell unit model contains the viscous constant $\eta_1$ in the denominator. On the other hand, if the representation of snow by the Maxwell unit model is correct, its elastic constant $E_1$ must be equal to $E$ of which the change with temperature was found, as shown in Fig. 28, to be very small as compared to that of $Y$ shown in Fig. 29. Therefore from the adoption of the Maxwell unit model as the representation of snow it follows that the constant $Y$ is a quantity which changes practically in inverse proportion to the viscous constant $\eta_1$ so far as the effects of change in temperature are concerned. In this way the results of experiments described in the previous paragraph can be explained by representing the snow by the Maxwell unit model.

In order to learn the general order of magnitude of $\eta_1$ of the Maxwell unit model representing the vibrating snow, let the value of $\eta_1$, for example, be computed with respect to the snow of density 0.29 at the temperature $-10°$C. Figs. 27, 28 and 29 give $\omega = 2\pi \times 250 = 1500$ radians/sec, $E = 2 \times 10^9$ dyne/cm$^2$, $Y = 2 \times 10^5$ dyne·sec/cm$^2$ respectively. Then formula (11) yields $\eta_1 = 9 \times 10^6$ dyne·sec cm$^2$. In the previous section, where the statical compression of snow was described, the snow was represented by a combination of a Maxwell unit model and a Voigt unit model in series connection. The first viscous constant $\eta_1$ of snow which corresponds to the viscous constant of the dash pot within the Maxwell unit model was then found to be about $10^8$ dyne·min/cm$^2$ as shown in Fig. 11(b) of §2 for the same density and temperature as the above example. The snow in this manner shows different values

of $\eta_1$ in the cases of vibrational motion and of statical compression: in the case of vibration, $\eta_1$ is comparatively small amounting only to certain thousandths of its value in the case of statical compression.

A Maxwell unit model and a Voigt unit model each constitutes individually a vibrating system having a characteristic resonance frequency. When a system composed of these two models is acted on by a periodic force of the same frequency as the resonance frequency of one of the component models, for example, of the Maxwell model, only the Maxwell unit model will vibrate violently while the Voigt unit model shows no or little response to the applied force. Then the whole system will appear as if it were composed only of the Maxwell unit model. Therefore the composite model employed in the case of statical compression of snow may seem to be applicable with no alteration also to the case of vibrating snow bar, the Voigt unit model, one component of the composite model, being still existent but being kept inactive in this case. But the above indicated large difference in the values of viscous constants in both the statical and vibrational cases shows that the Maxwell unit models cannot be the same in the two cases. Therefore the rheological model used to represent the snow must be changed essentially in accordance with the influences to which the snow is subjected.

Not only the viscous constant $\eta_1$ but also the elastic constant $E_1$ is very different in the vibrational and statical cases. As noted above, $E_1$ in the case of vibration is equal to $E$ of formula (1) and $E$ was found experimentally to be of the order of magnitude $10^9 \sim 10^{10}$ dyne/cm$^2$ as shown in Fig. 28. On the other hand it was shown in §2 that the snow responded to the statically applied compressive pressure with the first elastic constant $E_1$ of the order of magnitude $10^7 \sim 10^8$ dyne/cm$^2$. Here $E_1$ is the elastic constant of the spring within the Maxwell unit model comprised in the composite model which was used to represent the snow. Therefore $E_1$ of the vibrating snow is about one hundred times as large as that of snow subjected to the statical compression.

The relaxation time $\tau = \eta_1/E_1$ was found to be of the order of several minutes in the case of statical compression. In the case of vibrating snow $E_1$ and $\eta_1$ are so such enlarged and diminished respectively compared to those of the statical case that the relaxation time comes to be exceedingly reduced. The relaxation time $\tau = \eta_1/E_1 = 1/2\lambda$ (cf. formula (11)) of the vibrational case ranges from 0.001 sec to 0.1 sec, increasing as the temperature is lowered. If the period of vibration is denoted by $\theta$, the relaxation time $\tau$ and the vibrational loss $tan\,\delta$ can be put into the relation:

$$\tau = \theta/(2\pi\, tan\,\delta).$$

Therefore the mode of change in $\tau$ with temperature will be given more accurately by reference to Fig. 26 in which $tan\,\delta$ is plotted against tempera-

ture. In that case $\theta$ may be considered to have a constant value lying between 1/200 sec and 1/300 sec, since the change in $\theta$ with temperature is much smaller than that in $tan\,\delta$.

The snow samples used in the present vibrational experiments were not those freshly taken out from the snow cover lying on the ground but were those which had been stored in the cold room. For example the snow of density 0.29 used in the experiments had been stored about half a year. It must have undergone during this time a metamorphosis by sublimation. Accordingly its structure must have become different from that of snow of the same density in the natural state on which the experiments by statical compression were performed. Such a difference in the structure may be thought to have been the cause of the above described large difference of the constants $E_1$, $\eta_1$ in the vibrational and statical cases. But the present authors believe that the difference of the structure could constitute at greatest only a small portion of the cause and that the major part of it lay in the large difference of the rapidity with which the strain was changed respectively in the statical and vibrational experiments.

When the surface of the snow bar was observed by a microscope, it appeared as shown in the photographs of Fig. 31. Photograph (a) shows the still surface. Some of the ice grains on the surface reflected light so strongly that they appeared as bright spots on the dark back ground. When the bar began to vibrate such bright spots turned to bright streaks of which the length was obviously equal to the amplitude of vibration. Photograph (b) of Fig. 31 shows the bright streaks at the central point of the neutral line of vibration which bisects the thickness of the side surface of the snow bar. They were found to be 0.195 mm long. Photograph (c) is the appearance near one of the points at which the snow bar was suspended by the strings. The bright spots here were not lengthened to streaks—showing that this point was actually the node of vibration.

The neutral plane of vibration bisecting the vibrating bar horizontally along its length underwent no strain while every other horizontal plane which deviated from the neutral one was elongated and contracted alternately. Let the distance between the two nodes of vibration, the deviation of a horizontal plane from the neutral one and the amplitude of vibration at the central point of the neutral plane be denoted by $2l_0$, $y$, $A$ respectively. Then the maximum strain $e$ to which the horizontal plane was subjected is given by

$$e=2yA/l_0^2\,.$$

In the case of the photographs of Fig. 31, $2l_0$ was 27.3 cm while $A$ was $0.195/2=0.098$ mm as shown above. The thickness of the bar was 4.0 cm. Then the above formula yields $e=2\times10^{-4}$ for the maximum strain which the

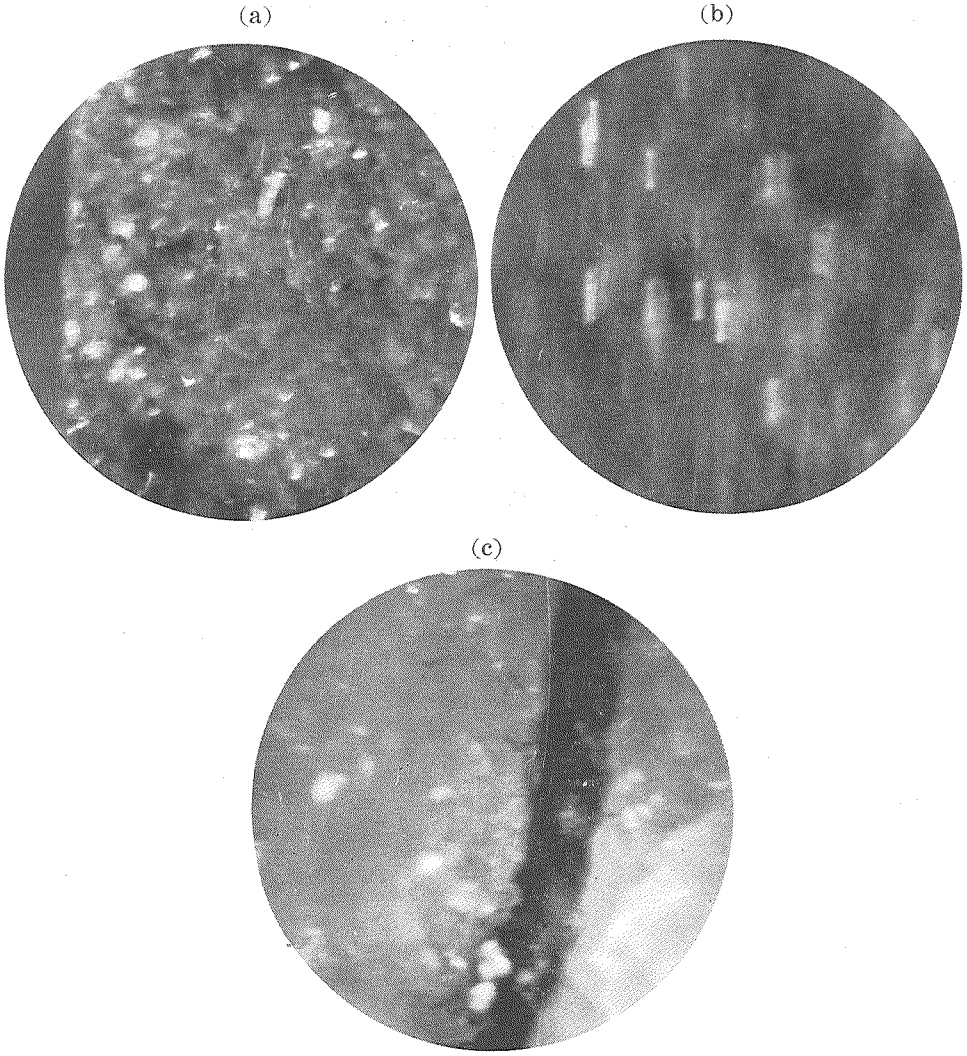


Fig. 31 Microphotographs of the surface of snow bar. (a) when snow bar is still, (b) at the centre of vibrating snow bar, (c) at the node of vibration.

top and bottom surfaces of the snow bar underwent while it was vibrating. It was found above that the elastic constant $E$ of the snow in vibrational motion amounted to more than $10^9$ dyne/cm$^2$. Therefore the maximum stress $Ee$ to which the top and bottom surfaces of the vibrating snow bar were subjected is found to have been more than $2\times10^5$ dyne/cm$^2$ or 200 gr-wt/cm$^2$.

The snow of Fig. 31 had the density 0.29 gr/cm$^3$. When the snow with density of this magnitude is pulled or pushed with a force stronger than 100 gr-wt cm$^2$ or thereabouts it is usually fractured or broken. Therefore the

vibrating snow bar of Fig. 31 should have been fractured at its top and bottom surfaces, since they were acted on by a large stress far exceeding the fracture stress. But these surfaces actually did not show even the slightest signs of fracture. It should be noticed that such a large stress acted not continually but intermittently, each period of action being only a fraction of the period of vibration. When one applies a force $f$ to glass rods to break them, they withstand the force for some while $t$ before they are broken, which phenomenon F. W. Preston called 'static fatigue' (14). The increase of $f$ shortens $t$; Preston and his co-workers found the following relation between them:

$$1/f = a + m \log t,$$

where $a$ and $m$ are constants. The phenomenon of static fatigue has not yet been studied on ice and it is entirely unknown whether ice shows such a phenomenon or not. But the above described fact that the top and bottom surfaces of the vibrating snow bar withstood a stress much greater than the fracture stress, determined on snow in the usual case of statical application of force, could be explained by the shortness of duration of the stress, if the phenomenon of static fatigue were ascertained on ice or snow. The present authors have heard that a motor lorry could traverse a frozen lake running at high speed while it would break the ice if it were driven at a low speed. Such an experience may be considered to be an indication of the existence of the phenomenon of 'static fatigue' in ice.

### §5 Load supporting strength of snow cover.

When a load is put on the surface of a snow cover, the load sinks a certain depth into it and is supported there. Of course, the depth $D$ by which the load sinks should depend on its weight $W$, but this dependency is not so simple that it can be represented by a continuous mathematical function as pointed out by S. Izumi (15) and R. Saito (11). These authors could add small loads to a plate which had already sunk into snow by having been weighted by a heavy load without making the plate sink still further. This fact shows that not one value of weight $W$ but a range of values of $W$ corresponds to one value of $D$.

The upper limit of the range of $W$ can be determined by adding small weights one by one to the plate until it sinks anew into the snow, but the determination of the upper limit by such means is a difficult task. The present authors devised a method by which the upper limit can be determined automatically (16). The lower limit of the range of $W$ will be considered later. In Fig. 32, F is a frame work of iron stood on the snow cover. An iron drum with handle H is attached to the top of the frame work and wire rope T wound around the drum suspends the stout helical spring S. At its bottom S

holds the cylindrical weight W, 14 cm or 20 cm in diameter and about 40 kg in weight. The iron frame J fixed at its upper end to the top of spring S holds a rectangular frame R made of iron wire along which wooden plate P can slide horizontally. A sheet of paper is placed on plate P and pencil N connected to the bottom of spring S registers the elongation of S on the paper. String Q of which one end is fastened to the top of the iron frame work F passes through wire ring M attached to R and ends at the extreme right of plate P.

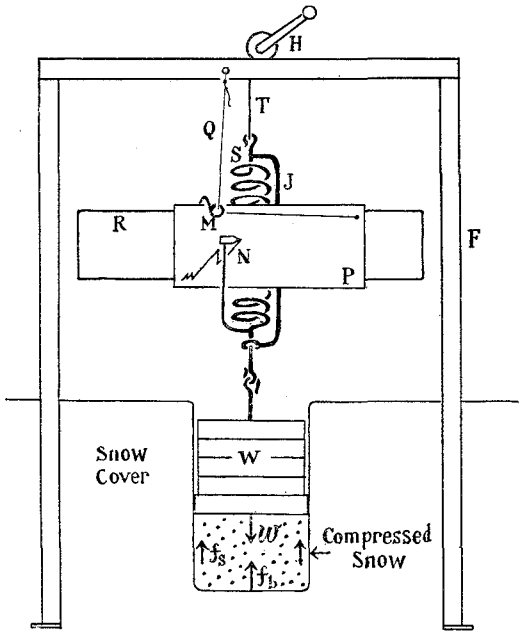


Fig. 32 Apparatus for registering the load supporting strength $W$ and the subsidence depth $D$ automatically.

Starting from the state in which the bottom of weight W is above the snow surface, wire rope T is unrolled slowly by rotating handle H by hand. Wooden plate P which has been placed to the right of the centre of rectangular wire frame R is moved towards the left by being pulled by string Q as the top of spring S is lowered. Until the bottom of W touches the snow surface, spring S is being elongated to the maximum and pencil N draws a horizontal straight line O'O on the paper near its lower edge as shown in Fig. 33. As soon as the bottom of W touches the snow surface at point O spring S begins to contract with the result that the bottom of W begins to press the snow below it with increasing pressure which is proportional to the amount of contraction of the spring. So long as the weight keeps its position by being supported by the snow, the amount of contraction of the spring is equal to the distance by which wooden plate P is shifted and consequently the pencil draws sloping straight line $OW_0'$ which makes an angle of 45° to the hori-

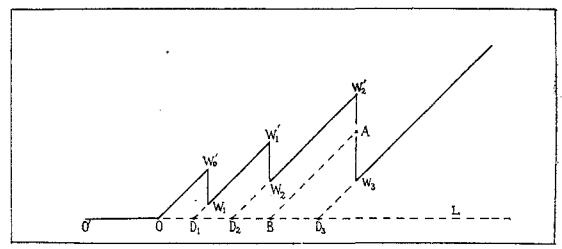


Fig. 33 Schematical illustration of the curve registered by the apparatus shown in Fig. 32.

zontal direction. When the load on snow attains a value represented by point $W_0'$ in Fig. 33, the snow breaks down under the weight and it sinks suddenly into the snow, the spring being elongated while no movement is imparted to the wooden plate. The pencil draws a vertical segment $W_0'W_1$ at this instant. In this way $W_0'$ is determined as the upper limit of the range of $W$ for $D=0$. On further lowering of the top of the spring, the pencil draws the second sloping line $W_1W_1'$ followed by vertical segment $W_1'W_2$ which corresponds to the second break-down of the snow. Depth $D_1$ corresponding to $W_1W_1'$ is given by the distance from point $O$ to point $D_1$, the point at which the downward elongation of $W_1'W_1$ intersects with the straight elongation L of horizontal segment $O'O$. The upper limit of weight corresponding to depth $D_1$ is given by $W_1'$. Such a process is repeated as wire rope T continues to be unrolled, till the bottom of the weight sinks to the depth where the snow is sufficiently compact to support the whole mass of the weight. In this way the upper limit of the range of weight which can be supported at a depth $D$ under the snow surface can be determined at once from the figure drawn by the pencil.

Generally the depth corresponding to any point on the curve of Fig. 33, for example such a point as A, is equal to the distance between points O and B, point B being the intersection point of line L with the line drawn through the point in question, point A in this example, making an angle of 45° with line L.

The greatest pressure $P_m$(gr-wt/cm$^2$) with which the bottom of the weight can press the snow without breaking it down at a deph $D$(cm) is plotted in Fig. 34, $P_m$ and $D$ being counted horizontally rightwards and vertically downwards respectively. $P_m$ is the same thing as the ratio of the force represented by such points as $W_1'$, $W_2'$, $W_3'$, shown in Fig. 33, to the area of the bottom of the weight. In Fig. 34 solid circles belong to the case in which the weight of 14 cm diameter was used while crosses belong to the case in which the weight of 20 cm diameter was used. The distribution of both the solid circles and the crosses can be represented nearly by the smooth curve $P_m=4+2.2D^2$. The figure in the right portion of Fig. 34

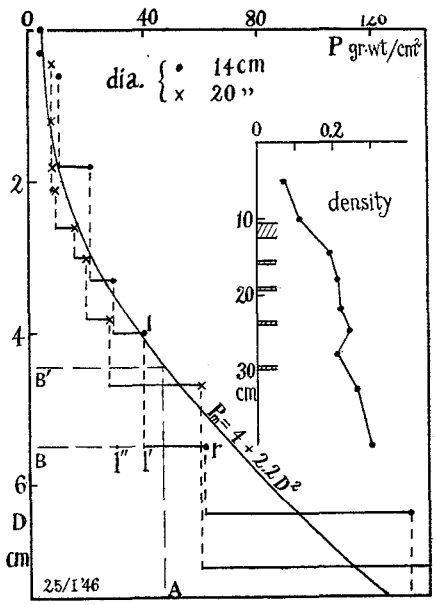


Fig. 34 $P$: pressure with which the bottom of the weight presses snow lying beneath it. $D$: subsidence depth of the bottom of the weight. Figure in the right portion shows the vertical distribution of snow density.

shows the vertical distribution of density in the snow cover. The hatched zones in this figure give the positions of crust sheets embedded in the snow cover.

The mathematical function representing such a smooth curve as given above does not apply to any value of $D$ but is available only at discrete values of $D$. Consequently the function cannot be used to determine the subsidence depth of a load of a given weight $W$ when it is placed on the snow surface. Let the pressure with which the bottom of a circular weight 14 cm in diameter presses the snow be denoted by $P$ corresponding to point A in Fig. 34. When such a weight is placed on the snow surface, the depth of its subsidence is given by point B but not by point B′ which corresponds to point A by way of the smooth curve. $P$ is a little larger than the pressure $P_l$ represented by the solid circle marked $l$, which pressure is the same as that represented by point $l'$ lying to the left of point A. At the level of point $l$ the snow cannot bear any pressure larger than $P_l$ and in order to support such a pressure the snow must subside to the next granted level B where it can afford to stand a pressure larger than $P$ provided that the pressure does not exceed the value $P_r$ represented by solid circle $r$ lying to the right of point A. In this way the actual relation between $P$ and $D$ is represented by the stepped curve composed of horizontal full lines and vertical broken lines which meet each other at the solid circles or crosses in Fig. 34.

The width of a step of the stepped curve, that is, the width from point $l'$ to point $r$ in the above example, is the range of pressure which the snow can bear at the depth of that step. Of course the snow can also hold any pressure less than $P_l$ at level B and the range of pressure at this level may have to be taken as extending from zero to $P_r$ in the strict sense of the word. But, since the levels located above level B have sufficient rigidity to hold pressure less than $P_l$, there is no need to use level B in order to support such pressures. Hence it will be more adequate to take $l-r$ as the range of pressure belonging to level B rather than to take $0-r$. Then the lower limit of weight $W$ of a load which is to sink down to one of the allowed depths is given by the product of the lower limit of pressure range belonging to that depth into the area of bottom of the load.

But in the actual case of the experiment of Fig. 34 the pressure which the load exerted on the snow immediately after it had fallen the height of stair $l-l'$ of the stepped curve was smaller than $P_l$ by the amount corresponding to the elongation $l-l'$ of the spring. That is to say, the experimental value of pressure descended from point $l$ directly, not to point $l'$ but to point $l''$ shown to the left of point $l'$ in Fig. 34. Such a descent occurred because the weight of the load was changeable and was made to exceed $P_l$ in order to break down the snow under the load. The weakened structure of the broken snow allowed the load to fall although the pressure upon it became smaller

than $P_l$ as it fell. Therefore the transfer of the experimental point from point $l$ to point $l''$ in Fig. 34 arose from the special circumstances that the weight of the load was changeable in the experiments. In the case of the load being merely placed on the snow surface such a change in weight is impossible and the load should descend directly to level B provided that the pressure due to its weight lies in the range from $P_l$ to $P_r$.

In the above case the strong crust sheet at the depth of 11–13 cm kept the weight from sin ing more than about 8 cm under the snow surface. In the case of another example shown in Fig. 35 the crust sheet at the depth of 10 cm was so weak that the weight broke through it and reached the depth of 20 cm. Here the circular and triangular marks represent the values of $P_m$ in the cases of weights 14 cm and 20 cm in diameter respectively. For each of the weights two experiments were performed; blackend and white marks belong to the different experiments. The marks are distributed near the smooth curve $P_m=4+1.7D+0.28D^2$, although those marks corresponding to depths somewhat above the crust sheet 10 cm deep deviate from the curve towards the larger values of $P$, being influenced by the rigidity of the crust. Blackened and white marks of the same shape seem to be located near each other in pairs while there can be seen no such relationships between the marks of different shapes. This pairing of the marks of the same shape indicates that the process of subsidence of weights into snow is nearly reproducible when the process is subjected to the same experimental conditions. But the fact that no definite relation is found between the distribution of marks of different shape, the same having been true also in the case of Fig. 34, shows that the discrete values found for $D$ are not only dependent on the property of the snow but are also influenced by the difference of experimental conditions such as the difference in diameter of

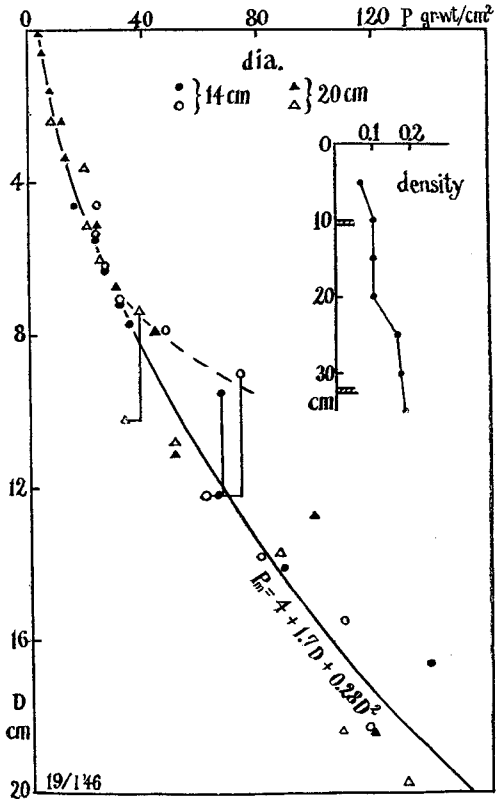


Fig. 35 Relation between $P$ and $D$ in the case of deep soft snow.

the weight.

Now that the discrete values granted to $D$ are known not to be determined by the property of snow alone, it will be of little practical significance to make any effort to determine accurate relations such as the stepped curves in Fig. 34 existing between the subsidence depth $D$ and the load supporting strength $P$. The smooth curves as shown in Figs. 34 and 35 may be rather useful in that they give relations between $D$ and $P$, even though not very accurately, regardless of the property of the weight.

When a load sinks into snow cover, as a matter of course, the snow under the load is compressed. If the snow cover is cut by a vertical plane through the centre of the load, the region of compressed snow can be clearly distinguished on the cut plane by its increased density. The region is bounded on the sides by a vertical cylindrical surface through the periphery of the load while it is bounded on the bottom by a plane parallel to the bottom of the load. The photograph of Fig. 36 shows the region of compressed snow made in a vertical sheet of snow held between two parallel glass plates. The

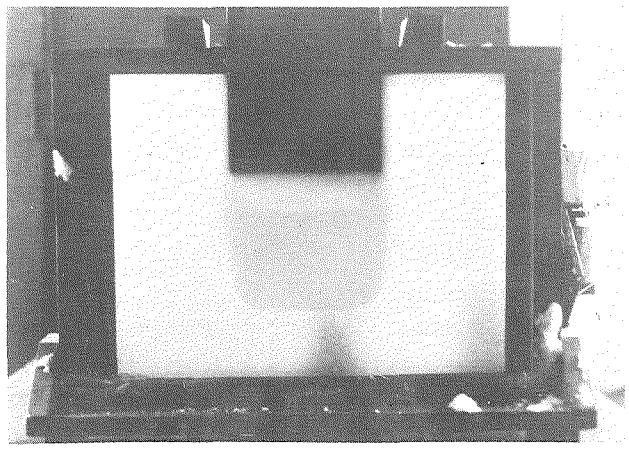

**Fig. 36** Region of compressed snow developed under the bottom of the weight.

pressure was applied from above by means of a wooden board of which the lower part is seen in the photograph. It should be noticed that the boundaries of the region of compressed snow are very sharp.

The load with the whole of its weight $W$ presses down upon the top of the region of compressed snow while this region is supported by the snow mass surrounding it by way of forces $f_b$ and $f_s$ as indicated in Fig. 32. $f_b$ is a force acting against the bottom of the region of compressed snow and $f_s$ is a shearing force acting on its side surface. For the load to be supported by the snow, $W$ must be equal to $f_b+f_s$. The snow surrounding the region of

compressed snow has not yet been broken down and must have the visco-elastic properties explained in the preceding sections § 1 and § 2. The forces $f_b$ and $f_s$ have their source in those properties. R. Saito placed plates of the same area and of the same weight but differing in shape upon the snow surface and found that the plates with shorter periphery sank more deeply into the snow (11). The shorter the periphery of the plate, the smaller $f_s$ must be with the result that $f_b = W - f_s$ becomes larger. Hence the load with short periphery should sink more deeply than that with a long one owing to the larger $f_b$ pressing down the snow lying below the region of compressed snow. Saito concluded that the shearing force $f_s$ exists by explaining his experimental results by such a reasoning.

Then it will be worth while to question whether or not $f_s$ influences the granted values of $D$ described in the preceeding paragraphs. For the purpose of solving this problem the present authors made the following experiments. As shown in the upper right portion of Fig. 37 a pillar of snow was made in the snow cover by shoveling out snow around the pillar. Weight W of the apparatus shown in Fig. 32 was lowered onto it. It is obvious that $f_s$ was completely eliminated in this case. The pillar was usually tilted to one side or burst sideways as the weight descended but in one case it was compressed straight downwards although a little bulging out of the side surface of the pillar occurred. The curve marked III in Fig. 38 is the one drawn by the pencil in this case. The granted value of depth $D$ and the magnitude of $P_m$ are shown by crosses connected by curve III in Fig. 37. In the next experiment the pillar of snow was surrounded by a cylinder made of galvanised iron sheet so that the snow pillar might not be tilted down or burst sideways. Since the friction between the snow and the galvanised iron sheet is small the magnitude of $f_s$ must be much reduced in this case. The results of experiment are shown by the triangles connected by curve II

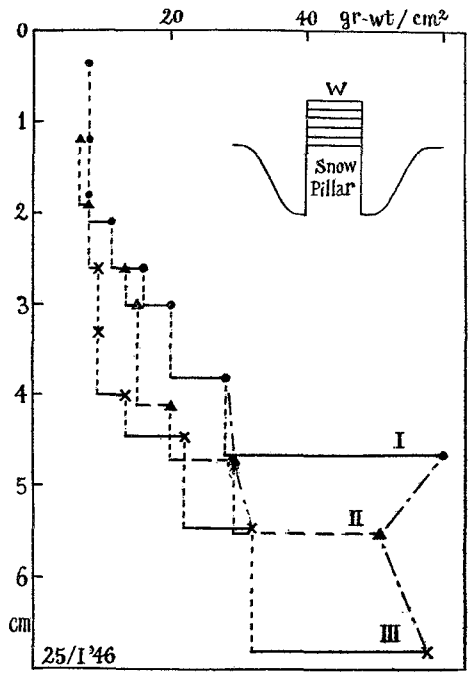


Fig. 37 Relation between $P$ and $D$. I: weight was lowered onto the snow surface in its natural conditions. II: weight was lowered onto snow pillar surrounded by a cylinder of iron sheet. III: weight was lowered onto unprotected snow pillar.

in Fig. 37 and by curve II in Fig. 38. The dark circles and curve I in Fig. 37 and curve I in Fig. 38 show the results of experiment made on the snow cover under natural conditions.

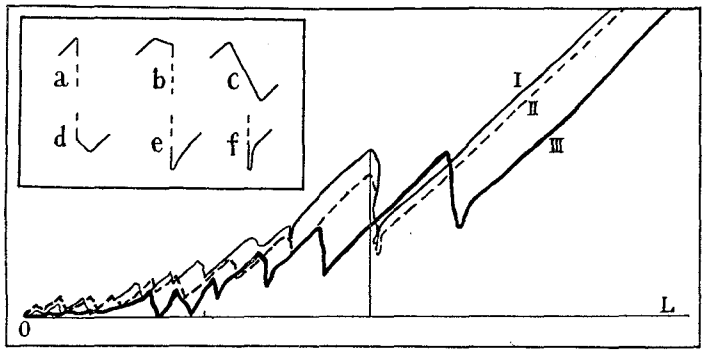


Fig. 38 Actual records registered by the apparatus of Fig. 32. Three curves I, II, III of Fig. 37 are obtained from the curves shown in this figure.

In Fig. 37 curves I, II, III are placed from above downwards in that order. The largest $f_s$ gives the least $D$ while the least $f_s$ gives the largest $D$, or, more strictly speaking, reduction of $f_s$ brings about the increase of each of the obtained values of $D$. This is in accord with the above described explanation by Saito of his experimental results. But the experiment made on the pillar of snow shows that $D$ still changes discontinuously with lowering of the weight even if $f_s$ is completely eliminated. Therefore the discreteness of values of $D$ must have its source in that character of snow which governs its response to compressive force. The shearing force $f_s$ is effective only in shifting the values of $D$ but has nothing to do with whether $D$ takes continuous or discrete values. If now the cause of restriction of $D$ to discrete values in the above experiments has been shown to lie in the compression of snow, such a phenomenon may be thought to have arisen from the fact that the weight was hung by the helical spring. But as will be shown later in the next paper of this series which will be published in the near future even a load merely dropped down onto snow meets resisting force which increases intermittently to large values even when the snow takes the form of a free pillar as in Fig. 37. Therefore the present authors believe that the influence of the spring hanging the weight in the former experiments was of little importance if any in respect to the discreteness of the values of $D$.

With regard to the above stated subject the following experiments conducted by I. Furukawa and Y. Shirai may be cited (17). They enclosed a circular pillar of snow 10 $cm^2$ in cross section and 10 cm long in a metal cylinder and compressed it longitudinally at a constant slow speed lying in

the range from 0.1 mm/sec to 2 mm/sec. The resistance $w$ of snow against compression increased as time went on with increasing strain $e$, $e$ being here the ratio of amount of contraction to the initial length of pillar. $w$ increased continuously with time in the case of wet snow, but, in the case of dry snow, the increase of $w$ was interrupted by intermittent abrupt decreases due to breakdown taking place somewhere in the body of snow. After all the resisting force of the pillar of dry snow showed discontinuous changes even if its length was diminished continuously at such a small rate. In this way it may be concluded that discontinuity comes to appear in the compressive nature of snow when the time rate of change in its strain exceeds some limit of very low value. In other words, snow shows the phenomenon of break-down in the same way as a solid does when subjected to compression proceeding at a rate larger than a certain limiting value while under the action of compression proceeding at a rate less than that limit snow behaves like a viscous liquid as described in §'s 1 and 2 above.

The actual recordings reproduced in Fig. 38 differ in details from their schematical copies shown in Fig. 33. The actual curve is not so pointed at its turning points as shown in the scheme; the appearance of the actual curve at these points respectively is shown in the upper left portion of Fig. 38. Such portions of curves b, c, d as run down rightwards indicate continuous depression of the weight unlike the vertical portion which shows discontinuous depression due to break-down of snow. The continuous depression shown here will be the same thing as the continuous contraction of snow taking place between the intermittent decreases of resistive force in the above described experiments of Furukawa and Shirai. Curve f shows that the weight was forced up slightly after it had fallen to certain depth by the break-down of snow. Curve e shows the case in which the weight was forced up slowly. Such a phenomenon must arise, as described in §'s 1 and 2, from the visco-elastic property of the snow underlying the bottom of the region of compressed snow developed below the weight.

### §6 Development of the region of compressed snow below the bottom of load.

The following experiments were performed to observe how the region of compressed snow described in the previous section develops under the descending load. The region of compressed snow is in the interior of the snow mass and cannot be seen from the outside under ordinary conditions. The present authors taking a sheet of snow as the snow sample pressed it on a portion of one of its edges by the edge of a wooden board and took motion pictures of the changes occurring in the sheet of snow. They considered that the sheet of snow could be regarded as a two-dimensional model of a vertical section through the centre of the actual region of compressed snow, the lower edge of

the wooden board being the bottom of the load.

A sheet of snow 2.5 cm thick was cut out horizontally or vertically from the snow cover and stood vertically between two sheets of organic glass plate. In this position the sheet of snow was 34 cm high and 42 cm wide. A wooden board 15 cm wide was attached vertically to the bottom of the weight hung through the spring of the apparatus shown in Fig. 32 and lowered onto the top of the sheet of snow by unwinding the wire rope suspending the spring. The photograph in Fig. 36 of the previous section illustrates the state when the plate has intruded some distance into the snow sheet, the region of compressed snow being shown distinctly by illumination from a light source placed behind the snow sheet. But, since such an illumination was too weak to be used to take a motion picture, the authors drew dark lines horizontally on the cut surface of the snow sheet with soot, before enclosing in glass, at intervals of 5 cm and took motion pictures of the soot lines by illuminating the snow sheet from the near side. Sometimes vertical soot lines were drawn in addition to the horizontal ones. Fig. 39 presents a schematical figure of the apparatus. The soot lines L were deformed in their portions lying under the wooden board P, by which deformation the development of the region of compressed snow will be displayed. In this figure S is the spring suspending weight W to the bottom of which wooden board P is attached. B is the wooden frame supporting the two sheets of organic glass plate between which the snow sheet is held. The organic glass plates must have some influence on the motion of the snow sheet. But

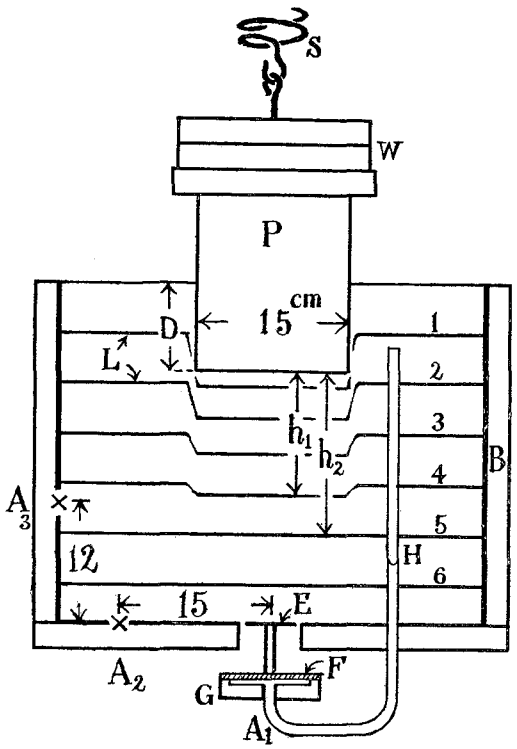


Fig. 39 Equipment for studying the development of the region of compressed snow under the load. Wooden frame B holds two organic glass plates between which a sheet of snow is held upright. Lines marked 1, 2, ..., 6, are soot lines drawn on the surface of the snow sheet. Wooden board P attached to the bottom of weight W presses down the sheet. The instrument marked $A_1$ at the bottom of the figure is a pressure gauge to be used for measuring the pressure in the snow sheet.

it will be shown below in § 8 that such an influence remains within a tolerably low limit.

Cinematographic pictures were taken at the rate of 16 pictures per second. In Figs. 40–46 at the end of this book are shown several series of photographs reproduced from the cinematographic films illustrating how the soot lines are deformed under the load (18). In each of the six series from Fig. 40 to Fig. 45 the sheet of snow was cut out horizontally from one snow layer in snow cover, consequently the snow sheet was of the same property from top to bottom. In the case of Fig. 46 the snow sheet was cut out vertically from the snow cover and was accordingly composed of several layers of different nature. The numerical figure attached to each of the photographs is the number of the picture counted from the beginning of photographing. Since one-sixteenth of a second belongs to a picture the picture numbered 51, for instance, in Fig. 40 shows the state 20/16 sec = 1.67 sec after the one numbered 31.

Fig. 40 shows the case of newly deposited snow. The central portions of the soot lines are cut and displaced downwards, the cut portions being maintained nearly straight. In the first photograph numbered 31 the uppermost line alone is deformed showing that the region of compressed snow has developed down to somewhere between this line and the second one next below it. In the following photographs numbered 51, 71, 91 the deformation of soot lines has proceeded to the second, the fourth and the fifth line respectively. The lowest soot line is deformed in the fifth picture numbered 111, which shows that the region of compressed snow is reaching the bottom of the snow sheet. Up to this picture the spacings between the cut portions of the adjacent lines have been kept constant while in the last picture numbered 141 they are narrower than before, showing that the region of compressed snow has been subjected to an additional compression after the time of the fifth picture. This additional compression must have been caused by the arrest of development of the region of compressed snow by the bottom of the wooden frame. In this final state the pressure acting on the region of compressed snow is 630 gr-wt/cm$^2$.

Three cases of compact snow of different densities 0.21, 0.36, 0.45 gr/cm$^3$ are shown in Figs. 41, 42 and 43, the temperature of snow being $-3.5$, $-2.4$, $-3.0$°C in each case respectively. Contrary to the first case of soft snow, the displaced portions of soot lines lying under the wooden board are irregularly distorted instead of being straight in the first two cases of Figs. 41 and 42. But such a distortion of soot lines comes to be much reduced in Fig. 43, the case of compact snow of such a large density as 0.45 gr/cm$^3$. The compact snow has coherent structure, that is, it is composed of small ice grains connected to each other by stout ice bonds. But with increasing density in nature the ice grains composing snow become large and this makes

its structure rather like that of sand, an assemblage of sand grains merely touching but not coherent to each other. This does not mean however that the compact snow of large density is incoherent in its structure. The ice grains are still connected by ice bonds, but they come to appear very weak in relation to the strength of the ice grains which are now large. This makes the structure of dense compact snow look like sand and such a sand-like structure seems to be the cause of reduced distortion in those parts of the soot lines belonging to the region of compressed snow in the case of such a snow sample. In the case of granular snow which is almost completely incoherent in structure—like sand—the displaced portions of the soot lines form smooth curves with slight distortions as shown in Fig. 44. The compact snow of Fig. 42 and the granular snow of Fig. 44 have almost the same densities; the above described difference in the degree of distortion of soot lines in these two cases cannot be attributed anything else than the difference in the structure of the snow. Among the cases which have hitherto been described, the least distortion is found in the case of newly deposited soft snow of Fig. 40. In such a soft snow the snow crystals have not yet cohered to each other and its structure is incoherent in spite of its small density.

The remarkable distortions of soot lines found in the case of compact snow samples of small and medium density seem to be the result of downward development of fracture planes which precede the descending bottom of the region of compressed snow while it is developing. Parts of snow located between fracture planes will move in different directions and by different amounts, making the portions of soot line which they carry take an irregular arrangements. The present authors suppose that the coherent structure of compact snow of small and medium density causes the development of the fracture planes, although no success has yet been attained in attempts to ascertain their development by means of experiments.

Fig. 45 shows the case of wet snow. As may be seen from this figure the wet snow responds to the compressive pressure much like a very viscous liquid such as gelatine gel. As stated in § 1, when the mechanical property of snow is considered to be represented simply by the rheological model of Maxwell, the snow should behave like a viscous liquid under a certain force provided that it is applied for a period of time longer than the relaxation time of snow. The relaxation time is given by the ratio of viscous constant $\eta_M$ to elastic constant $E_M$ of snow. In the present experiments the weight was lowered to the lowest position in a period less than 10~20 sec. The viscous constant $\eta_M$ of wet snow must be so small that it reduces the relaxation time to far less than this period; in other words, the fluidity of the wet snow which can be represented by the reciprocal of $\eta_M$ is sufficiently large to relax the concentrated stress produced in the snow near the bottom of the wooden board by the lowering weight to such an extent that the snow is

not fractured. But such a relaxation of the stress is effective only up to the time of the fourth picture numbered 99, Pl. VIII. Up to this time deformation of soot lines is continuous and there can be found no definite boundaries

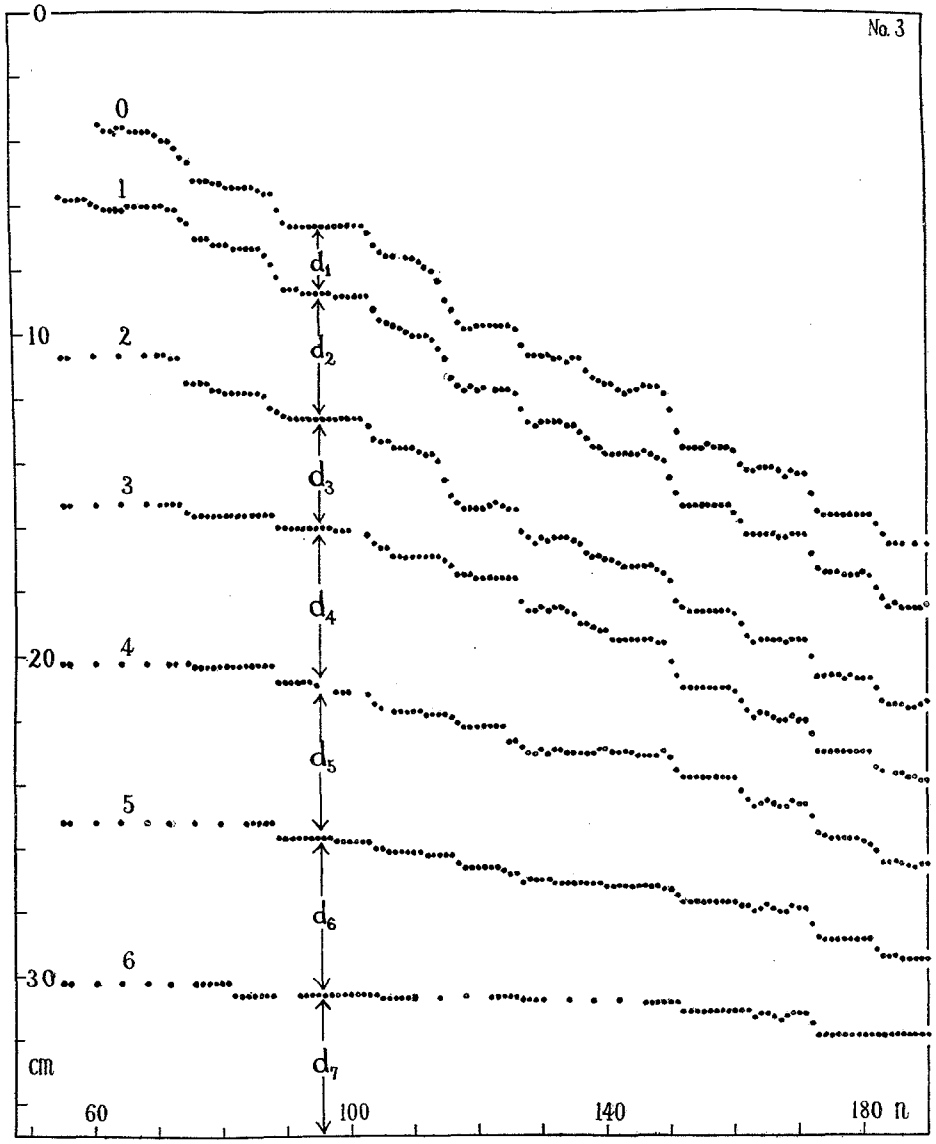


**Fig. 47** Compact snow. Density: 0.21 gr/cm³. Snow of Fig. 41. The following three figures, including this, show the course of change in position of each soot line. Number $n$ of picture of the cinematograph is taken along the abscissa. Time interval of one-sixteenth of a second corresponds to one picture.

dividing deformed and undeformed regions. But at the stage of picture numbered 126 the deformation of the snow sheet has become so large that it fractures at the corners of the wooden board. The relaxation time of dry snow amounts to several minutes as demonstrated in § 2 and this value of relaxation time is much longer than the period of the lowering of the weight. Owing to such circumstances opposite to those of wet snow, the dry snow is fractured and broken down in the same manner as a solid substance as shown in the previous paragraphs describing Figs. 40–44.

The snow sheet of Fig. 46 being a vertical section is not homogeneous; granular and compact snow compose the upper and lower halves of the snow sheet respectively, the two halves being divided by an ice layer located just below the third soot line from above in the figure. The region of compressed snow has already developed to the level of the ice sheet in the second picture but hereafter its development is stopped there until the ice sheet is broken after the fourth picture, numbered 66. In pictures numbered 101 and 121 the region of compressed snow has already intruded into the lower half composed of compact snow and one can see the soot lines belonging to the lower half to be more distorted than those belonging to the upper half.

Trains of dots in Figs. 47, 48, 49 and 50 show the change with time in position of the central point of the displaced portions of soot lines. The position is shown vertically downwards by the unit cm and the time is counted horizontally rightwards by the unit 1/16 sec, the time interval belonging to one

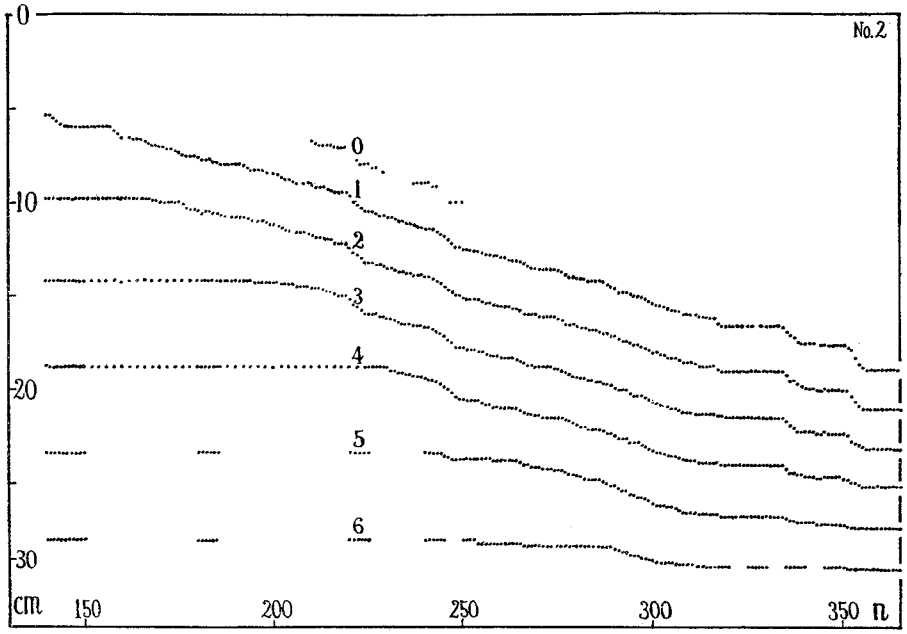


Fig. 48 Compact snow. Density: 0.3 gr/cm³. Temperature of snow: −3°C.

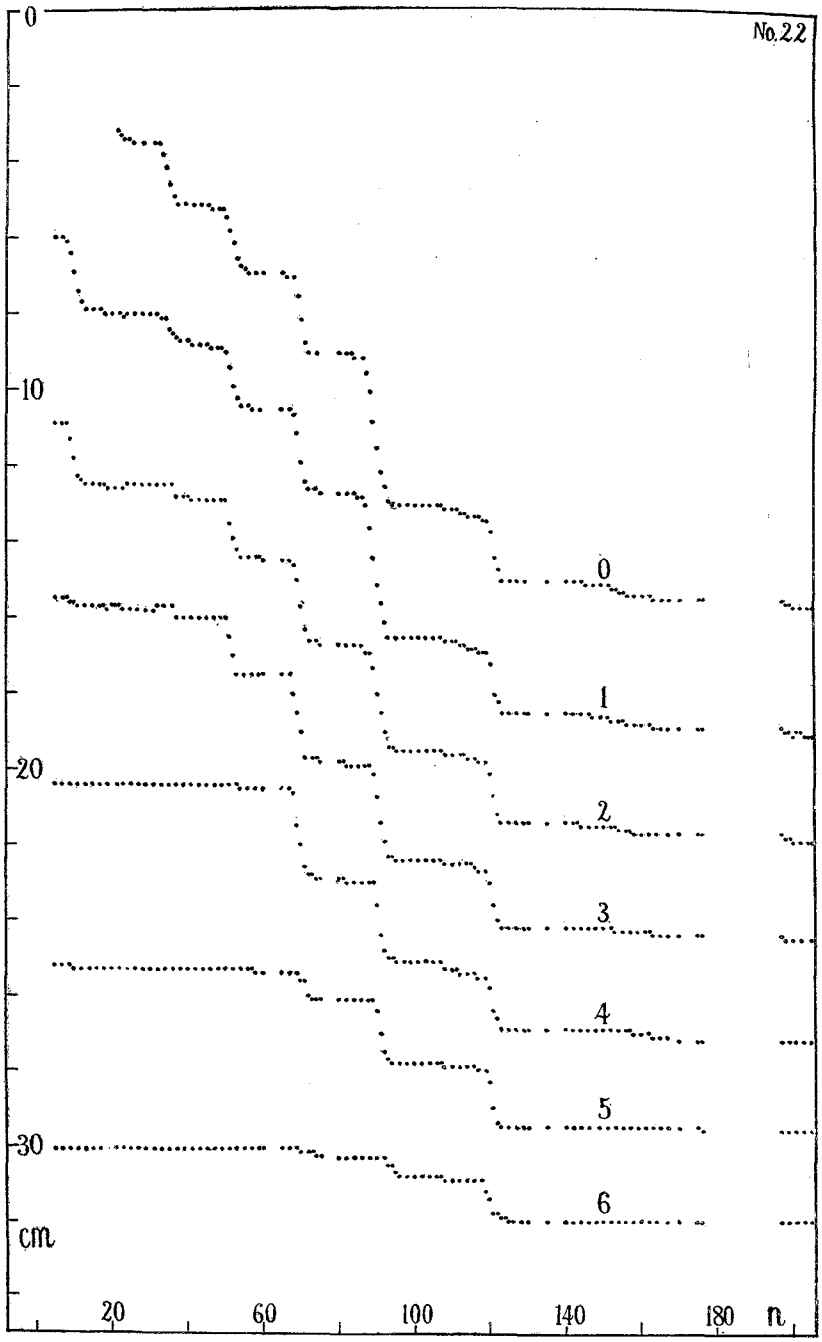


Fig. 49 Granular snow. Density: 0.32 gr/cm³. Snow of Fig. 44.

picture of the cinematograph. Each dot corresponds to the position of the soot line photographed in one picture which was determined in the following way. A large sheet of paper on which parallel lines had been drawn horizontally at equal spacing was placed on the wall and each of the cinematographic pictures was projected one after another on the paper by a magic lantern apparatus. The position of the thus projected soot lines was determined at the central point of their displaced portions in reference to the parallel lines drawn on the paper. As stated above, the displaced portions of soot lines are not straight and their central point cannot be considered to

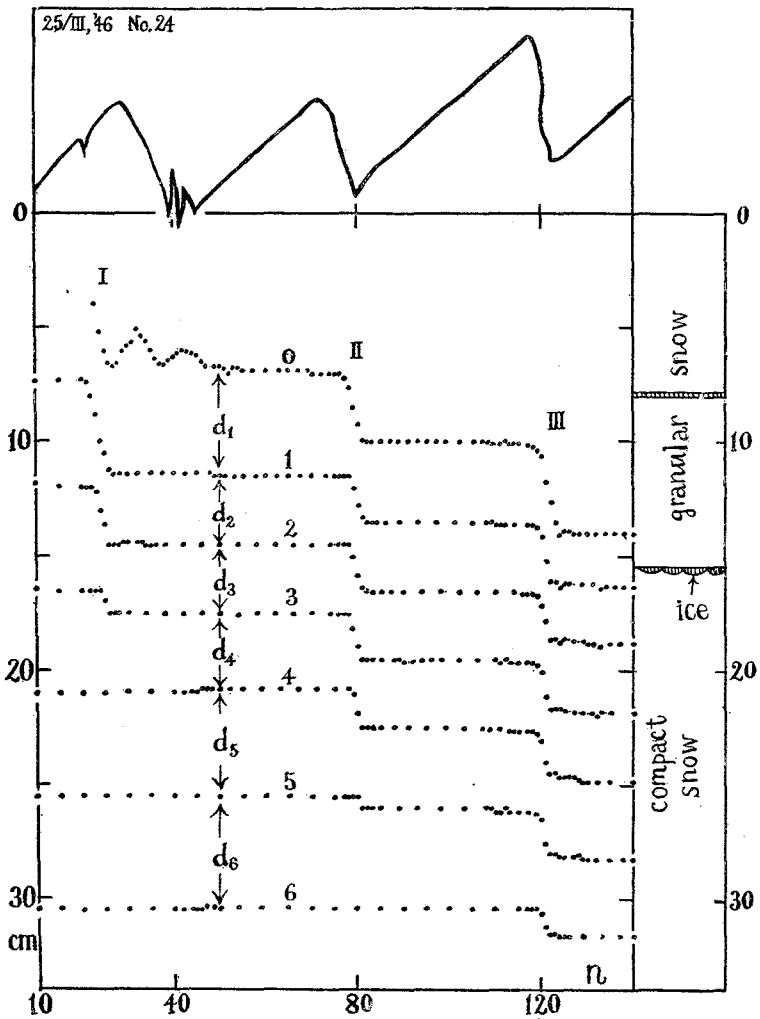


Fig. 50 Composite snow. Snow of Fig. 46. The figure looking like saw teeth at the top shows by its height the pressure acting on the snow sheet.

represent the average position of the whole length of the displaced portions. It was merely for the sake of practical convenience that the central point was chosen as the reference point. There are seven trains of dots numbered 0, 1, ····, 6 in each of the figures from Fig. 47 to Fig. 50. The uppermost train numbered 0 shows the position of the bottom of wooden board pressing the snow downwards. The positions of displaced portions of the six soot lines are shown by the other six trains numbered 1, 2, ····, 6.

The snow samples of Fig. 47 and Fig. 48 are both naturally compacted snow. The snow of Fig. 47 is the same as that of the series of photographs shown in Fig. 41, its density being 0.21 gr/cm$^3$. Fig. 48 illustrates the case of compact snow of density 0.30 gr/cm$^3$, but its photographs are not shown in this publication. In Fig. 47 the trains of dots decline stepwise towards the right with many steps of low elevation of only 1 cm or thereabouts while the number of steps becomes so abundant in the case of Fig. 48 that all the trains come to appear to be sloping down rightwards almost continuously without steps. In contrast to the cases of compact snow having such abundant steps the granular snow yields trains of dots declining with a small number of steps of high elevation from 2 cm to 4 cm as shown in Fig. 49. This figure is obtained from the series of photographs of Fig. 44. It should be noticed that the density of snow is nearly the same in the cases of Fig. 48 and Fig. 49; it is 0.30 in the former case of compact snow while it is 0.32 in the latter case of granular snow. The snow of Fig. 50 is a composite one, the upper and lower halves being granular and compact snow respectively as shown by the annexed figure beside the main figure. Here too the trains of dots have a small number of steps with high elevations. The curve shown on the top of Fig. 50 is of the same sort as those of Fig. 38 showing the pressure with which the bottom of wooden board presses the snow.

It is the general tendency for the compression of the zones between the soot lines to begin at the uppermost zone and proceeds downwards into the underlying ones. That is, the zones are generally thicker than or of the same thickness as the ones lying above them. But one can find an exception to this general tendency by inspecting Fig. 47. The second zone between the first and the second soot lines remains thicker than the third zone next below it to the right of $n=80$, where $n$ is the number of the cinematograph picture counted rightwards along the abscissa of the figure. Such a reversal of the general trend in thickness of zones is more clearly shown by Fig. 51. Here the zones are represented separately by the black blocks in which the displacement of the zones as a whole is disregarded and only their thickness is represented. In addition to the above described reversal of general trend between thickness $d_2$ of the second zone and thickness $d_3$ of the third zone, another reversal is found between the fifth and sixth zones; $d_5$ is larger than $d_6$ to the right of $n=125$, although the difference between $d_5$ and $d_6$ is not so

remarkable as in the case of $d_2$ and $d_3$. Since the thickness of zones presented here is that appearing at the centre of the displaced portions of the soot lines which are not straight, as stated above, it is a question whether such reversals in thickness of zones found here is also true at their other parts. But one will find by inspecting the photographs of Fig. 41 that the displaced parts of the zones show these reversals almost throughout their entire lengths. If the snow is a composite one such a reversal in thickness of zones will not be strange since any zone can be stronger than those lying below it. But, as noted above, the sheet of snow in the case of Figs. 47 and 51 is composed of homogeneous compact snow, having been cut out horizontally from the snow cover. Hence the reversal in thickness of zones cannot be ascribed to any difference in strength of zones.

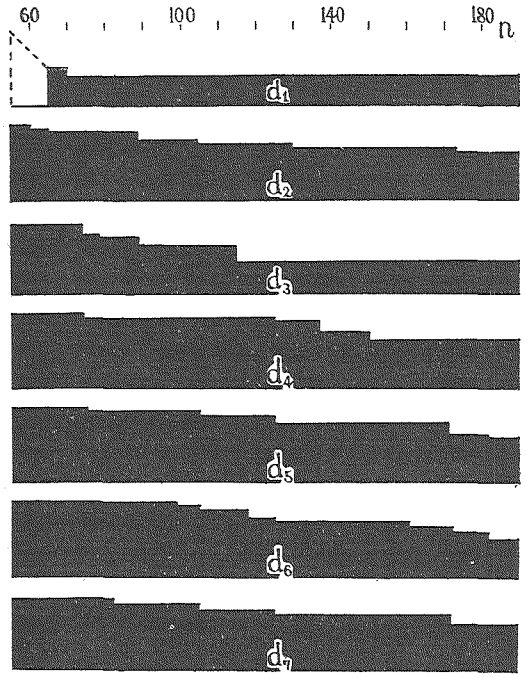


Fig. 51 The course of change in thickness $d_1$, $d_2, \ldots, d_6$ of zones between soot lines in Fig. 47 are shown here by the thickness of black blocks.

The bottom of the region of compressed snow under the load must lie between the lowest deformed soot line and the undeformed one next to it. Soot line 4 is deformed but soot line 5 is undeformed in the schematic figure of Fig. 39 and the region of compressed snow must have developed up to somewhere between these two soot lines. Therefore the height $h$ of the region of compressed snow can be determined by the present method only to the limit of the range from $h_1$ to $h_2$, where $h_1$ and $h_2$ are distances from the bottom of the weight to the lowest deformed soot line and to the undeformed one next below it respectively. (Here and in the following the bottom of the wooden board which was attached to the weight to press down the snow sheet will be called merely 'the bottom of the weight'.) In Fig. 52 $h_1$ and $h_2$ are plotted against depth $D$ of the bottom of the weight for snow samples of different sorts. The lower and the upper ends of vertical segments respectively show $h_1$ and $h_2$. The segments are located in the interior of the sectoral domain bounded by two straight lines $h=1.5D$ and $h=4D$, provided that $D$ is not larger than 13 cm. The upper ends of the vertical segments lie along

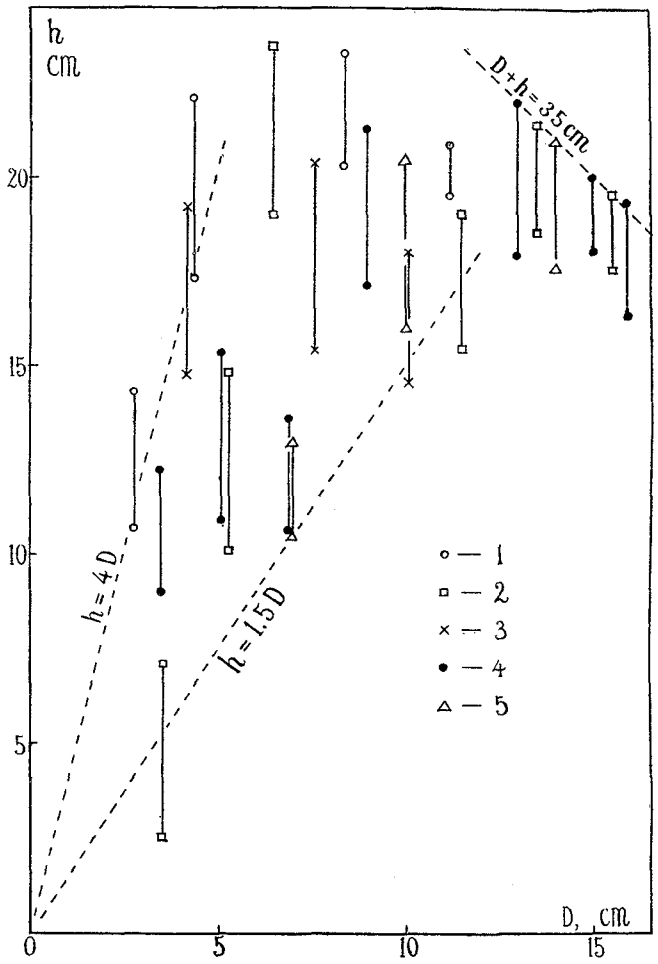


**Fig. 52** Relation between the height $h$ of the region of compressed snow and the subsidence depth $D$ of the weight. The value of $h$ is represented by some point on the vertical segment. The data here are taken from experiments on five snow samples, each sample being distinguished by different marks: 1 Newly deposited snow of Fig. 40; 2 Compact snow of Figs. 41, 47; 3 Compact snow of density 0.4 gr/cm$^3$; 4 Granular snow of Figs. 44, 49; 5 Composite snow of Figs. 46, 50.

straight line $D+h=35$ cm for the values of $D$ larger than 13 cm. This shows that the bottom of the region of compressed snow has reached the lowest zone of the snow sheet because the height of the snow sheet is 35 cm which value $D+h$ cannot exceed. Such segments come to lie outside the sectoral domain as value of $D$ becomes larger. Then it will be concluded that the height of the region of compressed snow is 1.5~4 times as large as the subsidence

depth of the weight as long as the region of compressed snow does not reach a rigid bed which stops its further development. When the development of the region is arrested its height diminishes and approaches to the depth of subsidence of the weight.

### §7 Propagation of break-down in the sheet of snow.

In the experiments described in the previous section the sheet of snow was broken down at first at its top following which action the process of break-down propagated downwards as the sheet was being pressed by the lowering weight. The broken down part was compressed by a finite amount discontinuously, that is, there took place a plastic compression. The break-down and the plastic deformation are quite different things in the cases of metals or other solid substances. The relation between strain and stress have been thoroughly investigated in respect to metals and such and the plastic deformation and the break down are seen to be distinctly distinguished on the stress-strain curve. But no such investigation has yet been reported on snow. Accordingly behavior of snow is left obscure beyond the elastic limit or the yield point. The structure of snow is very different from that of ordinary solid substances in that the snow is a porous substance with considerable vacant space in its interior. When snow is stressed beyond the yield point and is subjected to plastic deformation, some of the ice bonds connecting the ice granules in the snow will be broken down. In this sense the break down of snow will here be regarded as the same thing as plastic deformation. In order to study the propagation of the plastic compression in the sheet of snow, parts of Figs. 47 and 49 of the previous section showing the change in position of soot lines are reproduced in detail in Figs. 53 and 54, together with black blocks to represent the thickness of zones bounded by the soot lines.

The portion showing dotted lines on the left side of Fig. 53 is a copy of the part of Fig. 47 for the range of $n$ from 65 to 95. The uppermost dotted line marked 0 which represents the bottom of the weight began to descend at point a and, two units of $n$ after this, soot line 1 began to descend at point b. In this interval the upper most zone 1 between dotted lines 0 and 1 was compressed plastically by 3 mm as shown by the black block marked 1. Soot line 2 began to descend at point $c_1$ which is the same time point as b, showing that zone 2 between soot lines 1 and 2 descended as a whole at this time point. But the black block marked 2 shows that zone 2 underwent no compression at this descent. Therefore the plastic compression which had started at point a and proceeded downwards in zone 1 must have not intruded into zone 2. But, on the other hand, it cannot be said for certain that this plastic compression arrived actually at the bottom of zone 1. The small descent of zone 2 without compression rather suggests the arrival of only the forerunner of

the plastic compression at the bottom of zone 1 at point b. However, let it be here assumed for the sake of definiteness that the plastic compression had propagated through zone 1 and had reached its bottom, for there was no means to witness the displacement of snow by which the position of the head of plastic compression was to be determined except where the soot lines were drawn. Then it turns out that the plastic compression has traversed zone 1 which was 2.3 cm thick in two units of $n$, namely, in the time of 2/16 sec, which gives $C=18.4$ cm/sec as the velocity of propagation of plastic compression. Zone 2 which underwent no plastic compression only transported the pressure with infinite velocity to zone 3 underlying it. Zone 3 began to be

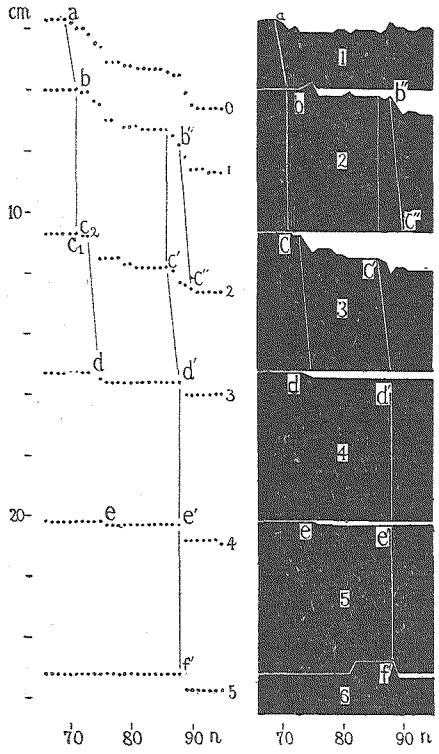


Fig. 53 The same compact snow as that of Fig. 47. Density: 0.21 gr/cm³.

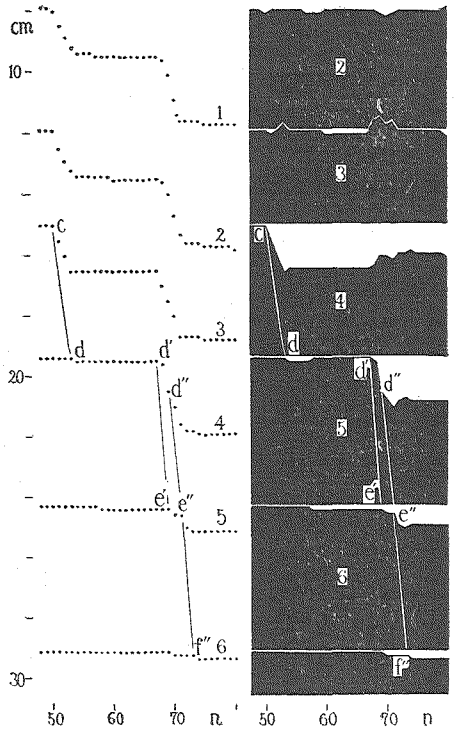


Fig. 54 The same granular snow as that of Fig. 49. Density: 0.32 gr/cm³.

compressed at point $c_2$ and the plastic compression reached its bottom at point d two units of $n$ later, in the same sense as explained above. The distance traversed by the plastic compression was 4.8 cm in this case; the velocity of its propagation is then equal to $C=38.4$ cm/sec.

The depression of the top of zone 1 which was the cause of starting the propagation of plastic compression in this zone was 0.3 cm, as shown in Fig.

53. Since this depression took place in 2 16 sec, the velocity $V_1$ of downward displacement of the top of zone 1 was equal to 2.4 cm/sec. The descent of soot line 2, the top of zone 3, starting at point $c_2$ proceeded with the velocity $V_1=5.6$ cm/sec to be stopped after having descended a distance 0.8 cm.

Zone 3 was subjected to another plastic compression starting at point c′ and reaching point d′ with velocities $V_1=4.0$ cm/sec and $C=30.4$ cm/sec. Immediately after the plastic compression in this zone had ended zone 2 lying above it began to be compressed at a rate $V_1=6.4$ cm/sec, the plastic compression propagating downwards with velocity $C=37.6$ cm/sec from point b″ to point c″. Two zones underlying zone 3 descended as a whole without undergoing any compression.

Fig. 54 represents the case of granular snow. The dotted line portion on the left side is the reproduction of Fig. 49 for the part from $n=50$ to $n=80$. There are three propagations of plastic compression: from point c to point d in zone 4, from point d′ to point e′ in zone 5 and from point d″ to point f″ through point e″ in zones 5 and 6. The last is the only case in which the plastic compression traversed two successive zones. Black blocks 5 and 6 show that these two zones underwent compressions of nearly the same amount in this process. The following table shows velocities $V_1$ and $C$ concerning these three propagations of plastic compression, together with those of the above described cases of Fig. 53.

| | Fig. 53 (compact snow) | | | | Fig. 54 (granular snow) | | |
|---|---|---|---|---|---|---|---|
| | a–b | c–d | c′–d′ | b″–c″ | c–d | d′–e′ | d″–e″–f″ |
| $V_1$ (cm/sec) | 2.4 | 5.6 | 4.0 | 6.4 | 8.0 | 8.0 | 10.4 |
| $C$ (cm/sec) | 18.4 | 38.4 | 30.4 | 37.6 | 23.5 | 35.2 | 32.8 |
| $\rho$ (gr/cm$^3$) | 0.41 | 0.21 | 0.25 | 0.22 | 0.32 | 0.32 | 0.48 |
| $e_1$ | 0.064 | 0.107 | 0.107 | 0.128 | 0.34 | 0.23 | 0.13 |
| $S$ (dyne/cm$^2$) | 116 | 130 | 138 | 135 | 153 | 190 | 295 |

According to the theory of plastic waves their front proceeds with a small velocity $C$ following the elastic waves which propagate ahead with the large velocity $c_0$ of sound (19). Let a matter distributed in an semi-infinite space bounded by a plane and extending in the range of co-ordinate $x$ greater than 0 be considered. When the boundary plane begins to be displaced with constant velocity $V_1$ at the time $t=0$, elastic compression starts to proceed into the matter with velocity $c_0$ followed by the plastic wave of compression of which the front advances with velocity $C$. The compressive strain $e$ due to the elastic wave is small. But $e$ increases gradually behind the elastic wave front and reaches a value $e_1$ at the plastic wave front to keep this value in the space swept already by it. This is shown in Fig. 55. The forerunner of the plastic compression referred to above concerning the small descent of

zone 2 in Fig. 53 may be considered to represent the range of strain $e$ between the fronts of the elastic and plastic waves. Let the modulus of deformation of the matter, elastic or plastic, be denoted by $S(e)=ds/de$ ($s$: stress) which is assumed to be determined by the value of strain $e$ alone imparted to the matter. $S(e)$ becomes equal to the compressive Young's modulus $E$ when the strain $e$ is reduced to below the yield strain of the matter. Then there hold the following relations:

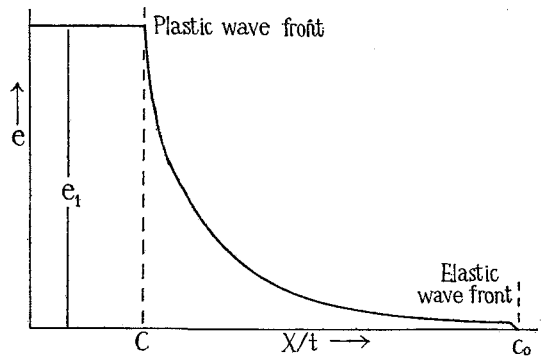


**Fig. 55** Distribution of strain $e$ in the proceeding elastic and plastic waves.

$$C^2=(S/\rho)_{e=e_1} \qquad (1)$$

$$c_0^2=E/\rho \qquad (2)$$

$$V_1=\int_0^{e_1}\sqrt{S/\rho}\,de, \qquad (3)$$

where $\rho$ denotes the density of the matter.

These results of the theory will be applicable at least approximately to the propagation of plastic compression in the snow sheet treated above in reference to Figs. 53 and 54. Then $V_1$ and $C$ in the above table correspond to $V_1$ and $C$ of the above formulae. The front of plastic compression proceeded downwards in the snow sheet with the velocity $C$, imparting to the snow which it swept a constant strain $e_1$ shown in the table. The values of $e_1$ were determined from Figs. 53 and 54 by dividing the depression of the soot line from which the plastic compression started by the height of zone which it traversed. The values of the modulus of deformation $S$ corresponding to the strain $e_1$ in the table are those computed by means of formula (1) and by the use of the values of $C$ and $\rho$ (density of snow) listed in the table. The table shows that $S$ comes to be reduced to the order of magnitude of $10^2$ dyne/cm$^2$ when the strain $e$ becomes as large as 10%, while $S$ takes values of the order of $E\sim10^7$ dyne/cm$^2$ for so small values of $e$ as 0.1% as stated above in §2.

The velocity $c_0=\sqrt{E/\rho}$ of the elastic wave front turns out to be of the order of magnitude $10^4$ cm/sec or 100 m/sec, since $E$ and $\rho$ are of the orders of magnitude $10^7$ dyne/cm$^2$ and 0.1 gr/cm$^3$ respectively. This is very much larger than the velocity $C$ of the plastic wave front shown in the above table. When the elastic strain alone but no plastic strain propagated as in the cases of zone 2 at $n=71$ and of zones 4 and 5 at $n=88$ in Fig. 53, the front of

elastic strain proceeding with the velocity $c_0$ made the displacements of the zones appear as if they propagated through the zones instantly with 'infinite' velocity.

The above described theory is valid only when the modulus of deformation $S$ remains finite and is determined uniquely by the strain $e$ alone. But these conditions appear to have not perfectly been satisfied in the case of snow of the present experiments. The weight which was used to compress the snow in the experiments intruded into snow stepwise, being held at a level for some time and then dropped suddenly to another level below. It is obvious that the strain $e$ of snow was maintained at a constant value while the weight was being held at a level. But the stress $s$ was increasing in this while. Therefore the modulus of deformation $S=ds/de$ must be infinitely great in this case (rigorously speaking, $S=E$ which is very large, in this case). While the weight was descending the strain $e$ as well as the stress $s$ were changing and the modulus of deformation $S$ must have a finite value. Fig. 34 of §5 contains two $D-P$ curves composed of vertical and horizontal segments. $D$, the subsidence depth of the weight into the snow cover, may be considered as a measure of the strain imparted to the snow lying below the weight. P, the pressure exerted by the weight to the snow, may be taken as stress produced in it. The horizontal segment shows that the weight was held by the snow at a certain depth below the snow surface and the vertical one shows the period while the weight was dropping in the snow towards another depth. Now two curves in Fig. 25 cross each other at several points. The snow must have the same strain $e$ on both the two curves at the cross point, since they are the results of experiments performed on snow of the same nature. But, as stated above, the modulus of deformation $S$ is infinitely large and of a finite value on the crossing horizontal and vertical segment at each cross point respectively. Hence the snow showed different values of $S$, one infinite and the other finite, for the same value of strain $e$.

Snow is a visco-elastic body as demonstrated in §1 and consequently its mechanical behavior depends largely on the rate of change $de/dt$ in strain imparted to it. Different values of $de/dt$ corresponded to two values of $S$ shown by the snow for one and the same value of $e$ in the case of the above paragraph: zero value of $de/dt$ for the infinite value of $S$ and a finite value of $de/dt$ for the finite $S$. Hence it seems promising to make $S$ a finite one-valued function of $e$ by attaching some conditions to the values of $de/dt$. Let the magnitude of strain of snow at its yield point be denoted by $e_y$, when the strain is increased at an infinite speed, that is, when $de/dt=\infty$. Then, if the relaxation time of snow is represented by $\tau$, $(de/dt)_0=e_y/\tau$ turns out to be a reference value of $de/dt$ in the following sense. When the snow is subjected to strain increasing at a rate much smaller than $(de/dt)_0$, the stress which is being produced in the snow by the increasing strain has sufficient time to be

relaxed and does not attain the yield value needful to break down the snow. On the other hand when the strain $e$ of snow is increased much more rapidly than at the rate $(de/dt)_0$, the stress $s$ also increases rapidly to break down the snow at the yield point, because $s$ has no or little time to be relaxed in this case. After the snow is broken down, $s$ will be reduced to a small value and the modulus of deformation $S=ds/de$ will come to show a small value.

In this way $S$ will come to be represented by a finite and unique function of $e$ provided that $e$ is increased at a rate $de/dt$ much larger than the reference rate $e_y/\tau$ given above. Such a large value of $de/dt$ checks the flow of snow due to its viscosity making the snow appear like a solid substance with no flowing property. Then the theory of plastic waves will be applicable to the propagation of plastic compression in the snow sheet under the condition that the function of $e$ determined in the above stated manner is used as the modulus of deformation $S$. Of course, for such an application to be valid, it must be shown that $de/dt$ was actually much greater than its reference value in the case of compression of zones of the snow sheet.

Haefeli showed that snow yielded at compressive pressure $s_y$ lying in the range $(0.14\sim1.6)\times10^6$ dyne/cm$^2$ (2). But he determined $s_y$ by increasing slowly the compressive pressure $s$ applied on the snow sample. The structure of snow is not uniform in microscopic scale. Hence, when the applied stress $s$ is rapidly increased, there must appear in the interior of the snow sample many spots of concentrated stress which are apt to become the starting points of fracture. But, when the stress is slowly applied, the concentrated stress has sufficient time to be relaxed with the result that the snow is not fractured. In this way the slow increase of the compressive pressure, that is, the small $ds/dt$ must have the same effect as that of a small $de/dt$ in this case. Hence $s_y$ determined by Haefeli must be much larger than that for infinite $de/dt$ and $s_y$ for infinite $de/dt$ may be taken as less than $10^5$ dyne/cm$^2$. Then $e_y=s_y/E$ is found to be $10^{-3}$ or thereabouts since Young's modulus of snow has the value of several $10^7$ dyne/cm$^2$. The relaxation time $\tau$ of snow is $4\sim15$ min or $(2\sim9)\times10^2$ sec as shown in § 2. Therefore the ratio $e_y/\tau$, the reference value of $de/dt$, will be of the order of magnitude $10^{-5}$/sec. The value of $de/dt$ in the case of the snow sheet of the present experiments can be obtained by dividing $V_1$ by the height $h$ (5 cm) of a zone of the snow sheet. Then the values of $V_1$ shown in the above table give $de/dt$ the value 1/sec or thereabouts which is $10^5$ times as large as the reference value.

The modulus of deformation $S$ of snow becomes very small compared with Young's modulus $E$ when the strain $e$ attains such a large value as $e_1$ shown in the table. Therefore snow can be regarded approximately as a perfectly plastic solid of which $S$ completely vanishes for the strain exceeding the yield strain $e_y$. Then the integral $\int_0^{e_1}\sqrt{S/\rho}\,de$ in formula (3) may be

replaced by $e_y\sqrt{E/\rho}=e_y\cdot c_0$ which yields the value 10 cm/sec for $e_y=10^{-3}$. The value of $V_1$ shown in the table which must be equal to the integral are somewhat smaller than its above computed value of 10 cm/sec. Such a discrepancy may be ascribed to the fact that the conditions demanded by the theory were not perfectly satisfied in the experiments.

## §8 Relaxation of stress in the snow sheet.

When a weight is being held by snow at any depth below the snow surface, the snow surrounding the region of compressed snow developed under the weight must be in a stressed state. The stress will be most intense at the bottom of the region of compressed snow and will be gradually diminished as the distance from that bottom is enlarged. But such an uneven distribution of stress will not be maintained as it is first spread, since the flowing property of snow must tend to make the stress be distributed uniformly throughout the snow. In order to study such a change in stress, pressure gauges were applied to the margin of the snow sheet described in the preceding two sections and the force exerted on them by the compressed snow was observed (16). The force measured by the pressure gauges is equal to the integral $\int X_x\,ds$, where $X_x$ is the component of stress tensor at the margin of the snow sheet expressed in the usual way in reference to the co-ordinate $x$ taken normal to that margin. The integral should be taken over the surface area of the metal plate E as will be described below in the next paragraph.

The pressure gauge used was such as shown at the bottom of the snow sheet in Fig. 39 of §6. G is a thick iron disc with a shallow hollow space which is covered by a plate of organic glass F. H is a glass tube connected to the hollow space in G. This closed hollow space in G and the lower half of the bore of H are filled with a mixture of water and alcohol. A clearance is made in the bottom of the wooden frame holding the snow sheet upright by cutting out a small portion of it and in this clearance a metal plate E is applied to the lower edge of the snow sheet. E is placed on the top of a metal rod stood on the organic glass plate F of the pressure gauge at its centre. When the snow presses E with a force, the centre of F is depressed and the mensiscus of the mixture in the bore of H is lifted by an amount proportional to that force. Such pressure gauges were mounted also at points $A_2$ and $A_3$ shown in Fig. 39 in addition to the one at point $A_1$, at the centre of the bottom of the snow sheet. Point $A_2$ is 15 cm distant from point $A_1$ on the bottom line of the snow sheet while point $A_3$ is located on the side edge of the snow sheet 12 cm above its bottom.

The metal plate E of the pressure gauge was applied to the edge of the snow sheet in such a way that E received no force from the snow at the begin-

ning of the experiment. If the snow were perfectly rigid and showed no deformation when pressed by the lowering weight, no force would be transmitted to the plate E even though the snow were much stressed. The bottom of the wooden frame would support all the force sharing out none of it to E. Therefore it is necessary for the force to be transmitted to E that the snow is so deformable that the edge of the stressed snow sheet intrudes into the clearance in the wooden frame when E is not in place. When E is put in place it can receive the force from snow by stopping the intrusion of snow into the clearance which would take place if E were not there.

The metal plate E was taken off and the weight was lowered into the snow sheet. Then its bottom actually intruded into the clearance made in the bottom of the wooden frame keeping itself horizontally straight. The observation by microscope showed that the intrusion was 0.07 mm and 0.90 mm respectively for 11 cm and 18 cm of the subsidence depth of the weight. Hence the intrusion would be about 0.02 mm for 2 cm of the subsidence depth. When E was put in place no such large intrusion occurred and the pressure gauge showed that a force of 100 gr-wt was exerted on E when the weight subsided 2 cm into the snow sheet. On the other hand it was learned by another experiment that a force of 100 gr-wt applied to E depressed it only by so small an amount as 0.0004 mm. Thus it is found that the metal plate E stopped 98% of the intrusion of snow amounting to 0.02 mm which the snow would have shown at the subsidence depth 2 cm of the weight if E had not been there.

The sensitivity of the pressure gauges was such that the meniscus of the mixture in the glass tube H is displaced by 25 mm when the metal plate is pressed by a force of 100 gr-wt. The mensiscus rose also in the case when the temperature was raised. Rise of temperature by 1°C made the meniscus rise by 45 mm. But such an effect of change in temperature could be completely eliminated by enveloping the pressure gauges thickly with snow.

The results of experiments on the snow sheet which are now being described hold good under the assumption that the two sheets of organic glass plate holding the snow sheet between exert no influence upon its motion. But such a situation cannot be realized in the actual case since the glass plates must be acting on the snow sheet with a certain frictional force. Therefore, for the experimental results to be significant, the frictional force $F_r$ acting on any portion of the snow sheet needs to be small as compared to the force $F_s$ with which the stress in the snow sheet is tending to move that part. $F_r$ will be shown to amount at greatest to one-twentieth of $F_s$ from the results of experiments which will be described in the next.

Fig. 56 represents an example of the results of experiments in which the wire rope suspending the weight by way of the helical spring was unrolled in two or three minutes. Since the time of the experiment was shorter than the relaxation time of snow the change in force due to the flow of snow did not

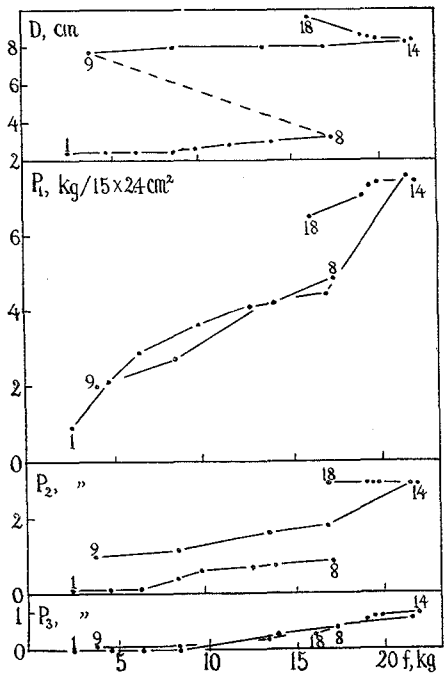


Fig. 56 $D$, $P_1$, $P_2$, $P_3$ versus $f$. $D$: depth by which the bottom of the wooden board attached to the hanged weight of Fig. 39 of §6 subsides into the snow sheet. $P_1$, $P_2$, $P_3$: pressure measured by the pressure gauges mounted on the margin of the snow sheet at points $A_1$, $A_2$, $A_3$ of Fig. 39 respectively. $f$: force with which the bottom of the wooden board presses the snow sheet. Density of snow: 0.30. Temperature: −1.2°C.

appear on the pressure gauges distinctly. The top figure of Fig. 56 shows the relation between the subsidence depth $D$ of the weight and force $f$ with which the bottom of the weight presses the snow sheet. $f$ can be determined by the length of the helical spring. The figure shows the process which went on after the weight had subsided to $D=2.4$ cm. $f$ increased gradually as the wire rope suspending the weight was unrolled. While $f$ remained less than 8.7 kg-wt, $D$ was subjected to no change, but after that, $D$ began to increase slowly to attain the value 3.2 cm at the point marked 8 when $f$ became as large as 17.4 kg-wt. Then the weight suddenly fell; $D$ increased to 7.8 cm while $f$ was diminished to 3.8 kg-wt as shown by point 9. After this the process went on as shown by the line from point 9 to point 14 with little change in $D$. At point 14 the weight came near falling again and the unrolling of the wire rope was stopped. Then, instead of falling rapidly, the weight began to settle slowly with decreasing $f$ along the line from point 14 to point 18.

The other three portions of Fig. 56 show the pressures $P_1$, $P_2$, $P_3$ determined by the pressure gauges against $f$; $P_1$, $P_2$, $P_3$ refer to the gauges placed at points $A_1$, $A_2$, $A_3$ respectively. Here kg-wt/(15×2.4 cm²) is used as the unit to express the pressures. 15×2.4 cm² is the area of the bottom of the weight, that is, that of the bottom of the wooden board pressing down the snow sheet with the force $f$. Therefore $f$ expressed by the unit kg-wt comes to be numerically equal to the average pressure at the bottom of the weight if it is expressed by the above-stated pressure unit. Use of such a conception of a pressure unit will make it easy to consider the relations between $f$ and $P$'s.

$P$'s increase nearly in proportion to the increase of $f$; $P_1$, $P_2$, $P_3$ are about 1/3, 1/10, 1/25 of $f$ for any value of it respectively. The bottom of the wooden frame is about three times as wide as that of the wooden board pressing the

snow sheet. $P_2$ is the pressure at the centre of one of the side thirds of the bottom of the wooden frame while $P_1$ is the pressure at the centre of the central third. Then the above described ratios between $P$'s and $f$ make it plausible that the whole length of the bottom of the wooden frame supports about one-third of the force $f$ with which the weight presses down the snow sheet. The side uprights of the wooden frame may be supporting some part of $f$ by frictional force. But this will be left out of consideration since it cannot be great because of the smallness of $P_3$. Then it turns out that the organic glass plates participate in supporting the weight by imparting to the snow sheet a frictional force amounting to two-thirds of $f$. Hence, if the frictional force per square centimeter on the surface of the snow sheet is denoted by $F_r$, its average value $\overline{F_r}$ comes to be equal to $(2f/3)/(34\times42)$, since the snow sheet is 34 cm high and 42 cm wide.

Let here a rectangular column of unit sectional area standing perpendicular to the surface of snow sheet be imagined somewhere on the vertical central line of it. The gradient $dX_x/dx$ of pressure of snow ($X_x$: one component of the stress tensor which was explained in the first paragraph of this section) along this central line is nearly equal to $(\frac{2}{3}f)/34$, since the difference between the pressures at the bottoms of the weight and of the wooden frame is about $2f/3$ while the distance between the two bottoms is about 34 cm. The height of the rectangular column is 2.5 cm, being equal to the thickness of the snow sheet. Therefore the force $F_s$ with which the pressure $X_x$ in the snow sheet tries to move downwards the snow contained in the rectangular column comes to be equal to $2.5\{(2f/3)/34\}$. On the other hand the organic glass plates try to prevent this movement with the above stated frictional force $F_r$. The larger the pressure $X_x$ in the snow sheet is, the larger $F_r$ will be. Hence $F_r$ acting on the rectangular column will be larger than its average value $\overline{F_r}$ since the presure is largest on the central line of the snow sheet. But the fact that the pressure is not zero even on the side margins of the snow sheet as shown by the finite value of $P_3$ shows that the pressure is not much concentrated on the central line but that its distribution is tolerably even throughout the whole snow sheet. Therefore it may be safely said that $F_r$ acting on the column is at greatest five times as large as its average value $\overline{F_r}$. Then the ratio of $F_r$ to $F_s$ acting on the rectangular column on the central line of the snow sheet comes to be $(5/42):2.5$, that is, about 1/20 as previously noted.

In addition to $F_r$ and $F_s$, one more force $F_s'=dX_y/dy$ acts on the rectangular column in the vertical direction. $F_s'$ arises from the shearing stress $X_y$ which is exerted upon the column through its vertical side surfaces. Here $y$ denotes the co-ordinate taken horizontally perpendicular to the vertical direction of $x$. Since $F_r+F_s+F_s'$ must be equal to or nearly equal to zero and since $F_r$ is very small as compared to $F_s$ as shown above, $F_s'$ must be of the same order of magnitude as $F_s$. Then the motion of the rectangular column is determined

for the most part by $F_s$ and $F_s'$ which arise from the stresses in the snow sheet, $F_r$ contributing only a little to the motion. In this way it is proved that the organic glass plates holding the snow sheet have little influence upon the state of the snow sheet whether it is in static equilibrium or is undergoing mechanical change.

Fig. 57 shows the course of change in $P_1$ when the weight was left to press the snow sheet without being suspended by the spring. Since the weight pressed the snow sheet with its whole force in this case, $f$ remained constant as long as the weight remained unchanged. $P_1$ rose to 0.37 as soon as the weight of 6.4 kg was applied at first and then increased to the maximum value 0.39 in 3 min. Then it began to decrease to reach 0.34 at $t=9$ min, where $t$ is the time counted from the application of the weight. After $t=10$ min, $P_1$ continued to decrease at a constant small rate. When the weight was increased to 12.4 kg at $t=30$ min, $P_1$ rose rapidly to a higher value and then continued to increase for about 5 min. Then it began to decrease again at a constant small rate. After the second increase of $f$ at $t=42$ min, $P_1$ continued to increase up to $t=54$ min, when the observation was discontinued.

The changes observed on $P_1$ before it began to decrease at a constant small rate were completed in several minutes; that period is of the same order of magnitude of the relaxation time of the snow as shown in § 2. There-

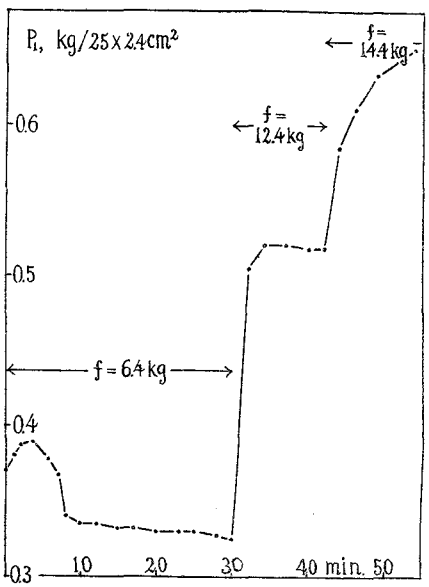


Fig. 57 Change in $P_1$ observed when the weight is pressing the snow sheet with its whole weight. The weight is not suspended in this case.

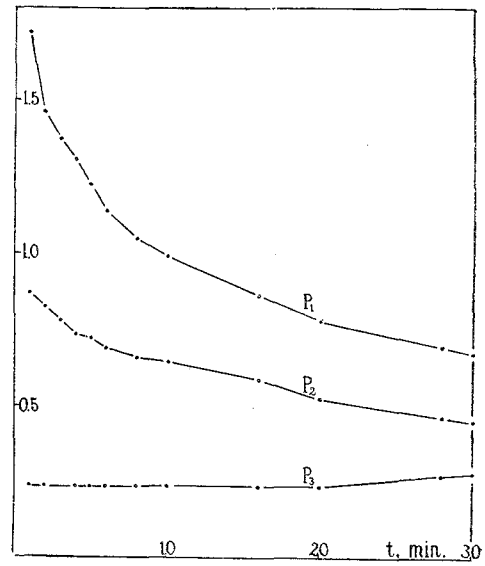


Fig. 58 Change in $P_1$, $P_2$, $P_3$ observed when the weight suspended by an unextensible wire rope is applied to the snow sheet. Density of snow: 0.35. Temperature: $-5$°C.

fore such changes in $P_1$ probably had their rise in the visco-elastic property of the snow. The pressure at the bottom of the snow sheet should continue to be largest at its central point if the snow were perfectly elastic, and $P_1$ is the pressure at this central point. But the snow actually has flowing property. Hence $P_1$ could not be maintained at its initially established largest value but could be gradually decreased because the flowing property of snow would tend to cause a spreading of the pressure uniformly throughout the snow sheet. The above described decrease in $P_1$ at a constant small rate seems to be an indication for this circumstance.

When the weight suspended directly by the wire rope but not through the helical spring was lowered into the snow sheet and was kept at a definite depth, $P_1$, $P_2$, $P_3$ changed with time as shown in Fig. 58. $P_1$ and $P_2$ continued to decrease while $P_3$ showed a slight tendency to increase as time went on. The final uniform distribution of pressure in this case should be such that the pressure is zero throughout the whole snow sheet since the weight was being suspended by an unextensible wire rope. The stresses initially established in the snow sheet would be allowed to relax without limit gradually delivering their initial load to the wire rope suspending the weight. The increasing tendency of $P_3$ shown above would be only a temporal occurrence taking place on the way of the general decrease of $P_3$ to a value of zero. Indeed in another experiment of the same sort performed under the same conditions as above, $P_1$, $P_2$, $P_3$ all continued to decrease towards zero.

## Summary

§1. **Compressive nature of snow.** A pillar of snow was loaded with a weight and the contraction to which the pillar was subjected was observed by means of a telescope and scale in the cold room attached to the Institute. At the moment of application of the load an instantaneous contraction appeared. After this the contraction slowly increased at a decreasing rate and finally it came to increase at a constant small rate. Then, when the load was removed, the pillar was elongated promptly by nearly the same amount as that of the initial instantaneous contraction to be followed by a slow elongation which gradually ceased. The amount of contraction which was produced in the period of contraction at the constant small rate was left behind as the permanent contraction without being recovered.

The strain-time curve obtained on the snow pillar in the above described way was shown to be brought into coincidence with the strain-time curve of the rheological model composed of Maxwell- and Voigt-unit models in series connection by giving suitable values to the four characteristic constants of the model. Therefore the compressive nature of snow comes to be represented by four characteristic constants $E_1$, $\eta_1$, $E_2$, $\eta_2$, where $E_1$, $E_2$ are elastic constants

while $\eta_1$, $\eta_2$ are viscous constants. It should be noticed, however, that the characteristic constants once determined on a snow sample cannot always preserve the same values since the snow changes its structure as time goes on.

## §2. Characteristic constants determining the compressive nature of snow.

(*a*) *Non-dependence of the constants $E_1$ and $\eta_1$ on the strength of compressive pressure.* When different compressive pressures were applied to different snow pillars of the same nature each of which had not previously been stressed, $E_1$ was shown to have nearly the same value on all of the snow pillars regardless of the strength of the compressive pressure. On the other hand $\eta_1$ was found to keep its value unchanged when the compressive pressure acting on one and the same snow pillar was increased stepwise.

(*b*) *The characteristic constants and the temperature.* All the four characteristic constants showed a tendency to increase with lowering temperature. The dependency of $\eta_1$ on the absolute temperature $T$ was found to be expressed by the formula:

$$\eta_1 = A \exp(Q/RT),$$

with $Q=20.8$ and 23.8 kcal/mole for two samples of snow.

(*c*) *The characteristic constants and the density of snow.* The following relations were found to hold, though not very precisely, between $E_1$, $\eta_1$ and the density $\rho$ of snow:

$$\begin{aligned} E_1(10^7\ \text{dyne/cm}^2) &= -1.5+(40/3)\rho \quad \text{for } -1\sim-3^\circ\text{C} \\ &= -5.4+36\rho \quad \text{for } -5\sim-15^\circ\text{C} \\ 1/\eta_1(10^7\ \text{dyne}\cdot\text{min/cm}^2) &= 2-6.5\rho \quad \text{for } -1\sim-3^\circ\text{C} \\ &= 0.85-3\rho \quad \text{for } -5\sim-15^\circ\text{C}. \end{aligned}$$

$E_2$ was found to be 2~4 times as large as $E_1$ for $\rho=0.1\sim0.2$ and temperatures higher than $-1.5^\circ$C. $E_2$ was reduced to less than $2E_1$ when $\rho$ exceeded 0.2 and temperature sank to below $-10^\circ$C. $\eta_2$ was generally less than $\eta_1$; $\eta_2$ lay between $0.7\eta_1$ and $0.9\eta_1$ for $\rho=0.1\sim0.2$ and temperatures higher than $-1.5^\circ$C, while it was reduced to about $0.1\eta_1$ for $\rho>0.2$ and temperatures lower than $-10^\circ$C. The relaxation time $\tau_1=\eta_1/E_1$ and the retardation time $\tau_2=\eta_2/E_2$ were found to be 4~15 min and 0.5~1 min respectively, independently of density and temperature.

(*d*) *The characteristic constants influenced by the compressive pressure which has previously been applied to the snow.* Let the increment of the strain produced elastically on a snow pillar at the moment when the compressive pressure $p$ acting on the pillar was increased by $\Delta p$, be denoted by $\Delta s$. Then the ratio $\Delta p/\Delta s$ showed the tendency to be increased as $p$ was increased

stepwise by the addition of $\Delta p$'s. Therefore $E_1$ appeared to increase as $p$ was enlarged step by step. As described in article (*a*) of this section $\eta_1$ kept its value unchanged when $p$ was increased stepwise. But, when $p$ was removed after it had been increased to some large value and then it was again increased stepwise, $\eta_1$ showed in this case a value larger than before.

(*e*) *Some notes on the present experiments.* (*i*) In order to examine whether the end effects of the snow pillar had any influence or not on the results of experiments, elastic and viscous constants were measured on two pillars of the same nature but of different lengths. The constants were found to be nearly the same independently of the lengths of the snow pillar. (*ii*) The snow pillars were found to give nearly the same elastic and viscous constants no matter whether they had been cut out from the snow cover in the horizontal direction or in the vertical direction. Therefore snow seems to be isotropic in its mechanical properties.

**§ 3 Viscous compression of snow layers composing snow cover.** In the experiments described in the previous sections the snow was subjected to compressive pressures which lasted only for ten minutes or thereabouts. The viscous response of snow to the compressive pressures lasting for many weeks was studied on the snow layers composing snow cover lying on the ground. The thickness $h$ and the density $\rho$ were measured on each of the snow layers every five or six days. The compressive pressure $w_i$ acting on the $i$-th layer could be determined by

$$w_i = \tfrac{1}{2}\rho_i h_i + \sum \rho_j h_j ,$$

where $\rho_j$'s, $h_j$'s are the density and thickness of the layers lying above the $i$-th layer respectively. Then the viscous constant $\eta_i$ of the $i$-th layer was given by

$$\eta_i = w_i / \{(d_i\rho_i/dt)/\rho_i\} .$$

The course of change in $\eta_i$ with time $t$ was found to be expressed by the formula

$$\eta = \eta_0 \, exp \, (a\sqrt{t}),$$

where $\eta_0$ and $a$ are constants. These constants varied from one snow layer to another but their variations were confined within narrow ranges. Therefore, as an average value, $\eta$ can be given by

$$\eta = 10 \, exp \, (\sqrt{t}) \text{ gr-wt} \cdot \text{day/cm}^2 ,$$

where $t$ should be counted by days. Not only $\eta$ but also the density $\rho$ of snow increased with time. The following average relation was found between $\eta$ and $\rho$.

$$\eta = 1.5\, exp\,(21\rho)\ \text{gr-wt}\cdot\text{day/cm}^2\,.$$

Throughout the period of observation the snow layers on which the observations were made were neither cooled down to below $-3°C$ nor so warmed as to be melted.

**§ 4. The visco-elastic constants in the case of lateral vibration of snow bar.** In order to study the visco-elastic properties of snow in the case of rapidly changing strain, the resonance vibration and the attenuation of vibration were observed at various temperatures below 0°C on a rectangular bar of snow which was excited by an oscillating electric current to vibrate laterally. The dimensions of the snow bar were so chosen that it vibrated with a resonance frequency $f$ lying in the range 200~300 cycles/sec.

The amplitude $A$ of vibration attenuated after the formula

$$A = A_0 e^{-\lambda t} \sin 2\pi f t\,,$$

after the exciting electric current was cut off. The attenuation constant $\lambda$ was found to change with temperature in such a way that $1/\lambda$ is related to the absolute temperatur $T$ by

$$1/\lambda = B\, exp\,(Q/RT)\,,$$

which formula holds generally for the viscosity of solids and liquids. Moreover the constant $Q$ in that formula was found between 10 and 20 kcal/mole which values are not far apart from those found on the viscous constant of snow in the case of the statical experiment. If the mechanical properties of the vibrating snow bar are represented by a single Maxwell unit model, it can be shown that the mathematical expression of the constant $Y$ respecting the internal friction of snow must contain the viscous constant $\eta_1$ of snow in the denominator. On the other hand $Y$ is generally a quantity which is proportional to $\lambda$. Therefore it may safely be concluded that the snow is represented rheologically by a Maxwell unit model when it is subjected to vibrational motion.

The elastic constant $E_1$ of the vibrating snow was found to be about a hundred times as large as that which the snow shows when influenced by statical compression. On the other hand the viscous constant $\eta_1$ was reduced to a few thousandths of its value in the case of statical compression. Hence the relaxation time $\eta_1/E_1$ comes to lie in the range 0.001~0.1 sec in the case of vibrating snow.

The amplitude of vibration of the snow bar was determined by a microscope; the geometrical calculation showed that the top and bottom surfaces of the bar were subjected to stress more than 200 gr-wt/cm$^2$—a value greater than the yield stress of snow in the usual case.

**§5. Load supporting strength of snow cover.** When a load of weight $W$ is put on the surface of snow cover, the load sinks to a depth $D$ in it and is supported there. In order to find the relation between $W$ and $D$ promptly, a cylindrical weight suspended by a wire rope through a helical spring was lowered onto the snow cover. As soon as the weight touched the snow surface the spring began to contract and the weight began to press the snow surface with increasing pressure $P$. When $P$ reached some value $P_0$ the snow broke and the weight fell a distance $D_1$ abruptly, at the same time the spring being lengthened and $P$ being reduced to a value less than $P_0$. As the upper end of the spring was lowered further, $P$ again increased with the weight at this new position until it attained a value $P_1(>P_0)$ when the snow broke for the second time. On further lowering of the spring such a process was repeated and the maximum pressure $P_n$ which the snow could bear at the depth $D_n$ was determined. Then the load supporting strength of the snow at the depth $D_n$ may be said to be represented by the range of pressure from $P_{n-1}$ to $P_n$.

The discrete values, $D_n$'s, of the depth at which the weight was held were found to be changed when weights of different diameters were used. Hence $D_n$'s are not depths which are determined by the nature of the snow cover alone.

There developed under the bottom of the weight a cylindrical region of compressed snow. The weight pressed the top of this region and the latter must be held by a force $f_b$ which the surrounding snow exerted on its bottom. But, in addition to $f_b$, there might be acting another force $f_s$ which acted on the side surface of the region of compressed snow and took part in holding it. When the weight was applied to a pillar of snow with the same diameter as that of the weight each of the $D_n$'s was found to be larger than in the case of the above described experiments on the snow cover in the ordinary conditions. Obviously the force $f_s$ was absent in the case of snow pillar. Hence the above fact can be considered as an item of evidence for the existence of the force $f_s$.

**§6. Development of the region of compressed snow below the bottom of load.** A sheet of snow 2.5 cm thick was held upright between two plates of organic glass and pressure was applied on a portion of its top surface by lowering a wooden board which was attached vertically to the bottom of the weight described in the previous section. Horizontal dark lines which had been drawn with soot on the surface of the snow sheet were deformed as the wooden board intruded into the snow sheet. The process of deformation of the soot lines was taken by a cinematograph, which displayed how the region of compressed snow developed beneath the lowering wooden board. The deformation of soot lines was found to differ in accordance with the different sorts of snow.

The height of the region of compressed snow was found to be 1.5 to 4 times as large as the depth by which the bottom of the wooden board subsided below the top surface of the snow sheet as long as the region of compressed snow did not reach the rigid bed at the bottom of the snow sheet. When the development of the region was arrested by the rigid bed its height began to diminish to approach the depth of subsidence of the wooden board.

§7. **Propagation of break-down in the sheet of snow.** The change with time in the height of the zones bounded between adjacent soot lines drawn horizontally on the snow sheet described in the previous section was examined in detail and a study was made of the downward propagation of the plastic compression through the snow sheet caused by the lowering wooden board. It was found that the front of the plastic wave propagated with the velocity $C=20\sim 30$ cm/sec in the snow sheet. From this value of $C$ and the results of the theory of plastic waves it was concluded that the modulus of deformation $S$ of snow was reduced to such a small value as $10^2$ dyne/cm$^2$ when the snow was plastically subjected to such a large strain as 10%, while $S$ is, for so small a strain as 0.1%, nothing other than the compressive Young's modulus which was shown in §2 to have such a large value as $10^7$ dyne/cm$^2$.

§8. **Relaxation of stress in the snow sheet.** Pressure gauges were mounted on the margin of the snow sheet and the pressure which was caused on that margin by the stress produced in the snow sheet was measured by these gauges while the wooden board described in the previous two sections was being lowered into the snow sheet. From the magnitude of pressure observed by the gauges it was found that the gradient of stress in the snow sheet was about twenty times as large as the frictional force exerted on the snow sheet by the glass plates holding it. This is an item of evidence for the belief that the glass plates had little influence on the motion of the parts of the snow sheet caused by the lowering wooden board, which was an important condition if the results of the present experiments on the snow sheet are to be considered valid.

The weight was applied to the snow sheet without being suspended and the pressure was observed for half an hour. In several minutes after the weight was applied or after the load of the weight was changed, the pressure continued to change with a considerable rapidity. After that, however, the pressure began to decrease slowly showing that the stress was tending to be distributed evenly throughout the snow sheet owing to the flowing property of snow. In another case the weight suspended by an unextensible wire rope was made to intrude into the snow sheet and was kept at a definite position in it. The pressure on the margin of the snow sheet continued to diminish tending to zero which value the pressure should have when the stress in the snow sheet would have been completely relaxed.

## References

"T. K." in the following is the abbreviation for "Teion-Kagaku" (Low Temperature Science), a scientific publication written in Japanese, issued by the Institute of Low Temperature Science, Hokkaido University, Sapporo, Japan.

(1) M. De Quervain 1946 Kristallplastische Vorgänge im Schneeaggregat II. Mitteilungen aus dem eidg. Institut für Schnee- und Lawinenforschung.

(2) R. Haefeli 1939 Schneemechanik mit Hinweisen auf die Erdbaumechanik. Beiträge zur Geologie der Schweiz—Geotechnische Serie—Hydrologie, Lieferung 3.

(3) Edwin Bucher 1948 Beitrag zu den theoretischen Grundlagen des Lawinenverbaus. Beiträge zur Geologie der Schweiz—Geotechnische Serie—Hydrologie, Lieferung 6.

(4) Zyungo Yosida, Masanobu Sasaya, Takehiko Utumi 1948 Elastic modulus and creeping velocity of snow. T. K. **4**, 11–16.

(5) Zyungo Yosida 1953 Visco-elastic property and break-down resistance of snow. T. K. **10**, 1–11.

(6) Kenji Kojima 1954 Visco-elastic property of snow. T. K. (Physics) **12**, 1–13.

(7) Tadashi Tabata 1955 A measurement of the visco-elastic property of sea-ice. T. K. (Physics) **14**, 25–31.

(8) J. W. Glen 1955 The creep of polycrystalline ice. Proc. Roy. Soc. London, (A) **228**, 519–538.

(9) Kenji Kojima 1955 Viscous compression of natural snow layer, I. T. K. (Physics) **14**, 77–93.

(10) Markus Reiner 1949 Twelve lectures on theoretical rheology, p. 31.

(11) R. Saito 1949 Physics of fallen snow. Geophysical Magazine (published by the Central Meteorological Observatory, Tokyo) **19**, 1–56.

(12) Kenji Ishiwara 1951 The forecast on the change of daily snow cover depth (in Japanese). Journ. of Japanese Society of Snow and Ice. **13**, 1–5.

(13) Kenji Yamaji, Daisuke Kuroiwa 1954 Study of elastic and viscous properties of snow by the vibration method. T. K. (Physics) **13**, 49–58.

(14) T. C. Baker, F. W. Preston 1946 Fatigue of glass under static loads. Journ. of Appl. Phys. **17**, 170–178.
J. L. Glathart, F. W. Preston 1946 The fatigue modulus of glass. Journ. of Appl. Phys. **17**, 189–195.

(15) Sueo Izumi 1928, 1931 Researches on snow, I, II (in Japanese). Kisho Zassan (Published by Central Meteorological Observatory, Tokyo) **5**, 101; **6**, 1.

(16) Zyungo Yosida, Tosio Huzioka 1950 Load supporting force of snow layer. T. K. **3**, 109–121.

(17) Iwao Furukawa, Yoshimi Shirai 1948 Resistance of snow against a slow compression. Journ. of Japanese Society of Snow and Ice. **10**, 128–132.

(18) Tosio Huzioka 1956 Cinematographic studies on the subsidence of a load into snow. (will be published in T. K. **15**)

(19) H. Kolsky 1953 Stress waves in solids. Chapter VII.

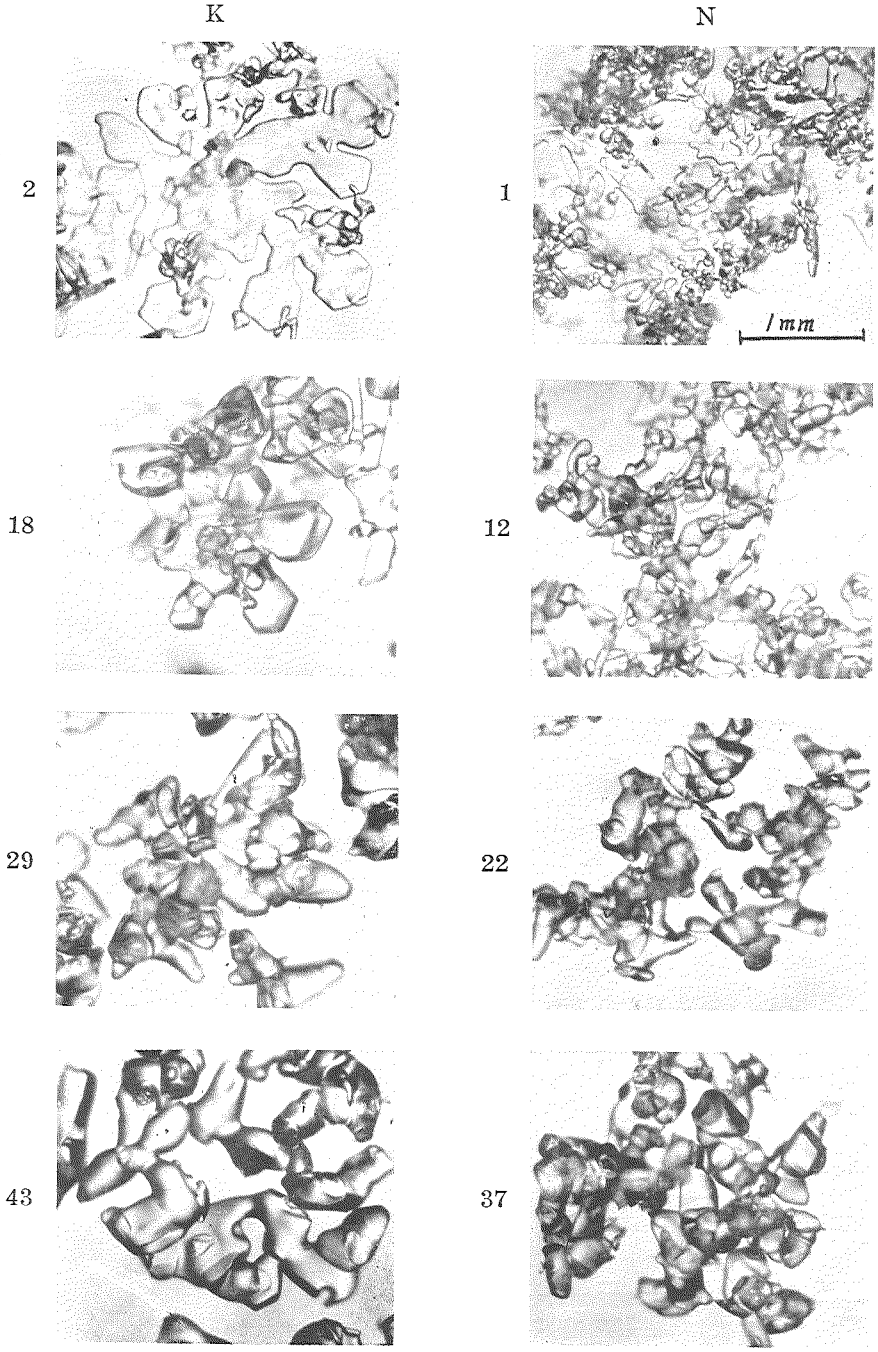


**Fig. 18** Metamorphosis of snow crystals which were deposited to form snow layers K and N. Numbers written beside the photographs are those of days passed since the crystals were deposited.

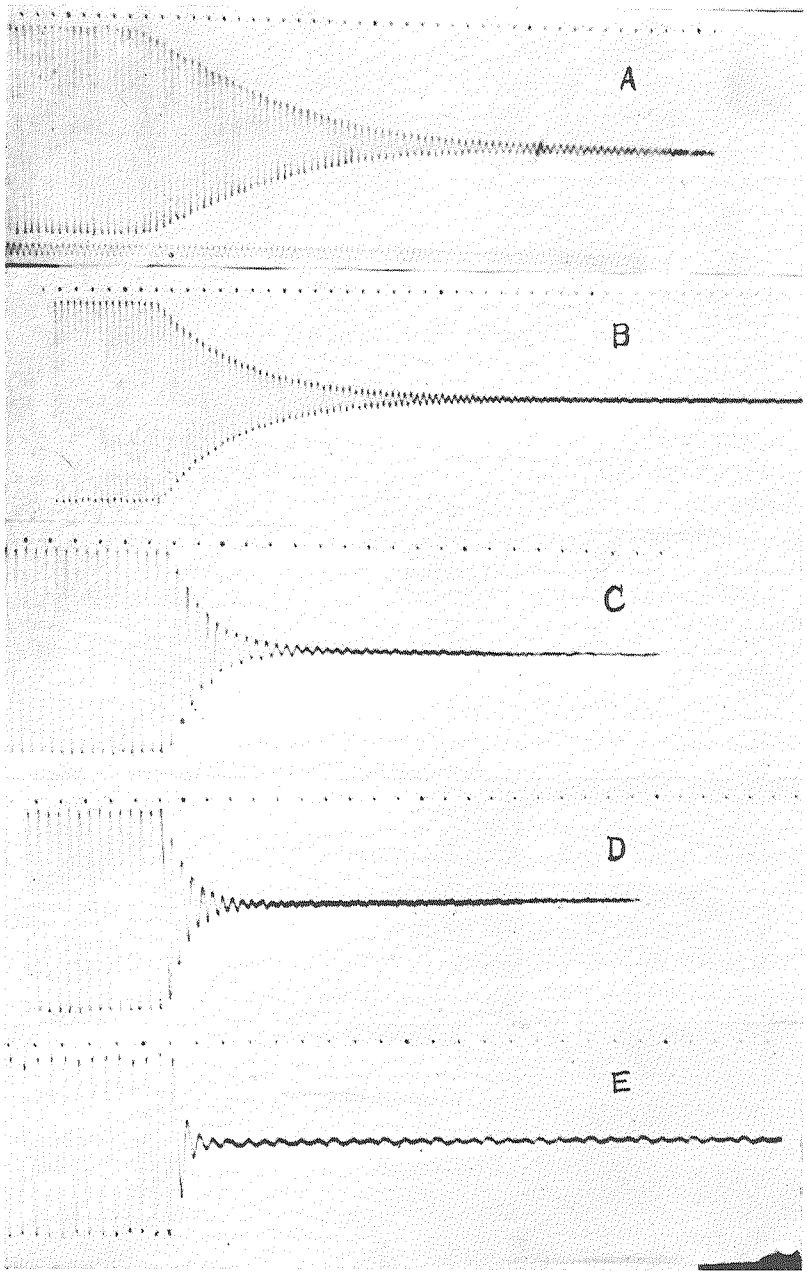


Fig. 24 Attenuation of vibration of snow bar (density: 0.33). Attenuation becomes weaker as the temperature is lowered. A: −37.0°C, B: −22.5°C, C: −15.5°C, D: −12.0°C, E: −3.0°C. Dots at the top of each figure are time marks, the interval between two adjacent dots corresponding to 0.01 sec.

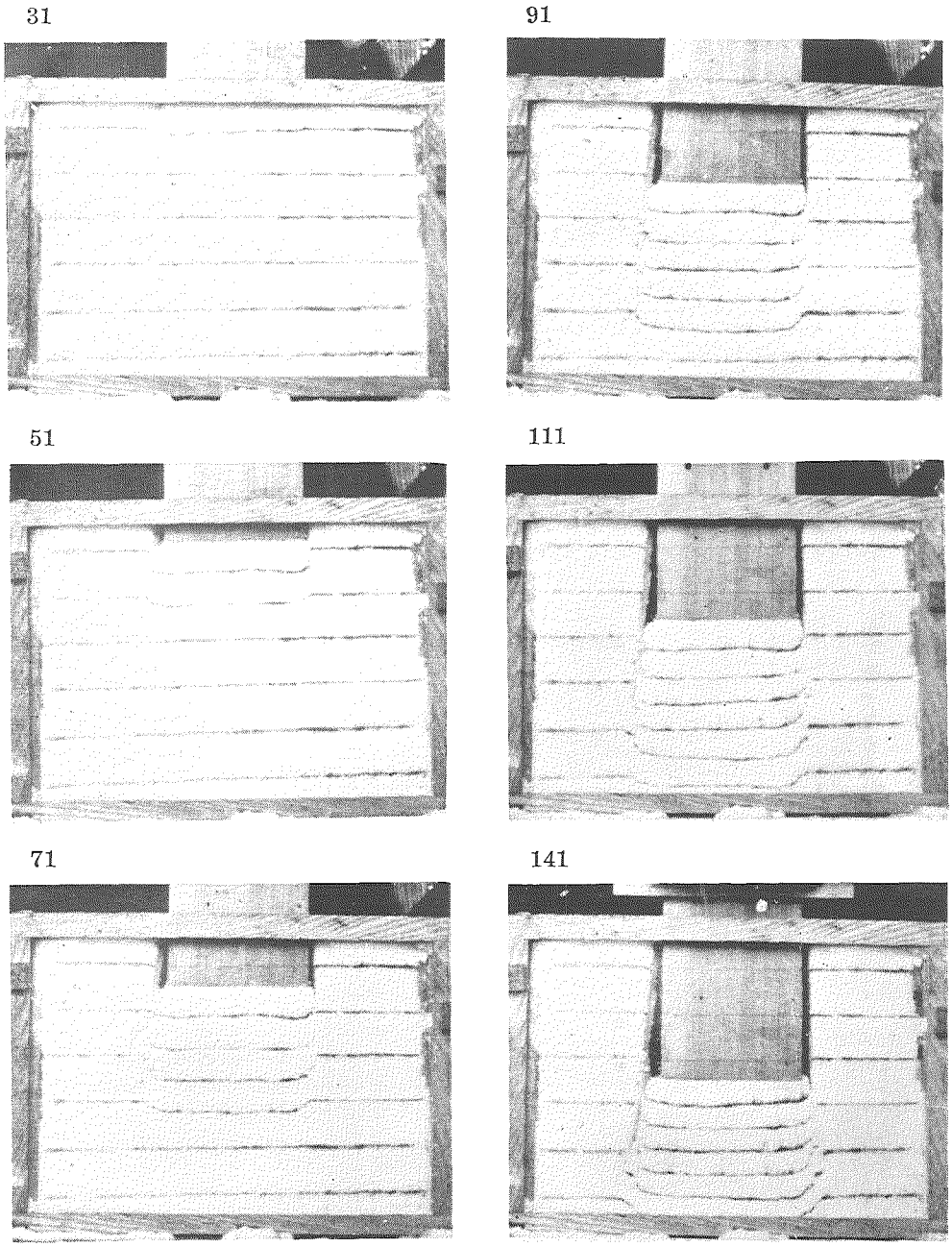


Fig. 40 Newly deposited snow. Density: 0.07 gr/cm³. Temperature of snow: −2.5°C. The series of photographs shown in Figs. 40 to Fig. 46 are picked out from the cinematographic films to show the development of the region of compressed snow under a load. The region is displayed by deformations of the soot lines. Numerical figure attached to the picture is the number of picture counted from the beginning of experiment. Sixteen pictures were taken per second.

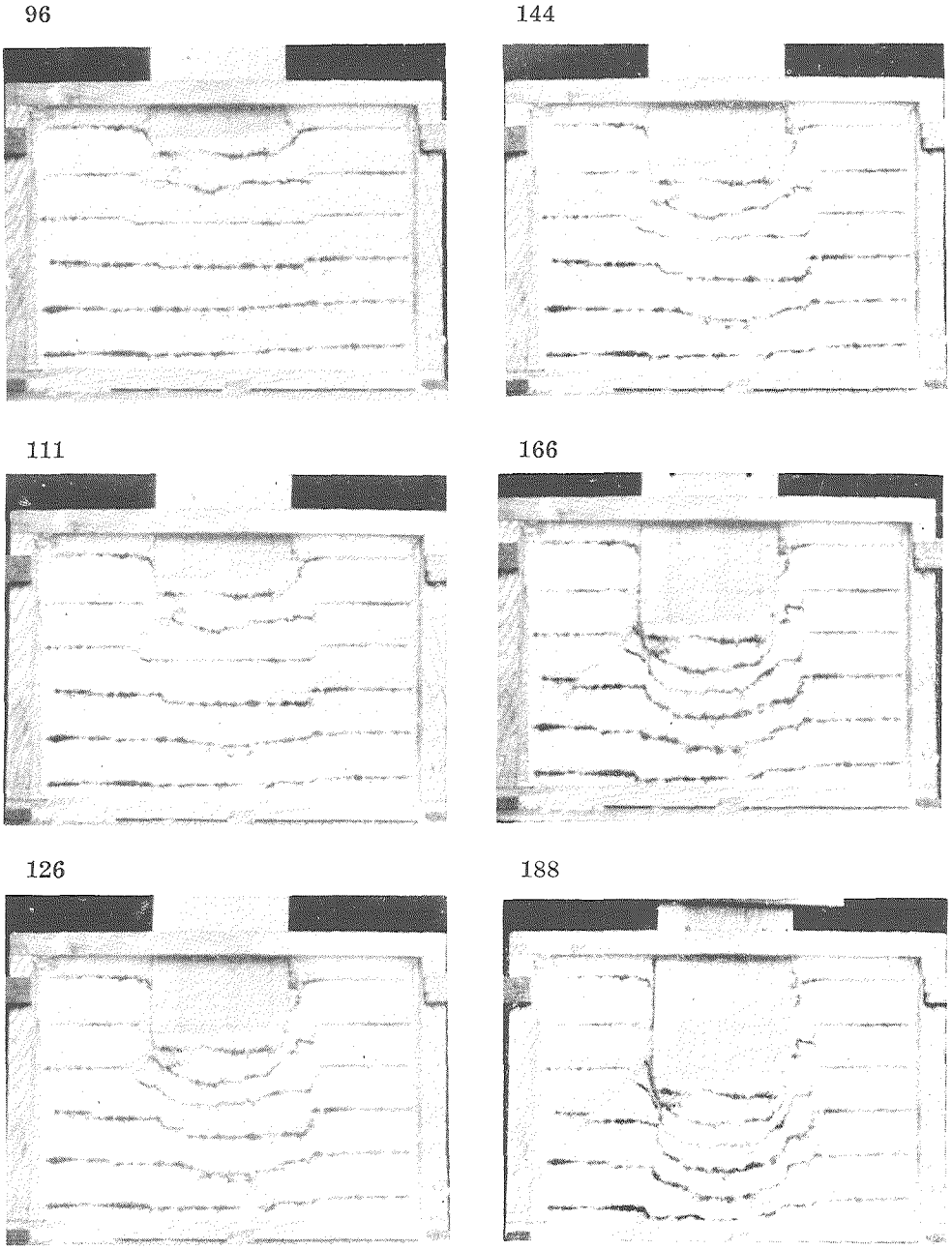


**Fig. 41** Compact snow. Density: 0.21 gr/cm³. Temperature of snow: −3.5°C. It should be noticed that the second zone between soot lines counted from above is thicker than the third zone. Such a reversal in thickness of zones is found also between the fifth and the sixth zones.

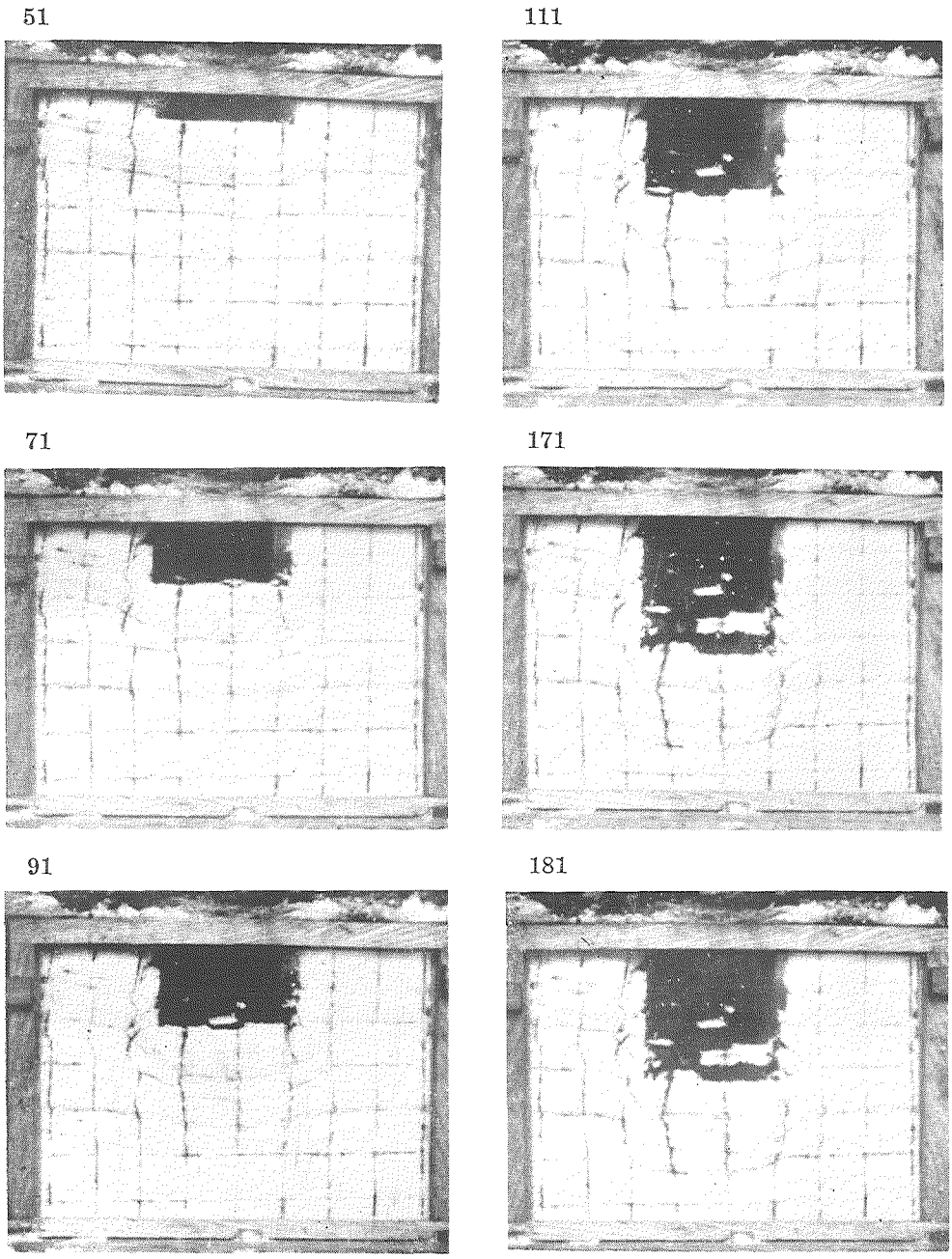


**Fig. 42** Compact snow. Density: 0.36 gr/cm³. Temperature of snow: −2.4°C. In this and the previous Fig. 41 the portions of soot lines belonging to the deformed part of snow sheet are remarkably distorted. Compact snow of these two Figs. are nearest to solid substance in this respect among the snows of all the series of pictures presented.

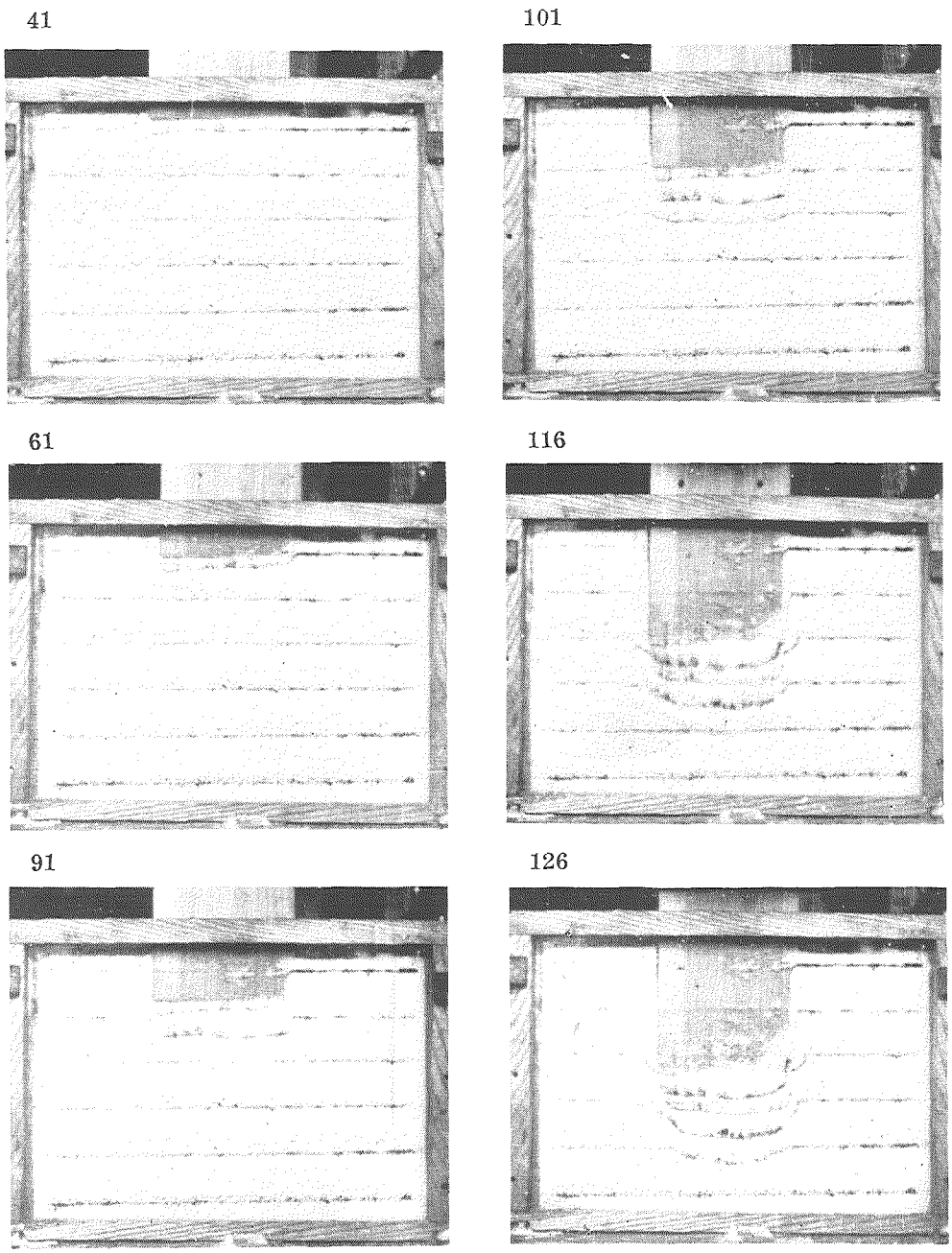


**Fig. 43** Compact snow. Density: 0.45 gr/cm³. Temperature of snow: −3.0°C. This snow shows little distortion in the displaced portions of soot lines in spite of being compact in character.

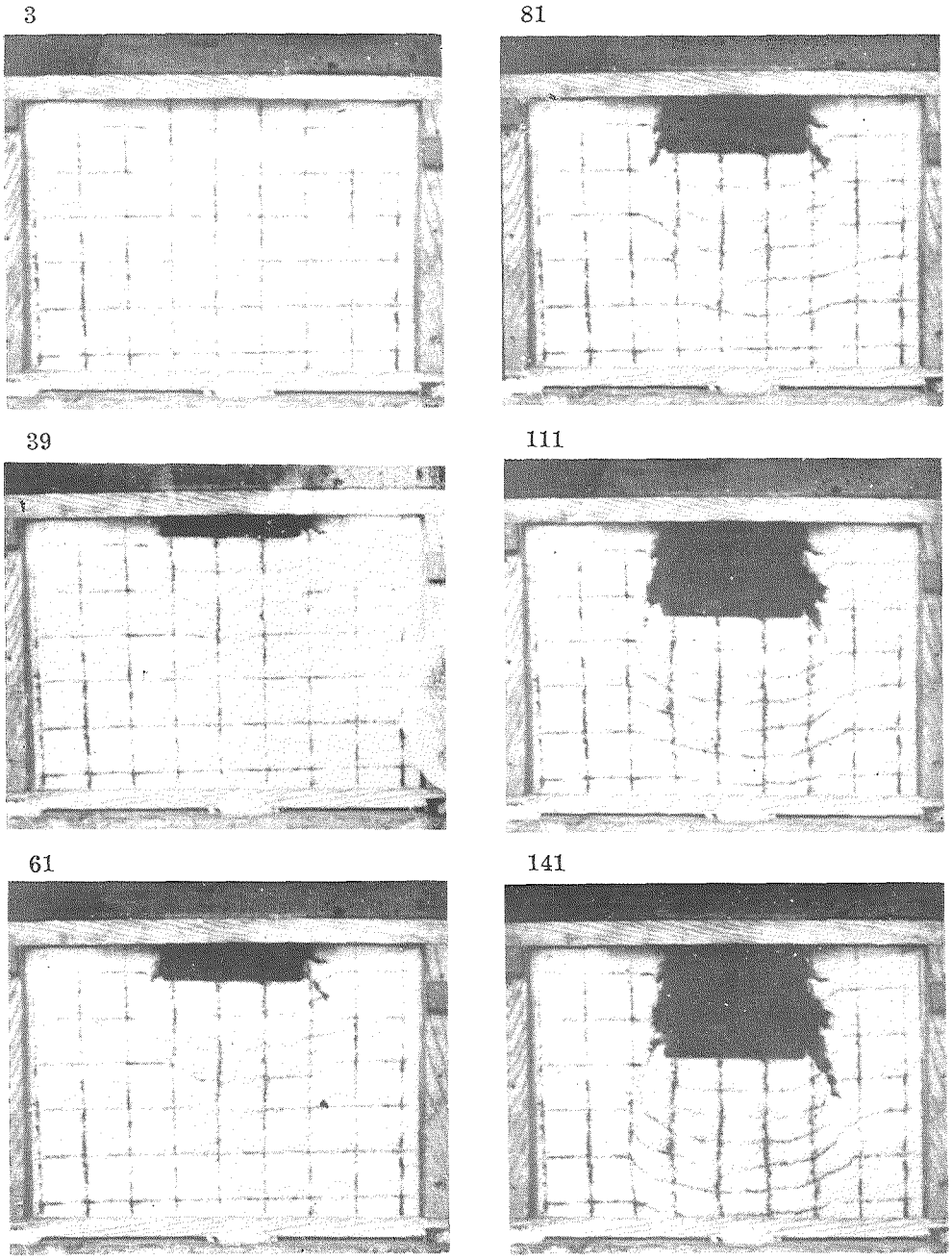


**Fig. 44** Granular snow. Density: 0.32 gr/cm³. Temperature of snow: −3.0°C. The soot lines appear smooth in contrast with the distorted soot lines of compact snow of nearly the same density of Fig. 42.

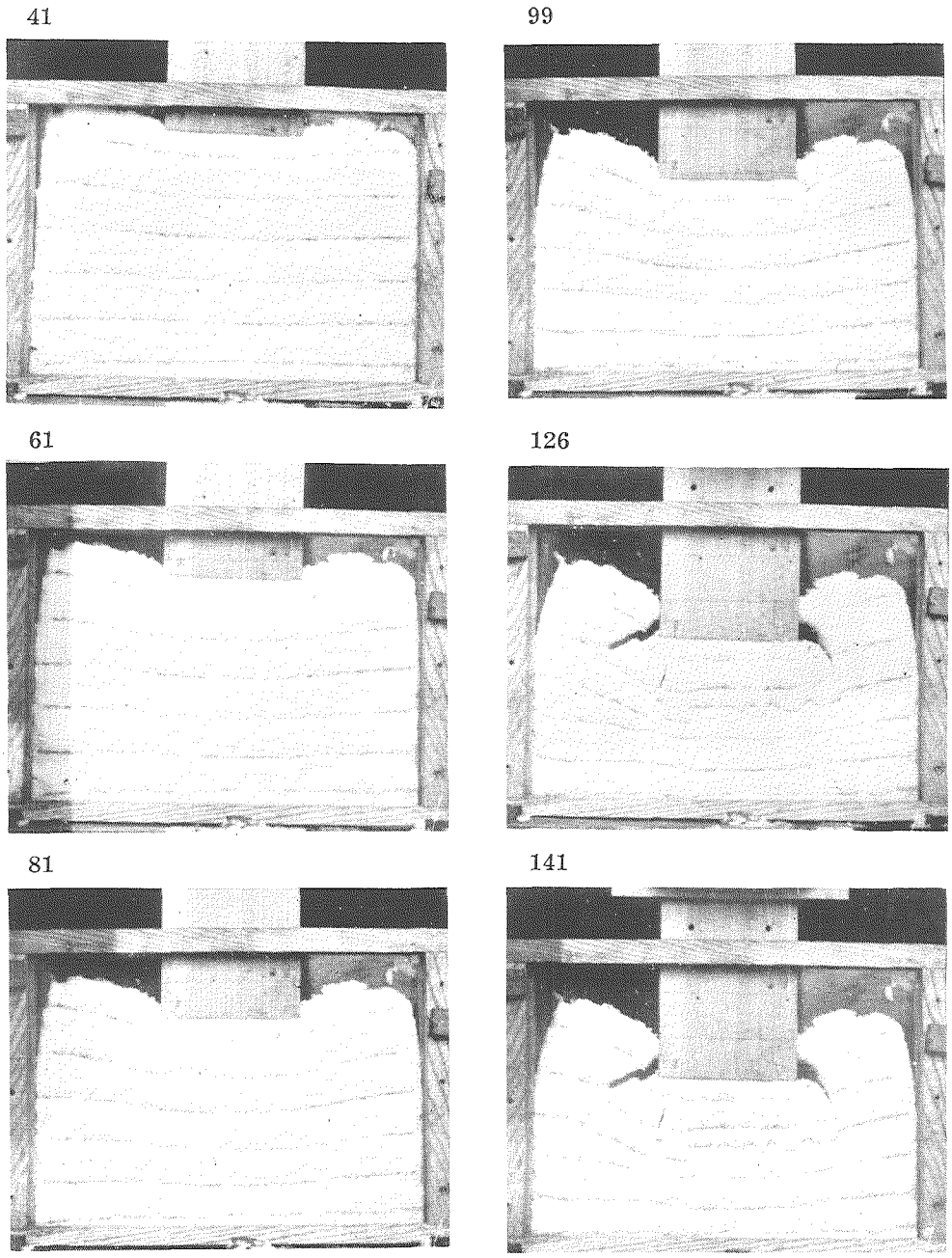


Fig. 45 Wet snow. Density: not determined. Temperature of snow: 0°C. Temperature of air: +0.6°C. The wet snow deforms much like a very viscous liquid such as gelatine gel.

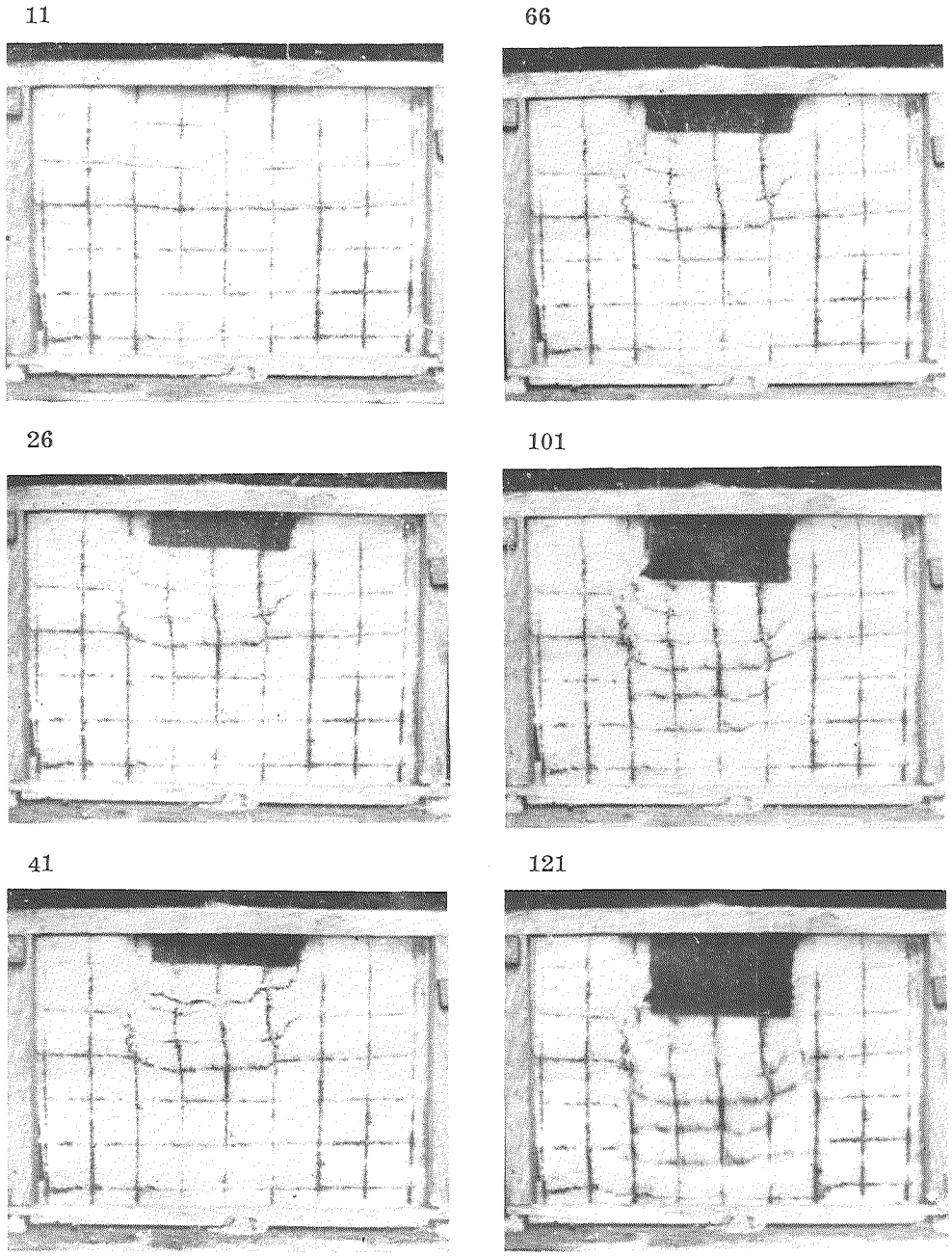


Fig. 46 Composite snow. Ice crust are embedded just below the uppermost soot line and near the third one. The part above the latter ice crust is granular snow while compact snow composes the part under it.